Kv1.1 RNA Editing: Physiological Roles and its Implications for Episodic Ataxia Type-1

By

Elizabeth Ferrick Kiddie

Dissertation
Submitted to the Faculty of the
Graduate School of Vanderbilt University
in partial fulfillment of the requirements
for the degree of

DOCTOR OF PHILOSOPHY
in

Molecular Physiology and Biophysics
May, 2017
Nashville, Tennessee

Approved:

Ronald B. Emeson, Ph.D.

Charles E. Cobb, Ph.D.

Roger J. Colbran, Ph.D.

Aurelio A. Galli, Ph.D.

Jennifer A. Kearney, Ph.D

.

This dissertation is dedicated to my family, friends, and especially my lab and my husband- who all in their own ways encouraged me forward scientifically, spiritually, and emotionally.

ACKNOWLEDGEMENTS

First and foremost, I would like to thank my adviser, Dr. Ron Emeson, for your mentorship that made my dissertation research possible and set me up with opportunities that will surely propel my scientific career forward. Thank you for demonstrating scientific curiosity and rigor for replicability. Dr. Chuck Cobb, thank you for being more than just my committee chair- you were a key support for helping me navigate my time at Vanderbilt. Thank you to Dr. Roger Colbran, Dr. Aurelio Galli, and Dr. Jennifer Kearney for serving on my committee and spurring me to think critically about the progression of my research. Thank you to the members of the Molecular Physiology & Biophysics department for asking thoughtful questions at seminars and for being a community of scientific rigor. Thank you to the members of my lab, past and present, Dr. Randi Ulbricht, Dr. Jennifer Hood, Dr. Richard O'Neil, Hussain Jinnah, Turnee Malik, Kayla Shumate, Chris Hofmann, Li Peng, Beth Sims, and Katie Patterson. You were my advisers, teachers of techniques, co-laborers of experiments, and listening ears for troubleshooting. Thank you to Li Peng for your expertise in cell culture and for aiding me in the cell experiments of my research. In particular, thanks to Katie Patterson whose superb mouse husbandry, expertise of behavioral tests, and peripheral tissue dissection skills made all the mouse experiments possible.

Thank you to the many, many collaborators who have contributed to the success of my project. Thank you to Dr. Roberts Reenan (Brown University) for developing and sharing the non-edited [Kv1.1(I)] and edited [Kv1.1(V)] mice

with us. Thank you to Dr. James Maylie (Oregon Health & Science University) who provided the Kv1.1 V408A/+ mice and was generous with his time by email and in person to discuss his expertise in the Episodic ataxia type-1 field. Thank you to Dr. Danny Winder and Dr. Samuel Centanni for your expertise in performing hippocampal slice electrophysiology for me. Huge thanks to Dr. Joshua Rosenthal (Woods Hole and University of Puerto Rico Medical Sciences Campus) for hosting me at his laboratory in Puerto Rico. You provided key mentorship for performing, analyzing, and writing all the data derived from the *Xenopus* oocyte electrophysiological experiments. Thank you to the members of Dr. Rosenthal's lab for being so welcoming and teaching and advising me in all the techniques I needed to learn in a short amount of time, Dr. Laura Fernández-Alacid, Dr. Nuria Vazquez, Dr. Maria Fernanda Montiel-Gonzalez. Isabel Vallecillo-Viejo, and Sonia Soto (who in particular isolated the *Xenopus* oocytes for my experiments). Thank you to Dan Ayers, the master statistician who helped build complex statistical models when he could and advised me on the statistics for the rest- you have made me care more about statistics then I ever thought I would. Thank you to the friends across departments who helped me find and fine-tune my dissertation story, in particular Amanda Meyer, Dr. Andrea Belovich, Britney Lizama-Manibusan, and, of course, my husband Dr. Bradley Kiddie.

Funding for this work was provided by the Vanderbilt Molecular Endocrinology Training Program (T32DK007563), the Ruth L. Kirschstein National Research Service Award (F31NS087911), a Vanderbilt Dissertation Enhancement Grant, and the Vanderbilt Joel G. Hardman Chair in

Pharmacology. Additional support for the research, which occurred in Dr. Joshua Rosenthal's lab, included NINDS (R0111223855, R01NS64259), the Cystic Fibrosis Foundation Therapeutics (Rosent14XXO), NIGMS (P20GM103642), NIMH (G12-MD007600), and NSF (DBI 0115825, DBI 1337284).

Finally, thank you to my supportive family and friends who made the time I spent at Vanderbilt and in Nashville a pleasant and formative time of life.

TABLE OF CONTENTS

Page

DEDICATION ii

ACKNOWLEDGEMENTS iii

LIST OF TABLES ix

LIST OF FIGURES x

LIST OF EQUATIONS xiii

LIST OF ABBREVIATIONS xiv

Chapter

I. INTRODUCTION 1

A brief history of our understanding of the variety of influences on genetic flow 1
A-to-I RNA Editing 2
Voltage-gated potassium channels 5
Kv1.1 and the Kv1 family 9
Episodic Ataxia type-1 16
Modulation of Kv1.1 function by RNA editing 18
Summary 26

II. FUNCTIONAL CONSEQUENCES OF KV1.1 RNA EDITING IN MOUSE MODELS 29

Introduction 29
Materials & Methods 34
Mouse Experiment Approval 34
Characterization of Kv1.1 editing in wild-type mouse tissues 35
Generation of non-edited [Kv1.1(I)] and edited [Kv1.1(V)] mutant mice 35
Kv1.1 RNA Expression Characterization in non-edited [Kv1.1(I)] and edited [Kv1.1(V)] mutant mice 38
Mendelian distribution of progeny 39
Behavioral Testing 40
Spontaneous Seizure Monitoring 42
Drug-induced Seizure Susceptibility 43
Hippocampal Slice Electrophysiology 46
Statistical analysis 47

Results 48
Characterization of Kv1.1 editing in wild-type mouse tissues 48
Verification of non-edited [Kv1.1(I)] and edited [Kv1.1(V)] mutant mouse models 49
Mendelian distribution of progeny 53
Behavioral characterization 56
Spontaneous Seizure Monitoring 67
Drug-induced Seizure Susceptibility 67
Preliminary Electrophysiological characterization 77
Discussion 79
Characterization of Kv1.1 editing in wild-type mouse tissues 79
Verification of non-edited [Kv1.1(I)] and edited [Kv1.1(V)] mutant mouse models 81
Mendelian distribution of progeny 84
Behavioral characterization 85
Spontaneous Seizure Monitoring and Drug-induced Seizure Susceptibility 91
Preliminary Electrophysiological characterization 95
Summary 96

III. INTERACTIONS BETWEEN KV1.1 RNA EDITING AND EPISODIC ATAXIA TYPE-1 MUTATIONS 98

Introduction 98
Materials & Methods 99
Kv1.1 and Kvβ1.1 constructs 99
In vitro analysis of RNA editing 100
In vivo analysis of RNA editing 102
Electrophysiological recording in Xenopus oocytes 103
Statistical analysis 105
Results 107
EA1-associated mutations alter RNA editing in vitro 107
A mouse model of EA1 (V408A/+) alters RNA editing in vivo 110
Gating properties are altered between non-edited and edited Kv1.1 channels harboring EA1 mutations 112
Inactivation kinetics are altered between non-edited and edited EA1 mutant proteins 122
Discussion 129
Proof of concept that existing mutations alter RNA editing 129
Edited Isoforms of EA1 mutants alter electrophysiological properties 131
Incorporating RNA editing into the complex interactions involved in the EA1 disorder 133

IV. CONCLUSIONS 135

Significance 135

Future Directions 138
Utilizing the newly developed mouse models of Kv1.1 editing 138
Continuing the study of RNA editing effects on EA1 145

Appendix

A. Comparative analysis of editing rates determined by Sanger sequencing versus High-throughput sequence analysis 150

B. Additional p-value tables 153

C. Human variants found in the Kv1.1 mRNA duplex 157

REFERENCES 161

LIST OF TABLES

Table		Page
2.1	Seizure threshold scale for scoring PTZ-induced seizures	44
2.2	Seizure threshold scale for scoring 4-AP-induced seizures	46
2.3	Conditional non-Mendelian distribution of non-edited [Kv1.1(I)] mutant offspring	55
2.4	Conditional non-Mendelian distribution of edited [Kv1.1(V)] mutant offspring	55
3.1	Free energy calculations of wild-type and EA1 human mutant duplexes	108
3.2	Voltage-dependence of activation	115
3.3	Kinetics of recovery from Kvβ1.1 inactivation	129
B.1	P-values corresponding to Figure 3.6 (time to half-activation)	154
B.2	P-values corresponding to Figure 3.8 (closing kinetics)	155
B.3	P-values corresponding to Figure 3.10 (kinetics of Kvβ1.1 inactivation)	156
C.1	Human variants found in the Kv1.1 mRNA duplex	158

LIST OF FIGURES

Figure		Page
1.1	ADAR Enzymes convert adenosine residues to inosine by hydrolytic deamination	3
1.2	Domain topology for the Kv1.1 α-subunit and accessory Kvβ-subunit	7
1.3	Conformational states of Kv channels	9
2.1	Targeting strategy to solely generate non-edited [Kv1.1(I)] or edited [Kv1.1(V)] isoforms in mutant mice	36
2.2	Design of duplex mutations to solely generate non-edited [Kv1.1(I)] or edited [Kv1.1(V)] transcripts in mutant mice	37
2.3	Quantitative analysis of Kv1.1 RNA editing (I/V site) in mouse	49
2.4	Confirmation of Kv1.1 isoform identity in mutant mice	51
2.5	Steady-state Kv1.1 RNA expression is unchanged in non-edited [Kv1.1(I)] and edited [Kv1.1(V)] mutant mice compared to wild-type mice	53
2.6	Initial behavioral analysis of non-edited [Kv1.1(I)] and edited [Kv1.1(V)] mice	57
2.7	Non-edited [KV1.1(I)] and edited [KV1.1(V)] heterozygous and homozygous mutant mice do not display locomotor dysfunction under the unstressed traditional rotarod paradigm	58
2.8	Non-edited [Kv1.1(I)] and edited [Kv1.1(I)] mutant mice do not display locomotor dysfunction under the unstressed modified rotarod paradigm	60
2.9	Non-edited [Kv1.1(I)] mutant mice display stress-induced locomotor dysfunction under the stressed modified rotarod paradigm	61
2.10	Non-edited [Kv1.1(I)] mice display reproducible stress-induced gait alterations	63
2.11	Non-edited [Kv1.1(I)] and edited [Kv1.1(V)] mice do not display stress-induced alterations by the inverted screen test	65

2.12 Open-field analysis of non-edited [Kv1.1(I)] and edited [Kv1.1(V)] mice 66

2.13 Flurothyl-induced seizures 68

2.14 PTZ-induced seizure threshold scores 69

2.15 Male versus female comparison of PTZ-induced seizure threshold scores 70

2.16 Latency to hindlimb extension following PTZ-induced seizures 71

2.17 4-AP-induced seizure threshold scores 73

2.18 Male versus female comparison of 4-AP-induced seizure threshold scores 74

2.19 Latency to hindlimb extension following 4-AP-induced seizures 76

2.20 Electrophysiological characterization of dentate gyrus granule cells of non-edited [Kv1.1(I)] and wild-type mice 78

2.21 Stress-enhancement of rotarod performance 89

3.1 Time course analysis to determine the linear range for the in vitro RNA editing rates 102

3.2 The proximity of the Kv1.1 editing site compared to the EA1 mutations responsible for V404I, I407M, and V408A 108

3.3 Quantitative analysis of *in vitro* RNA editing rates for wild-type and mutant Kv1.1 transcripts 110

3.4 Quantitative analysis of allele-specific Kv1.1 editing in V408A mutant mice 111

3.5 Voltage-dependence of non-edited compared to edited mutant channels 114

3.6 Editing alters opening (activation) kinetics of I407M channels 116

3.7 I407M E and V408A E channels display decreased currents at the most positive voltages 117

3.8 Editing alters closing (deactivating) kinetics of V404I channels 119

3.9 Long pulse characterization of WT and EA1 channels..... 121

3.10 Editing slows Kvβ1.1-induced inactivation kinetics of I407M and V408A channels 124

3.11 Long pulse characterization of Kvβ1.1-inactivation of WT and EA1 channels 126

3.12 Editing alters the recovery from Kvβ1.1-induced inactivation in V404I, I407M, and V408A channels..... 128

4.1 Human variants found in the Kv1.1 mRNA duplex..... 148

A.1 Comparative analysis of editing quantification by Sanger and High-Throughput Sequencing..... 152

LIST OF EQUATIONS

Equation		Page
3.1	Ohm's Law	105
3.2	Boltzmann Function	113

LIST OF ABBREVIATIONS

ΔG	Gibb's free energy
4-AP	4-aminopyridine
$5HT_{2C}$	2C-subtype of 5-hydroxytryptamine (serotonin) receptor
A	adenosine
A-type	rapidly inactivating
ADMS	autosomal dominant myokymia and seizures rat model
AP	action potential
ADAR	Adenosine Deaminase acting on RNA
AMPA	α-amino-3-hydroxy-5-methyl-isoxazole-4-propionate
ANOVA	analysis of variance
BCNU	1-3-bischloroethyl-nitrosurea
bp	base pair
C	cytidine
C-terminal	Carboxyl-terminal
CA1	Cornu Ammonis region 1
CA3	Cornu Ammonis region 3
$CaCl_2$	calcium chloride
$Ca_v1.3$	voltage-gated calcium channel, α-subunit 1D
cDNA	complementary deoxyribonucleic acid
DNA	deoxyribonucleic acid
dsRNA	double stranded ribonucleic acid

DTT	dithiothreitol
EEG	electroencephalogram
E#	embryonic day #
E	edited Kv1.1 isoform
EDTA	ethylenediaminetetraacetic acid
EGTA	ethylene glycol-bis(β-aminoethyl ether)-N,N,N',N'-tetraacetic acid
EMG	electromyography
EA1	Episodic ataxia type-1
ER	endoplasmic reticulum
FAAH	fatty acid amide hydrolase
Flna	filamin A, alpha
G	guanosine
GluA2	AMPA Glutamate Receptor subunit 2
Gabra3	$GABA_A$ receptor α3 subunit
Gapdh	glyceraldehyde 3-phosphate dehydrogenase
GABA	γ-aminobutyric acid
HEPES	4-(2-hydroxyethyl)-1-piperazineethanesulfonic acid
HgTx	rHongotoxin-1
HLE	hindlimb extension
I	inosine
I400V	isoleucine to valine change at amino acid position 400
I407M	isoleucine to methionine change at amino acid position 407
k	voltage sensitivity

K+	potassium ion
K-glutamate	potassium glutamate
KCNA1	human gene encoding Kv1.1
Kcna1	mouse gene encoding Kv1.1
Kv	voltage-gated potassium channel
Kv1.1	voltage-gated potassium channel, subfamily A member 1 (older names MBK1 and RCK1)
Kv1.x	heterotetramers of Kv1 channel subunits
Kv1.1(I)	protein encoding the non-edited isoform of Kv1.1 with isoleucine at amino acid position 400
Kv1.1(V)	protein encoding the edited isoform of Kv1.1 with valine at amino acid position 400
Kvβ	potassium channel, voltage-dependent, beta subunit
Kvβ1.1	potassium channel, voltage-dependent, beta subunit 1.1
Lgi1	leucine-rich glioma inactivated gene 1
LGN	lateral geniculate nucleus
loxP	locus of crossover X in P1
MAP	mitogen-activated protein kinase
mceph	truncation mutation in Kv1.1 causing megencephaly
mg/kg	mg drug administered per kg of mouse's body weight
$MgCl_2$	magnesium chloride
miRNA	micro ribonucleic acid
MNTB	medial nucleus of the trapezoid body
mRNA	messenger ribonucleic acid

MTLE+HS	mesial temporal lobe epilepsy with hippocampal sclerosis
N	non-edited Kv1.1 isoform
n	sample size number
N-terminal	amino-terminal
NAB	N-terminal A and B box domain
NaCl	sodium chloride
NADP+	nicotinamide adenin dinucleotide phosphate
NaOH	sodium hydroxide
P#	postnatal day #
Pin1	peptidyl-prolyl cis-trans isomerase NIMA-interacting 1
PIP_2	phosphatidylinositol 4,5-bisphosphate
PCR	polymerase chain reaction
PMSF	phenylmethylsulfonyl fluoride
PTZ	pentylenetetrazole
qRT-PCR	quantitative reverse-transcriptase polymerase chain reaction
RNA	ribonucleic acid
RT-PCR	reverse transcriptase-polymerase chain reaction
S#	transmembrane domain #
SEM	standard error of the mean
sIPSC	spontaneous inhibitory postsynaptic current
T	thymidine
T1	tetramerization domain
tRNA	transfer ribonucleic acid

U	uridine
$V_{1/2}$	voltage corresponding to the midpoint of channel activation
V404I	valine to isoleucine change at amino acid position 404
V408A	valine to alanine change at amino acid position 408
V408A/+	mouse heterozygous for the V408A mutation in Kv1.1
WT	wild-type
WWP2	WW domain containing E3 ubiquitin protein ligase 2 (also known as NEDD4-like E3-ubiquitin protein ligase)

CHAPTER I

INTRODUCTION

A brief history of our understanding of the variety of influences on genetic flow

Debates raged in the first half of the twentieth century- what is the molecular makeup of our genetic code? Proteins or DNA? Although DNA rightly won the title for our genetic material through elegant discoveries of its transformative properties and information-storing structure, the story of genetic flow was still incomplete (Avery et al., 1944; Franklin and Gosling, 1953; Griffith, 1928; Hershey and Chase, 1952; Watson and Crick, 1953). The central dogma in its simplest form lays the groundwork for genetics: DNA is the central genetic material that is stably housed in the nucleus of (almost) every eukaryotic cell and in the nucleoid of prokaryotic cells. Because DNA is (generally) stationary, our genetic material is copied into smaller, portable forms, RNAs, which can travel to the ribosome for translating genetic information into proteins. Each of these steps, though faithfully copied into every textbook, has a caveat associated with it- genetics are not actually this simple.

Indeed, when the human genome was completed, the gene count was surprisingly low compared to original estimates and nodded to our current understanding that our DNA sequences alone are not enough to explain life's

vast complexity (Consortium, 2004; Lander et al., 2001; Pertea and Salzberg, 2010; Venter et al., 2001). Beyond the simple DNA sequence, epigenetic discoveries of histone structure, its modification, and DNA modifications began to explain how post-translationally modified proteins and DNA modifications could shape our genetic landscape, even revealing how environmental impacts could alter gene expression (Feil and Fraga, 2012; Felsenfeld, 2014). RNA regulation was recognized as a key way to shape and change the flow of genetic information, through cell-specific RNA processing and splicing, miRNA-induced repression of RNA expression, piwi-interacting RNA-mediated protection from transposable elements, long non-coding RNAs functioning as epigenetic controllers, and post-transcriptional modification, including RNA editing (Licatalosi and Darnell, 2010).

A-to-I RNA Editing

RNA editing, in particular, involves endogenous RNA processing events, which add complexity to the process of genetic flow by altering genetic information post-transcriptionally. One form of RNA editing is adenosine-to-inosine (A-to-I) RNA editing, which is an enzyme-mediated, hydrolytic deamination of adenosine residues to inosine within regions of double stranded RNA (dsRNA) (Bass and Weintraub, 1988; Wagner et al., 1989) (Figure 1.1). This conversion can lead to recoding when it occurs within the open reading frame of an mRNA, because inosine base pairs with cytidine (in a similar manner

as guanosine) in the tRNA anticodon loop, thus A-to-I editing functions like an A-to-G conversion (Basilio et al., 1962).

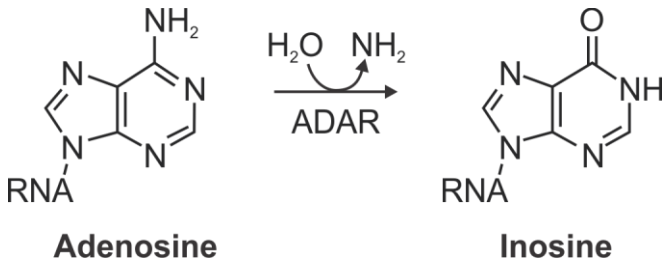

Figure 1.1. ADAR Enzymes convert adenosine residues to inosine by hydrolytic deamination.

This enzymatic reaction is catalyzed by the ADAR enzymes (Adenosine Deaminase acting on RNA), which are a family of dsRNA-binding proteins, including ADAR1, ADAR2 and ADAR3. ADAR1 and ADAR2 are the only catalytically active enzymes of the family, functioning as homodimers, and possessing varying selectivity regarding which RNAs, as well as which specific sites, they target (Chen et al., 2000; Cho et al., 2003; Gallo et al., 2003; Lehmann and Bass, 2000). ADAR1 and ADAR2 are found ubiquitously throughout the human body, whereas ADAR3 is brain-specific, and ADAR homologs are conserved from humans to the earliest branching metazoan lineages (including sponges, *C. elegans*, *D. melanogaster*, squid, rat, mouse) (Chen et al., 2000; Feng et al., 2006; Gerber et al., 1997; Grice and Degnan,

2015; Kim et al., 1994a). In shorter, imperfect duplexes, ADARs deaminate A-to-I in a site-specific manner, whereas in the context of extensive duplexes, ADARs are known to edit non-specifically, such as with invading viral dsRNA genomes (George et al., 2011; Nishikura, 2010). In mammalian tissues, A-to-I editing occurs prominently in the brain where it serves to modulate the function of many proteins important for nervous system function including the ion-selectivity and biophysical properties of the AMPA Glutamate Receptor subunit 2 (GluA2), altering activation and deactivation kinetics of the $GABA_A$ receptor α3 subunit (Gabra3), regulating G-protein coupling efficacy and constitutive activity for the serotonin 5-HT_{2C} receptor ($5HT_{2C}$), and modulating the calcium-dependent inhibition of a voltage-gated calcium channel subunit ($Ca_V1.3$) (Huang et al., 2012; Niswender et al., 1999; Rula et al., 2008; Sommer et al., 1991). The importance of these and additional editing events also is highlighted by the effects observed in mutant mice where the expression of ADAR1 or ADAR2 has been selectively ablated. ADAR1 knockout mice exhibit embryonic lethality between embryonic day 11 (E11) and E12.5, exhibiting widespread apoptosis and defects in hematopoiesis that can be partially rescued by inhibiting components of the innate immune system (Hartner et al., 2004; Mannion et al., 2014; Wang et al., 2004). ADAR2 knockout mice display postnatal lethality between postnatal day 0 (P0) and P20, coinciding with progressive seizures, which can be rescued through expression of the genomically edited GluA2 receptor (Higuchi et al., 2000).

Although ADAR2's role in creating the edited isoform of the GluA2 receptor leads to the most drastic phenotypic effects (lethality), editing regulation for other ADAR2 targets has the potential to modulate editing levels to allow for tissue-specific expression of edited isoforms. This is particularly evident in the tissue-specific expression of the $5HT_{2C}$ receptor, where five editing sites lead to 32 different mRNA species encoding 24 possible protein isoforms. RNA editing of these five sites varies across different brain regions, presumably leading to altered isoform ratios and altered contributions to neuronal function (Morabito et al., 2010). This editing-dependent fine-tuning of neuronal function in a brain region-specific manner is likely at play for another ADAR2 substrate, the voltage gated potassium channel α-subunit, Kv1.1.

Voltage-gated potassium channels

Voltage-gated potassium channels (Kv) are characterized by their conduction of potassium ions through the channel pore following a voltage change in the membrane potential. They are a diverse family of potassium channel subunits arising from at least 40 genes in humans, which are further characterized into 12 subfamilies (Gutman et al., 2005). Each subfamily contains multiple members, called α-subunits, which generally form homo- and heterotetramers in a subfamily-specific manner (as is the case for Kv1 channels) (Gutman et al., 2005). However, the Kv5, Kv6, Kv8, and Kv9 families encode

subunits which act as modifier subunits within Kv2 heterotetramers (Gutman et al., 2005).

Structural insights regarding these six helical transmembrane domain proteins has been gained through determination of the Kv1.2 crystal structure (Chen et al., 2010; Long et al., 2005). Each α-subunit is composed of six α-helical transmembrane domains (S1-S6): S1 through S4 together form the voltage-sensor domain while S5, the P loop, and S6 together form the pore domain (Sands et al., 2005) (Figure 1.2). The extracellular face of the pore is composed of a selectivity filter which allows for the selective flow of potassium (K^+) ions down their electrochemical gradient, with conformational control over the intracellular face of the pore conferred by the charged residues of the S4 helix, in the voltage sensing domain, which twists upon changes in the membrane potential (Glauner et al., 1999). A cytoplasmic N-terminal tetramerization domain (T1, also called the N-terminal A and B box domain, or NAB) of Kv channels is responsible for allowing the four α-subunits to associate with each other as well as with four accessory β-subunits (Yu et al., 1996).

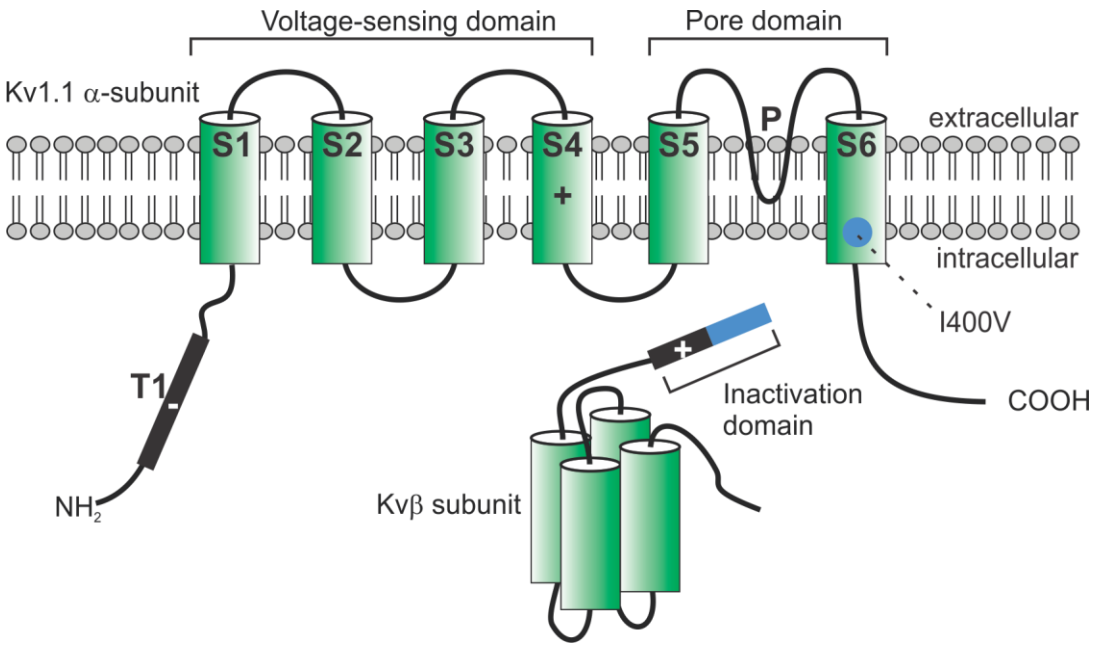

Figure 1.2. Domain topology for the Kv1.1 α-subunit and accessory Kvβ-subunit. The voltage-sensing domain is composed of the S1-S4 helices, with conformational control of the voltage sensor mediated by the positively charged S4 helix. The pore domain is composed of the S5-P loop-S6 region, and the I400V residue (determined by RNA editing) is contained within the S6 helix, within a hydrophobic region (shaded blue). Tetramerization of four α-subunits with each other and with four accessory Kvβ-subunits is mediated by the N-terminal T1 domain. The β-subunit contains an inactivation domain composed of hydrophobic (shaded blue) and positively charged residues which interact with the hydrophobic residues of the channel pore and the negatively charged residues of the T1 domain (Adapted from Hood and Emeson, 2012).

Potassium channels can exist in several states: closed, open, or inactivated (Figure 1.3). The closed and inactivated states occur when the pore is constricted or blocked at different locations within the central pore. The closed versus opened state occurs when the S6 transmembrane domains of each α-subunit constrict on the intracellular face of the channel, in a region called the bundle-crossing and the activation gate (Holmgren et al., 1998; Long et al., 2005;

Yellen, 2002). In addition to closing, there are two types of inactivation that can occur following opening of the channel, despite maintaining a continuous depolarizing voltage, slow (C-type) and fast (N-type) inactivation. Both types of inactivation are distinct from the closed state and represent stable, non-conducting states which are maintained for periods of time before the channels are closed and available to be opened again by depolarization (a process quantified as the recovery from inactivation) (Kurata and Fedida, 2006). C-type inactivation is generally slower than N-type and involves a change in the extracellular pore of the channel, proposed to be mediated either by pore constriction or pore dilation at the outermost face of the selectivity filter (Choi et al., 1991; Hoshi and Armstrong, 2013). N-type inactivation is a rapid inactivation which can be mediated by two types of auto-inhibitory peptides, either N-terminal domains which are part of some α-subunits, such as *Shaker* and Kv1.4 (Hoshi et al., 1990; Lee et al., 1996; Po et al., 1992; Zagotta et al., 1990), or from the N-terminal domains of accessory β-subunits (Rettig et al., 1994; Zhou et al., 2001). N-type inactivation is proposed to be a docking of these N-terminal inactivation peptides within the inner channel pore, representing approximately 20 amino acids (Zagotta et al., 1990). The peptides contain a string of 10 hydrophobic followed by 10 positively charged or hydrophilic amino acids which interact with the negatively charged amino acids within the T1 domain and the hydrophobic residues within the intracellular pore of the channel (Long et al., 2005).

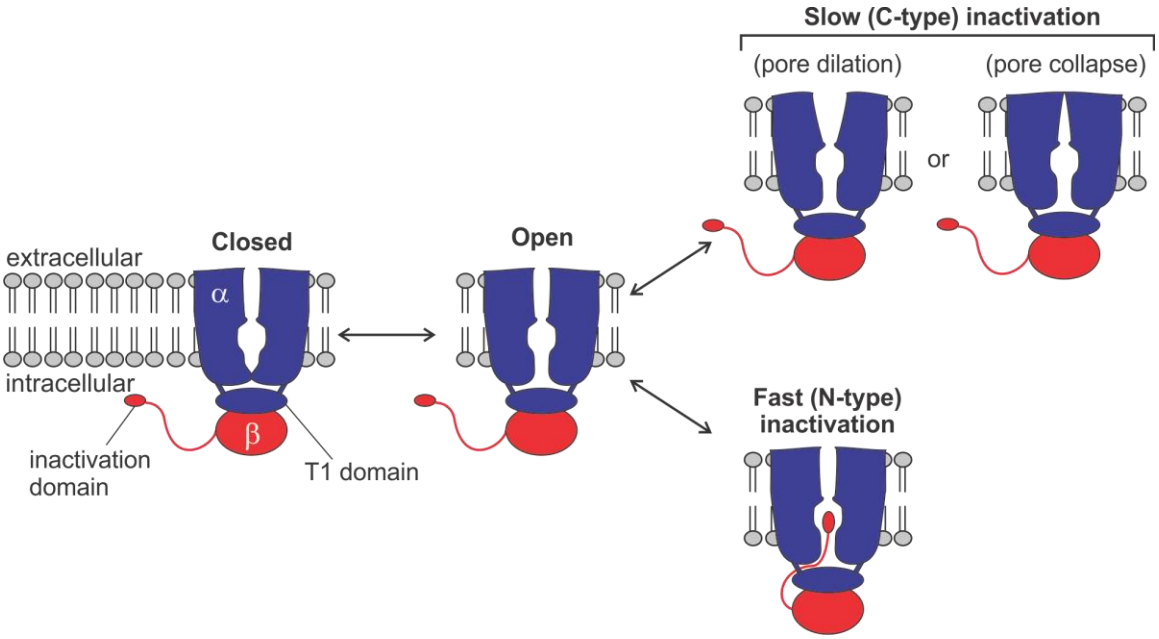

Figure 1.3. Conformational states of Kv channels. Kv channels (composed of four α-subunits) can exist in several conformational states, including closed, open, and inactivated either by slow (C-type) inactivation or fast (N-type) inactivation. Slow inactivation has been proposed to be either a pore dilation or pore constriction. Fast inactivation can be mediated by the inactivation domain of an accessory β-subunit (shown in red) or by an intrinsic inactivation domain of some Kv α-subunits (not shown) (Adapted from Bezanilla, 2004).

Kv1.1 and the Kv1 family

The homolog of the mammalian Kv1 family was first discovered in *Drosophila melanogaster*, and named *Shaker*, describing the rapid shaking phenotype of Shaker mutant flies upon treatment with ether (Kaplan and Trout, 1969). Cloning of the Shaker locus revealed it encoded a potassium channel and subsequent studies characterized its electrophysiological properties (Kamb et al., 1987; Tempel et al., 1987). The Kv1.1 mammalian *Shaker*-homolog, originally named MBK1 and RCK1, was first discovered by hybridizing *Shaker*

complementary DNA (cDNA) probes, directed against the transmembrane segments, under low-stringency to a cDNA library composed of either mouse brain or rat cortex mRNA (Baumann et al., 1988; Tempel et al., 1988). Rat and mouse Kv1.1 were found to have 68% and 65% sequence homology with *Drosophila Shaker*, respectively, highlighting the selective pressure to maintain these proteins' functions in evolutionarily distant organisms (Baumann et al., 1988; Tempel et al., 1988).

The Kv1 family is composed of eight *Shaker*-related family members, Kv1.1 through Kv1.8 (human gene names *KCNA1* through *KCNA10*), each with unique biophysical characteristics of activation, deactivation, and inactivation (Bardien-Kruger et al., 2002; Grupe et al., 1990; Gutman et al., 2005; Heinemann et al., 1996; Kalman et al., 1998; Kirsch et al., 1991; Lang et al., 2000; McKinnon, 1989; Stühmer et al., 1989; Swanson et al., 1990; Yao et al., 1995). These family members can be subdivided based upon their inactivation characteristics. For example, Kv1.4 is a rapidly inactivating (A-type) channel with N-type inactivation conferred by its intrinsic N-terminal inactivation domain (Gutman et al., 2005; Lee et al., 1996). The other Kv1 family members are delayed rectifiers that intrinsically inactivate only by C-type inactivation (Gutman et al., 2005). N-type inactivation can be conferred to channels containing most of the delayed rectifier subunits, by co-assembly with β-subunits or heterotetramerization with Kv1.4, though Kv1.6 contains an N-type inactivation prevention (NIP) domain (Gutman et al., 2005; Heinemann et al., 1996; Po et al., 1993; Roeper et al., 1998).

Kv1 channels can co-assemble with accessory β-subunits, in an $\alpha_4\beta_4$ configuration (Parcej et al., 1992). Multiple isoforms of β-subunits include Kvβ1 (alternative splicing isoforms: 1.1, 1.2, and 1.3), Kvβ2 (alternative splicing isoforms: 2.1 and 2.2), and Kvβ3 (England et al., 1995; Pongs and Schwarz, 2010). These isoforms differ predominantly in their N-terminal domains, which are responsible for mediating inactivation, whereas high homology is found throughout the rest of the proteins (Dolly and Parcej, 1996). Kvβ2.1 is the β-subunit with the highest abundance in the mammalian brain, whereas Kvβ2.2 has only been found in the C6 rat glioblastoma cell line, reactive astrocytes from a rat model of gliosis, and rabbit portal vein, but not normal rat brain (Akhtar et al., 1999; Rhodes et al., 1996; Thorneloe et al., 2001). Of these β-subunits, isoforms of Kvβ1 has been shown to interact and inactivate Kv1.1 channels, whereas Kvβ2 and Kvβ3 can co-assemble with Kv1.1 but do not inactivate it (Heinemann et al., 1996; Heinemann et al., 1995; Rettig et al., 1994). Kvβ2 is proposed to modulate the fast inactivation properties of other inactivating proteins, as it prevents Kvβ1 fast-inactivation when both β-subunits are co-expressed with Kv1 channels and speeds Kv1.4-induced inactivation (McCormack et al., 1995; Xu and Li, 1997). Pulldown studies have isolated Kv1.1-containing heterotetramers with Kvβ1.1 and Kvβ2.1 subunits in the human brain, whereas the Kvβ1.2 and Kvβ1.3 isoforms are predominantly found in the heart. One study did find Kvβ1.3 expression in the brain, but it was weakly inactivating for Kv1.1 (Coleman et al., 1999; England et al., 1995; Wang et al., 1996). Interestingly, another accessory subunit, Lgi1, can oppose Kvβ1 inactivation in tetramers of Kv1.1 and Kv1.4,

however inactivation by intrinsic inactivation of Kv1.4 remained intact (Schulte et al., 2006). Lgi1 mutations are associated with autosomal dominant lateral temporal lobe epilepsy; these mutations prevent Lgi1 function to regulate Kvβ1 inactivation, further underscoring the importance of tightly regulated β-mediated inactivation (Schulte et al., 2006).

Expression of the Kv1 family in mammals varies by family member and by tissue type. Most subunits are expressed in at least some tissues of the nervous system (including the brain and spinal cord), localized particularly in axons and nerve terminals, though Kv1.5 had very low expression and Kv1.7 was only found in peripheral tissues (Gutman et al., 2005; Kalman et al., 1998; Trimmer and Rhodes, 2004). Kv1 family members are also prominently expressed in heart, aorta, pancreatic islets, and skeletal and smooth muscle (Gutman et al., 2005). Particular family members also contribute to specific tissues, such as Kv1.1 and Kv1.2 in the retina, Kv1.3 and Kv1.6 in the lungs, Kv1.5 and Kv1.8 in the kidneys, and Kv1.3 in the spleen and lymphocytes (Gutman et al., 2005). These sites of expression underscore the ubiquitous role that the Kv1 family plays in maintenance of the membrane potential for a variety of cell and tissue types.

One of the main roles that the Kv1.1 α-subunit plays is the regulation of neuronal excitability. By dampening excitability at the axon initial segment and juxtaparanodal region (Robbins and Tempel, 2012), it can influence action potential initiation, propagation, and reduce nerve terminal excitability, permitting fine-tuning of neurotransmitter release (Ishikawa et al., 2003). Kv1.1 is widely

expressed throughout the mammalian brain, with high levels of expression in the hippocampus (notably in CA3 pyramidal cells and dentate gyrus granule cells) and cerebellum (particularly in basket cell nerve terminals synapsing to Purkinje neurons) (Kirchheim et al., 2013; Tsaur et al., 1992; Wang et al., 1993). Underscoring its physiological importance, genetic knockout studies have revealed that mice lacking Kv1.1 expression develop spontaneous seizures, cold-sensitive neuromyotonia, decreased motor coordination, hyperalgesia, and neurogenic cardiac dysfunction (Clark and Tempel, 1998; Glasscock et al., 2010; Smart et al., 1998). Kv1.1-knockout mice display an incompletely penetrant lethality due to increased developmental seizure susceptibility, with approximately half of the homozygous mutants dying before the sixth postnatal week (Rho et al., 1999; Smart et al., 1998; Zhang et al., 1999; Zhou et al., 1998).

Although Kv1.1 can form functional homotetrameric channels, Kv1.1 is predominantly found in heterotetramers with other Kv1 family members (denoted Kv1.x) that contribute to the large diversity of Kv1 channel kinetics and pharmacology throughout the mammalian central nervous system (Coleman et al., 1999; Koch et al., 1997; Rasband et al., 2001; Sokolov et al., 2007). Most often Kv1.1 is found in various heterotetrameric combinations with Kv1.2 and/or Kv1.4, as these three subunits are the most predominant Kv1 α-subunits in the mammalian brain (Coleman et al., 1999; Trimmer and Rhodes, 2004; Wang et al., 1999; Wang et al., 1993; Wang et al., 1994). Kv1.1 also is co-expressed with subunits of lesser abundance, co-localized with Kv1.3 in the choroid plexus and cerebellar cortex and with Kv1.6 in interneurons (Rhodes et al., 1997; Speake et

al., 2004; Trimmer and Rhodes, 2004; Wang et al., 1999). Heterotetrameric assembly leads to channels with biophysical properties intermediate to the characteristics of homotetrameric α-subunit channels, and the ratios of each type of α-subunit lead to dose-dependent contribution to the overall channel characteristics (Bagchi et al., 2014; Ovsepian et al., 2016; Sokolov et al., 2007). Kv1.1 has a unique role in influencing heterotetrameric voltage-dependence and the kinetics of activation, as it opens at an especially low voltage threshold (Kv1.1 $V_{1/2}$:-35 mV; Kv1.2 $V_{1/2}$: 5 and 27 mV; Kv1.4 $V_{1/2}$: 22 and 34 mV) and faster than other highly co-expressed Kv1.x α-subunits (Kv1.1 τ: 5 ms; Kv1.2 τ: 6 ms; Kv1.4 τ: 16.5 ms) (Ovsepian et al., 2016).

Subunit composition not only alters the biophysical characteristics of the heteromeric channel, but may also alter the trafficking of Kv1 channels to the plasma membrane. When subunits were expressed as homotetramers in transfected cell lines and primary hippocampal cultures, Kv1.1 was predominantly localized to the endoplasmic reticulum (ER), Kv1.4 to the cell surface, and Kv1.2 expression was split between the ER and the plasma membrane (Manganas and Trimmer, 2000). Increasing the ratio of Kv1.1 subunits in Kv1.x heterotetramers shifted the expression towards greater intracellular localization, whereas Kv1.4 had the opposite effect, and Kv1.2 had a neutral effect (Manganas and Trimmer, 2000). Extracellular pore residues within the P loop of homotetrameric Kv1.1 channels, which differ from other Kv1.x family members (A352P and Y379K), are thought to prevent Kv1.1 cell surface trafficking from the ER, though a mechanism has not been elucidated (Manganas

et al., 2001). Additional studies found that heterotetrameric assembly impacted subcellular localization in neurons, with Kv1.2 being a prominent determinant for Kv1.1 axonal trafficking (Jenkins et al., 2011).

Co-assembly with β-subunits increases the surface expression of homo- and heterotetrameric combinations of Kv1.1, Kv1.2, and Kv1.4, with the notable exception of Kv1.1 homotetramers (Manganas and Trimmer, 2000; Shi et al., 1996). The ability of β-subunits to facilitate surface expression was attributed to its oxidoreductase activity, as mutations to the NADP+ co-factor binding pocket abolished the β-subunits' ability to promote trafficking (Campomanes et al., 2002). Axonal targeting also has been attributed to the T1 domain interaction with β-subunits (Gu et al., 2003). Although these functions have been suggested for the role of β-subunits, based on studies in transfected mammalian cells and primary hippocampal cultures, surface expression and axonal localization of Kv1 proteins were not affected in Kvβ2 knockout mice and only affected in a subset of Kvβ1/Kvβ2 double-knockout animals (Connor et al., 2005; McCormack et al., 2002). These finding suggest that β-subunits may have additional unknown roles and that the inactivation and surface-promoting properties of Kv1.4, Kvβ1, and Kvβ2 serve redundant functions.

Episodic Ataxia type-1

The role of Kv1.1 and its effects on human health have also been studied in the context of a related genetic disorder. Genetic linkage analyses have identified over 30 heterozygous mutations within the gene encoding human Kv1.1 (*KCNA1*) that have been associated with the sporadic and autosomal dominant neurological disorder, episodic ataxia type-1 (EA1) (D'Adamo et al., 2015). EA1 occurs with an age of onset in patients between 2 and 15 years old and is characterized by stress-induced motor discoordination, involuntary, repetitive muscle contraction (myokymia), and can coincide with seizures (Graves et al., 2014). Types of stressors found to trigger ataxia vary between patients, most commonly including exercise/exertion, stress/emotional upset, and environmental temperature; additional triggers can include, but are not limited to, fever, caffeine, alcohol, startle, prolonged rest, sudden movement, and diet (Graves et al., 2014). The most common symptoms include imbalance, slurred speech, incoordination of hands, weakness, tremors, and muscle twitching or stiffness (Graves et al., 2014).

The majority of EA1-related mutations result in a loss of channel function, reduced surface expression, or a change in biophysical properties where the mutant subunits can exert a dominant-negative effect by association with wild-type α-subunits (Chen et al., 2016; D'Adamo et al., 2015; Eunson et al., 2000; Imbrici et al., 2006; Mestre et al., 2016; Petitjean et al., 2015; Tomlinson et al., 2013; Zerr et al., 1998). Deficits have also been observed in heterotetramers with other Kv1 family members as well as when co-expressed with auxiliary β-

subunits (Imbrici et al., 2006). Only one mouse model of EA1 has been developed in which an identified human EA1 mutation responsible for a valine to alanine change at amino acid position 408 (V408A) was introduced into the endogenous mouse *Kcna1* locus. The V408A mutation has been described to have altered the biophysical parameters of homotetrameric channels compared to wild-type Kv1.1, and have dominant-negative effects on heterotetrameric channels containing wild-type Kv1.1 and V408A (Adelman et al., 1995; Bretschneider et al., 1999; D'Adamo et al., 1999; D'Adamo et al., 1998; Imbrici et al., 2011; Imbrici et al., 2006; Maylie et al., 2002; Zerr et al., 1998). The homozygous (V408A/V408A) mutants die between E3 and E9, while the heterozygotes (V408A/+) exhibit stress-induced and temperature-sensitive motor dysfunction, with alterations in cerebellar signaling (Begum et al., 2016; Brunetti et al., 2012; Herson et al., 2003). In addition, Ishida *et al.* (2012) used a forward genetic screen for mutations leading to myokymia, neuromyotonia, and seizures in rats, which led to the development of the autosomal dominant myokymia and seizures (ADMS) rat model with relevance to EA1. A missense mutation was found in ADMS rats within the Kv1.1 S4 voltage sensor domain leading to S309T, which is in close proximity to two known human EA1 mutations, L305F and R307C (D'Adamo et al., 2015; Ishida et al., 2012). S309T channels displayed a dominant-negative dysfunction with wild-type Kv1.1 in heterotetrameric channels, leading to an 80% decrease in outward K+ current (Ishida et al., 2012). S309T/S309T homozygotes died around P16, whereas S309T/+ rats displayed

increased mortality from 16 to 30 weeks, both corresponding with increasing spontaneous seizures (Ishida et al., 2012).

Despite the broad distribution and altered functions resulting from these mutations throughout the channel protein, no clear correlation has been established between the diverse clinical phenotypes of EA1 patients and specific mutations within Kv1.1, or why stress triggers symptoms (though neuromyotonia and myokymia have been attributed to hyperexcitability of peripheral nerve endings) (Brunetti et al., 2012; D'Adamo et al., 2015; Graves et al., 2014; Graves et al., 2010). This lack of consistency in clinical presentation suggests that additional mechanisms could also be responsible for alterations in channel function and EA1 heterogeneity. One factor that has yet to be addressed is how the EA1 disorder is impacted by the endogenous Kv1.1 isoform variation arising from RNA editing.

Modulation of Kv1.1 function by RNA editing

RNA editing was first discovered in the *Drosophila* potassium channel, *Shaker*, and subsequently found in its mammalian homolog Kv1.1, though no editing was discovered in any of the other Kv1.x or Kv families (Decher et al., 2010; Hoopengardner et al., 2003). RNA transcripts encoding Kv1.1 are modified by a site-specific A-to-I RNA editing event in which a genomically-encoded isoleucine (AUU) is converted to a valine (IUU) codon at amino acid position 400 of the protein (I400V) (Hoopengardner et al., 2003). This amino acid lies within

the S6 transmembrane domain predicted to line the ion-conducting pore of the channel (Figure 1.2). Editing of Kv1.1 transcripts is dependent upon a region of dsRNA within exon 2 which forms intramolecular base-pairing interactions between imperfect, inverted repeat elements surrounding the targeted adenosine moiety (Bhalla et al., 2004). This process was determined to be catalyzed by ADAR2 through exogenous expression in HEK293 cells as well as the almost complete absence of Kv1.1 RNA editing in ADAR2-null mice (Bhalla et al., 2004; Horsch et al., 2011).

Although an isoleucine to valine substitution does not seem substantial, only resulting in an amino acid with one fewer methyl group, previous studies have revealed that Kv1.1 channels containing edited [Kv1.1(V)] subunits display a 20-fold faster rate of recovery from Kvβ1.1-inactivation, compared to non-edited channels [Kv1.1(I)] (Bhalla et al., 2004). More recent studies have indicated that only small alterations in the hydrophobicity of the editing site amino acid were needed to reproduce the editing-dependent alterations in recovery kinetics (Gonzalez et al., 2011). In addition, the extent of inactivation was heavily influenced by the accessible surface area of the hydrophobic amino acid at the editing site; thus the non-edited [Kv1.1(I)] isoform has a greater extent of inactivation than the edited [Kv1.1(V)] isoform (Gonzalez et al., 2011). Interestingly, the alteration in the recovery from inactivation following a slight change in the hydrophobic interactions has been recapitulated previously in a complimentary experiment, where the hydrophobic residues of the N-terminus of the auxiliary β-subunit were substituted for alanine or valine (Zhou et al., 2001).

The dissociation constants of the mutant β-subunits were generally faster compared to wild-type, further supporting the role of these hydrophobic interactions, between the α- and β-subunits, in setting the dissociation rate of β-inactivation (Zhou et al., 2001).

β-subunits are not alone in conferring hydrophobic-mediated inactivation of potassium channels, as endogenous lipids can not only induce fast inactivation (arachidonic acid induces fast inactivation in Kv1.1), but they also can prevent β-inactivation (such as PIP_2 preventing Kv1.1 inactivation by Kvβ1.1) (Honoré et al., 1994; Oliver et al., 2004). Extensive drug studies have elucidated that the editing status of Kv1.1 has a prominent effect on the efficacy of drug-mediated channel blockers. Edited Kv1.1 was insensitive to the channel block mediated by important endogenous signaling lipids, including arachidonic acid, docosahexaenoic acid, and the endocannabinoid anandamide, whereas non-edited channels were readily blocked (Decher et al., 2010). Although the binding rate of arachidonic acid was not different between non-edited [Kv1.1(I)] and edited [Kv1.1(V)] isoforms, the recovery from arachidonic acid-induced block was rapid for edited [Kv1.1(V)] and slow for non-edited [Kv1.1(I)] channels, mirroring the recovery from inactivation kinetics of the β-subunit (Bhalla et al., 2004; Decher et al., 2010). Several pharmacological open channel blockers displayed similar selectivity for the non-edited [Kv1.1(I)] channel, including the known Kv1 channel blockers, Psora-4 and 4-aminopyridine (4-AP) (Decher et al., 2010). When different ratios of non-edited [Kv1.1I(I)] and edited [Kv1.1(V)] channels were co-expressed to make a tetramer, only one edited [Kv1.1(V)] subunit was

needed to suppress the sensitivity to endogenous and pharmacological blockers, reducing the inhibition by 60% for arachidonic acid and 65% for Psora-4, compared to channels made entirely of non-edited [Kv1.1(I)] subunits (Decher et al., 2010). Similarly, heterotetrameric assembly of edited [Kv1.1(V)] with other Kv1.x family members significantly reduced the affinity of the channels to open channel blockers (Decher et al., 2010). These studies emphasize that even tissues with low levels of Kv1.1 RNA editing may be able to impact signaling kinetics through the effects of a single edited [Kv1.1(V)] subunit within a heterotetramer.

Kv1.1 editing also has been implicated in altering trafficking to the plasma membrane. Although homotetrameric Kv1.1 is known to be predominantly localized to the ER, some non-edited [Kv1.1(I)] channels still express at the cell surface. By contrast, edited [Kv1.1(V)] surface expression was significantly reduced compared to the non-edited [Kv1.1(I)] channels (Streit et al., 2014). Co-expression with Kv1.4 trafficked both the non-edited [Kv1.1(I)] and edited [Kv1.1(V)] channels to the plasma membrane, equalizing the surface expression of both isoforms (Streit et al., 2014). A caveat to these trafficking experiments was that they were performed in HeLa, HEK293, and CHO cells and in *Xenopus* oocytes, rather than in primary hippocampal cultures like previous Kv1.x trafficking experiments. It is unknown whether these cell lines contain all of the necessary components for Kv1.1 trafficking.

Kv1.1 editing has been found predominantly in nervous tissue, though some editing has been found in human aorta (but not in the heart) (Decher et al.,

2010; Hoopengardner et al., 2003; Li et al., 2009). The percentage of Kv1.1 editing is found to vary in dissected portions of the mammalian nervous system, with approximately 20% editing in human hippocampus compared to 70% in human spinal cord (Hoopengardner et al., 2003). In addition, Kv1.1 RNA editing is developmentally regulated in the mouse brain, with low editing (approximately 5-7%) in whole brain samples at E15, E19, P0, and P2, but by P21 levels rise to approximately 30%, near the adult levels of 45% (Jacobs et al., 2009; Wahlstedt et al., 2009). Although many other editing targets share similar trends in editing regulation, with low embryonic editing (except the GluA2 RNA which is always highly edited), most other targets have increases in editing at birth, whereas Kv1.1 RNA editing lags behind these other targets (Flna RNA has a similar lagging RNA editing trend to Kv1.1) (Jacobs et al., 2009; Wahlstedt et al., 2009). The same Kv1.1 developmental RNA editing trend was observed by transcriptome-wide RNA-seq, detecting editing patterns across development for human and mouse tissues, and these studies also further resolved that Kv1.1 editing began increasing at P7 in mice (Hwang et al., 2016). At this time, it is unknown whether adult neurogenesis occurring following a seizure leads to a similar lag in Kv1.1 RNA editing that has been observed during embryonic development.

As is the case with the quantification of Kv1.1 editing described above, most editing profiles are quantified from entire tissues or brain regions that may be composed of many different cell types. The heterogeneity of these tissues leads to different interpretations of what the editing percentages mean. Are

tissues composed of a few cell types with high levels of editing in the midst of other cells with no editing, or does editing occur in every cell at a variable ratio?

Although Kv1.1 RNA editing has not been determined in defined cell types, patch-clamp studies on acutely isolated thalamic LGN and hippocampal CA1 neurons by Decher *et al.* (2010) provide an indirect method for inferring single-cell editing. Using the differential pharmacological sensitivity to Psora-4 (blocks nonedited [Kv1.1(I)] and Kv1.x channels, but not edited [Kv1.1(V)] or Kv1.4) versus rHongotoxin-1 (HgTX) (blocks both nonedited [Kv1.1(I)] and edited [Kv1.1(V)] and Kv1.x, but not Kv1.4 or Kv1.5), investigators were able to determine estimates of edited Kv1.1 expression in individual neurons of each cell type (Decher et al., 2010; Koschak et al., 1998; Vennekamp et al., 2004). The currents which were Psora-4-resistant, but HgTX-sensitive, indicated the presence of the edited [Kv1.1(V)] protein isoform in these cell types. Sequencing reverse transcriptase-polymerase chain reaction (RT-PCR) amplicons derived from these isolated neuronal populations revealed that the average Kv1.1 RNA editing correlated well with the edited [Kv1.1(V)] protein expression estimated from the single-cell electrophysiological characterization; 63% of the current from LGN neurons was Psora-4 resistant, indicative of edited Kv1.1 expression, and 52% of the Kv1.1 RNA was edited in the population of these isolated cells (Decher et al., 2010). By contrast, 15% of the current from CA1 pyramidal cells was Psora-4 resistant, correlating with a 7% editing profile for Kv1.1 RNA in these cells (Decher et al., 2010). These studies provide evidence that intermediate editing ratios are observed within single cells, though they do not

exclude the possibility that editing could still vary by cell type within tissues.

Little is known about how Kv1.1 RNA editing is regulated *in vivo*, however, Kv1.1 editing levels are altered in two mouse models of epilepsy. In the first model, control rats displayed low Kv1.1 editing levels in the entorhinal cortex (5.1%), whereas, following epileptic induction by kainic acid, editing was increased (21.5%) (Streit et al., 2011). In normal rat entorhinal/hippocampal slices, 4-AP induces seizure-like events, however slices from kainic acid epileptic rats are resistant to 4-AP effects (Streit et al., 2011). These data suggest that increased editing may be associated with a decreased seizure-susceptibility in rats. The second model is a genetic model of epilepsy where editing of the GluA2 receptor was decreased in the mouse forebrain (in particular, GluA2 Q/R site editing in the hippocampus was decreased approximately 25%) (Krestel et al., 2013; Krestel et al., 2004). In this model, Kv1.1 RNA editing was also increased in the epileptic mice compared to controls (Krestel et al., 2013).

There are several possible mechanisms for these increases in Kv1.1 RNA editing following seizure induction. First, increases in editing may result from increased expression of ADAR2, as previous studies have indicated that, following kainic acid seizure induction, rats had a 40% increase in ADAR2 protein expression (O'Leary et al., 2016). Second, the kainic acid-induced seizure rat model has also been associated with increased activity of two MAP kinases, and the nuclear localization of ADAR2 is positively regulated by a phosphorylation-dependent interaction with the phosphorylation-dependent prolyl-isomerase, Pin1 (whereas localization in the cytoplasm can lead to degradation mediated by the

E3-ubiquitin ligase, WWP2) (Kim et al., 1994b; Marcucci et al., 2011). Third, ADAR2 gene expression is regulated by the CREB transcription factor and seizure-induction can activate CREB (in these cases, seizures were induced by pentylenetetrazole (PTZ) or 1-3-bischloroethyl-nitrosurea (BCNU)) (Moore et al., 1996; Peng et al., 2006; Pennacchio et al., 2015). Although editing regulation may occur by altering ADAR2 expression and activity, as detailed above, other unknown factors may be involved as well.

Aside from these mouse models displaying alterations in Kv1.1 RNA editing, one study has correlated Kv1.1 editing in epileptic patients. Tissue samples obtained from patients undergoing surgery for mesial temporal lobe epilepsy revealed an editing-dependent association, where levels of Kv1.1 RNA editing were inversely correlated with the duration of years that the patients had experienced epileptic activity, such that lower editing was correlated with a longer epilepsy duration (Krestel et al., 2013). These results could indicate that increased editing of Kv1.1 has a protective effect, dampening future seizures in chronic epilepsy, and that decreased editing could represent a risk factor for long-term seizures, though further experiments are necessary to test this hypothesis.

Of note, in two brain regions of interest, the hippocampus and the cerebellum, Kv1.1 expression is lower than other Kv1.x subunits (including combinations of Kv1.2, Kv1.4, and/or Kv1.6), thus Kv1.1-containing heterotetramers in these tissues may contain only one Kv1.1 subunit (Scott et al., 1994). Kv1.1 is an important subunit, even in heterotetramers, because it opens

at lower voltages and faster than other Kv1.x subunits (Ovsepian et al., 2016). This Kv1.1 subunit could be non-edited or edited, thus heterotetramers may be further stratified into groups defined by the unique and dominant characteristics conferred by the absence or presence of an edited subunit. The role of Kv1.1 in defining the opening kinetics of heterotetramers, and editing conferring rapid recovery from inactivation, may underlie the particular vulnerability of mutations and altered editing patterns in leading to dysfunctions related to hippocampal and cerebellar function.

Summary

Kv1.1 is an important regulator of neuronal signaling in normal physiology and its dysregulation leads to EA1, yet the role of Kv1.1 RNA editing as it contributes to healthy and EA1 physiology are still largely unknown. Although several studies have indicated that edited [Kv1.1(V)] channels have altered biophysical characteristics, these studies have been performed predominantly in cell culture and *Xenopus* oocytes, rather than in an endogenous context. In addition, no studies have been performed to understand how RNA editing impacts the human disorder, EA1, though several EA1 mutations are in close proximity to the editing site.

The data in Chapter II describe our attempts to understand Kv1.1 RNA editing in a physiological context. Thus we have generated two mutant mouse lines which solely express either the non-edited Kv1.1 [Kv1.1(I)] or edited Kv1.1 [Kv1.1(V)] isoform. We describe how globally regulating Kv1.1 editing leads to

phenotypic alterations in each mouse line compared to wild-type littermates. Both the non-edited [Kv1.1(I)] and edited [Kv1.1(V)] mice exhibited an incompletely penetrant postnatal lethality that appeared to be dependent upon environmental factors. Non-edited [Kv1.1(I)] mice displayed EA1-like stress-induced ataxia, with alterations in gait and locomotor activity. In addition, editing altered drug-induced seizure susceptibility of both mouse lines, with the non-edited [Kv1.1(I)] mice displaying an increased susceptibility and faster latency to 4-AP-induced seizures and the edited [Kv1.1(V)] mice displaying a decreased susceptibility to both 4-AP and PTZ-induced seizures. Initial electrophysiological analysis of Kv1.1 in mouse hippocampal slices did not find differences in signaling parameters for non-edited [Kv1.1(I)] mice that would explain this alteration in seizure susceptibility.

In Chapter III, we detail the impact of RNA editing on EA1 mutant RNAs and proteins. Although numerous Kv1.1 mutations have been associated with the human disorder EA1, three EA1 mutations, V404I, I407M, and V408A, are located within the RNA duplex structure required for Kv1.1 RNA editing. Each EA1 mutation decreased RNA editing *in vitro* and the V408A mutation was confirmed to decrease RNA editing *in vivo* using a mouse model bearing the heterozygous V408A allele. Editing of transcripts encoding mutant channels affected numerous biophysical properties including channel opening, closing, and inactivation. Thus, EA1 symptoms could be influenced not only by the direct effects of the mutations on channel properties, but also by their influence on RNA editing. These studies provide the first evidence that mutations associated with a

human genetic disorder can affect *cis*-regulatory elements to alter RNA editing.

Finally, Chapter IV summarizes the conclusions of these studies and describes future directions to address new questions spurred on by the discoveries made thus far.

CHAPTER II

FUNCTIONAL CONSEQUENCES OF KV1.1 RNA EDITING IN MOUSE MODELS

Introduction

Although initial studies have characterized the effects of Kv1.1 RNA editing on channel function, most have been performed in exogenously expressing *Xenopus* oocytes. Thus, further studies are needed to better understand the physiological impact of Kv1.1 RNA editing *in vivo*. We have developed mutant mouse lines that have been genetically modified to solely express either the non-edited [Kv1.1(I)] or edited [Kv1.1(V)] isoforms. These mutant mouse lines have allowed us to assess the phenotypic effects of dysregulating normal editing patterns for Kv1.1 transcripts, and serve as important tools to examine the native electrophysiological properties of Kv1.1-expressing neurons.

These novel mouse lines have been developed in the context of several other related mouse models, whose characterized defects could indicate that our editing mouse models will have similar dysfunctions. Three models of Kv1.1 dysfunction have been created thus far including a Kv1.1-null mouse in which expression of the *Kcna1* gene encoding Kv1.1 is ablated (Smart et al., 1998). Although Kv1.1-null mice exhibit a normal Mendelian distribution at birth, no overt

ataxia, and normal Kv1.2 distribution in the cerebellum, they display spontaneous seizures starting at 3 weeks of age, hyperalgesia, neurogenic cardiac dysfunction, and have an enlarged hippocampus and ventral cortex (Clark and Tempel, 1998; Glasscock et al., 2010; Persson et al., 2007; Smart et al., 1998). Half of Kv1.1-null mice die within 3-5 weeks after birth, often immediately following seizures, though surviving mice can live up to 12 months of age (Smart et al., 1998). Kv1.1-null mice also displayed a shorter latency to flurothyl-induced seizure onset, with seizures occurring 60% sooner than wild-type animals, and heterozygous null mice showed a modest change in the onset of seizures (9% sooner than wild-type) (Rho et al., 1999; Smart et al., 1998). Surprisingly, no differences were found in the intrinsic membrane properties of CA3 pyramidal cells, though other electrophysiological changes were observed, including lower threshold for antidromic action potentials and a subset of cells which displayed epileptic late burst discharges upon mossy fiber stimulation (Smart et al., 1998). In the cerebella of Kv1.1-null mice, Purkinje neurons displayed increased frequency of GABAergic spontaneous inhibitory postsynaptic currents (sIPSCs), and these mice displayed motor deficits walking across a stationary thin rod, but were not different from wild-type animals using the rotarod test (Zhang et al., 1999). Peripheral nerve transmission also was altered in Kv1.1-null mice, including recordings in the sciatic nerve that indicated that loss of Kv1.1 leads to a prolonged repolarization and a longer recovery period and hyperexcitable neuromuscular transmission following cooling of isolated phrenic nerve (Smart et al., 1998; Zhou et al., 1998).

The *mceph/mceph* mouse is a megencephaly mouse model resulting from an 11-bp deletion in Kv1.1, leading to a frame-shifted, C-terminally truncated protein (truncated at amino acid 230 out of 495) (Petersson et al., 2003). These mice have a 25% increase in brain size, shakiness in gait, and display complex partial seizures starting at 3 weeks of age (Donahue et al., 1996; Petersson et al., 2003). Electrophysiological characterization in mossy cells of the hippocampus revealed increased frequency of stimulus-induced pulse trains, but no change in action potential shape or membrane resistance (Petersson et al., 2003). The truncated protein was expressed in mice, though localized to the ER, and Kv1.2 and Kv1.3 protein expression was decreased in *mceph/mceph* hippocampus (Persson et al., 2005; Petersson et al., 2003).

Another Kv1.1 mutant mouse was developed which incorporated a human EA1 mutation, V408A, into the endogenous *Kcna1* locus (Herson et al., 2003). Mice homozygous for the V408A mutation die during embryonic development between E3 and E9, while heterozygous V408A mice (V408A/+) display stress-induced motor discoordination (Herson et al., 2003). Electrophysiological characterization of V408A/+ cerebellar Purkinje neurons indicated this mutation increased the frequency and amplitude of sIPSCs, attributed to action potential broadening at basket cell boutons leading to increased GABA release (Begum et al., 2016; Herson et al., 2003). Recordings from V408A/+ motor nerves also revealed spontaneous bursting activity, which was triggered by fatigue, ischemia, and low temperature (Brunetti et al., 2012).

In addition to mouse lines with introduced mutations in the Kv1.1 α-subunit, four β-subunit knockout models also have been developed. Kvβ1.1-null mice exhibited no changes in lifespan, brain morphology, seizure activity, or alterations in open field or bar hang behavioral tasks (Connor et al., 2005; Giese et al., 1998). However, electrophysiological characterization of CA1 pyramidal neurons in Kvβ1.1-null mice revealed several alterations compared to wild-type controls. Kvβ1.1-nulls showed a decreased amplitude of inactivation, faster action potential repolarization during trains of depolarizing pulses (a decrease in the frequency-dependent spike broadening), and a reduced amplitude of the slow after-hyperpolarization phase of the action potential following spike trains (Giese et al., 1998). Kvβ1.1-null mice did not have any overt impairment in spatial or contextual learning and extracellular field recordings in the CA1 region did not reveal any differences in synaptic plasticity, though subtle learning impairments were observed in some cases (including in an altered paradigm of the Morris water maze, where previously trained mice had to find a new hidden platform location, and in the social transmission of food preference test) (Giese et al., 1998; Need et al., 2003).

Kvβ2-null mice were found to have phenotypic alterations similar to the Kv1.1-null mice, including cold swim-induced tremors, shortened life span (though normal Mendelian distribution at weaning), and the presence of sporadic seizures, but no differences in PTZ-induced seizure susceptibility (Connor et al., 2005; McCormack et al., 2002). Phenotypes were altered in a strain-specific manner, with Kvβ2-null mice on a C57B/6J background demonstrating more

severe phenotypes than the 129/SvEv background, which could result from a strain-specific 5-fold higher expression of Kvβ2 in C57B/6J versus 129/SvEv wild-type mice (Connor et al., 2005; Sandberg et al., 2000). The presence of seizures in this model is consistent with human patient data where a deletion including the region of Kvβ2 was a significant risk factor for epilepsy or epileptiform activity observed by EEG analysis (Heilstedt et al., 2001). Surprisingly, none of the observed mouse phenotypes could be attributed to presumed functions of Kvβ2. Previous characterization of Kvβ2 in heterologous expression systems suggested that Kvβ2, which does not induce fast-inactivation, was involved in potassium channel trafficking and axonal targeting (Gu et al., 2003; Shi et al., 1996). However, characterization of Kvβ2-null mice indicated no change in trafficking of Kv1.1 and Kv1.2 in the cerebellum or in the juxtaparanodal localization of Kv1.1 and Kv1.2 within the sciatic nerve (McCormack et al., 2002). In addition to Kvβ2-null animals, an additional mutant line was developed in which the oxidoreductase catalytic domain was targeted, but no observable phenotype resulted (McCormack et al., 2002).

Double mutant animals, in which the expression of both Kvβ1.1 and Kvβ2 were ablated, were developed to assess whether these subunits perform redundant functions (McCormack et al., 2002). Kvβ1.1/Kvβ2 double mutants had decreased lifespan compared to the Kvβ2-null animals, however Kvβ1.1 loss did not further exacerbate the cold swim-induced tremors (Connor et al., 2005). Localization of Kv1.2 within the pinceau region of cerebellar basket cells was more variable for the double mutants, with 5/8 mutants displaying less robust and

more diffuse expression of Kv1.2 (Connor et al., 2005). However, 3/8 mutants had comparable expression to wild-type controls, still indicating that proper localization could occur without either β-subunit (Connor et al., 2005).

Mouse models containing alterations in either the Kv1.1 α-subunit or Kvβ subunits serve as important references to compare the phenotype of mutant animals in which the editing profile for Kv1.1 RNAs has been fixed. For these studies, we have focused specifically on phenotypic alterations in survival, stress-induced motor discoordination, seizures and seizure susceptibility, and brain slice electrophysiology. Our initial characterization indicates that Kv1.1 editing serves a modulatory function for motor coordination and seizure susceptibility.

Materials & Methods

Mouse Experiment Approval

All animal care and experimental procedures involving mice were approved by the Vanderbilt University Medical Center Institutional Animal Care and Use Committee and were performed in accordance with relevant guidelines and regulations.

Characterization of Kv1.1 editing in wild-type mouse tissues

To characterize wild-type Kv1.1 RNA editing levels, wild-type C57BL/6 mice were euthanized by cervical dislocation under anesthesia followed by decapitation. Seven tissues (whole brain, spinal cord, lung, heart, bladder, skeletal muscle, kidney) were dissected from four male wild-type adult mice. Six brain regions (cerebellum, hippocampus, hypothalamus, cortex, striatum, olfactory bulb) were dissected from three additional male wild-type adult mice. Tissues were flash-frozen in liquid nitrogen and RNA was isolated by sonication in TRIzol (Ambion) according to the manufacturer's instructions. RNA was reverse-transcribed with random primers using the High Capacity cDNA Reverse Transcription kit (Applied Biosystems) and Kv1.1 editing was quantified by high-throughput sequence analysis as described previously (Hood et al., 2014) (VANTAGE, Vanderbilt University).

Generation of non-edited [Kv1.1(I)] and edited [Kv1.1(V)] mutant mice

Our collaborator, Dr. Robert Reenan (Brown University), generated mice that were genetically modified to solely express either the non-edited [Kv1.1(I)] or the edited [Kv1.1(V)] subunit isoform. Mutations were incorporated at the endogenous *Kcna1* locus (knock-in) by homologous recombination with a replacement-type targeting vector in C57BL/6J embryonic stem cells (Figure 2.1). This targeting vector included a positive selectable marker (neomycin cassette flanked by loxP sites) within and a negative selectable marker (thymidine kinase)

outside the region of homology, respectively. Mice with the mutant-neo allele were crossed with a mutant line expressing Cre recombinase to excise the neomycin resistance cassette, leaving a single loxP site downstream of exon 2. The non-edited [Kv1.1(I)] targeting vector incorporated two point mutations surrounding the editing site, which have previously been shown to disrupt the critical RNA duplex structure required for editing (Bhalla et al., 2004), yet maintain the codon identities in this region (Figure 2.2). The targeting vector to generate edited [Kv1.1(V)] transcripts was designed to introduce a guanosine at the editing site to mimic the coding potential of the inosine normally generated by A-to-I conversion (Figure 2.2).

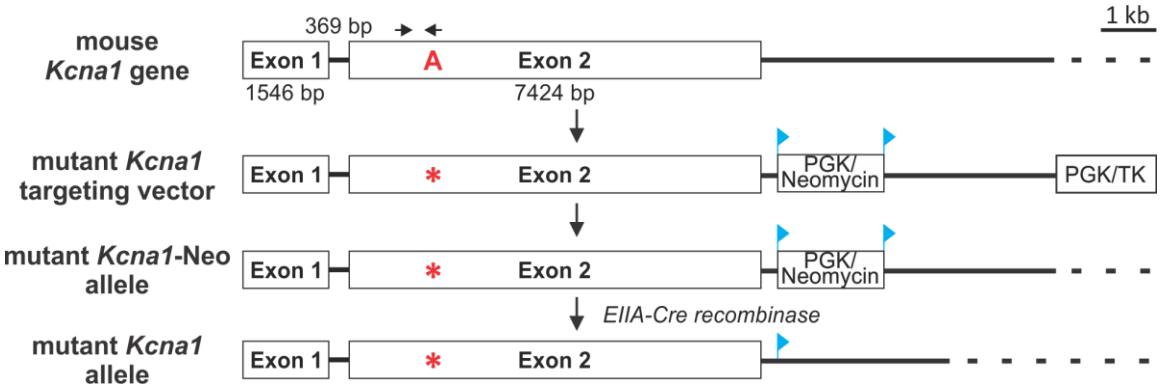

Figure 2.1. Targeting strategy to solely generate non-edited [Kv1.1(I)] or edited [Kv1.1(V)] isoforms in mutant mice. The targeting strategy for creating the non-edited [Kv1.1(I)] and edited [Kv1.1(V)] mutant mice is outlined. The *Kcna1* mouse gene is labeled with the editing site (indicated as a red A) within the RNA duplex region, indicated by arrows. Mutant constructs included the mutations required for either the non-edited or the edited isoform (indicated as a red asterisk) in conjunction with a positive selectable marker (neomycin cassette flanked by loxP sites) within the region of homology and a negative selectable marker (thymidine kinase) outside the region of homology. Mice with the mutant-neo allele were crossed with a Cre recombinase-expressing mouse to excise the neomycin resistance cassette, leaving a single loxP site behind (blue triangle).

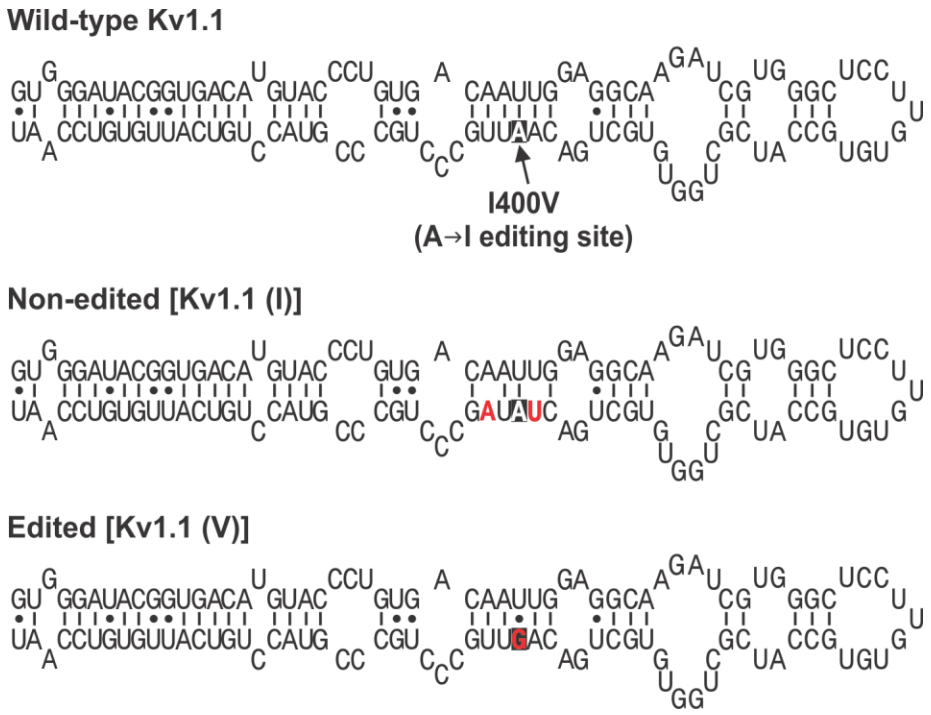

Figure 2.2. Design of duplex mutations to solely generate non-edited [Kv1.1(I)] or edited [Kv1.1(V)] transcripts in mutant mice. The predicted secondary structure for the wild-type mouse Kv1.1 pre-mRNA, in the proximal region of exon 2, is shown with the position of the I/V editing site indicated. The introduction of mutations to generate mutant mouse lines, solely expressing the non-edited and edited isoforms of the channel, are indicated in red.

Genotyping was performed by polymerase chain reaction (PCR) amplification of a 534 base pair (bp) region surrounding the editing site using sense (5'- TCCTCTTCATTGGGGTCATACTGT-3') and antisense (5'-GGGGTTTGTTTGGGGCTTTTGTTG-3') oligonucleotide primers in exon 2. The presence of the mutations incorporated into these mouse lines creates or destroys restriction sites for the non-edited (Sfc I) and edited (Mfe I) alleles, respectively, allowing accurate genotyping to be distinguished from heterozygous breeding crosses. Genotyping was performed using tail biopsies with the

REDExtract-N-Amp Tissue PCR Kit (Sigma-Aldrich).

To ensure expression of the mutant allele at the RNA level, RNA from mouse cerebellum for each genotype was isolated with TRIzol and subjected to RT-PCR, as described previously, and directly sequenced by Sanger sequencing (VANTAGE, Vanderbilt University). To further ensure that the non-edited [Kv1.1(I)] mice did not have undetectable RNA editing occurring, spinal cord cDNA was subjected to high-throughput sequence analysis as described previously (Hood et al., 2014) (VANTAGE, Vanderbilt University).

Kv1.1 RNA Expression Characterization in non-edited [Kv1.1(I)] and edited [Kv1.1(V)] mutant mice

Six adult mice each (mixed sex) of non-edited [Kv1.1(I)], edited [Kv1.1(V)], and wild-type animals were euthanized by cervical dislocation under anesthesia followed by decapitation. Six brain regions (cerebellum, hippocampus, hypothalamus, cortex, striatum, olfactory bulb) were dissected from each mouse. RNA was extracted and used as a template for reverse transcription with random primers using the High Capacity cDNA Reverse Transcription kit (Applied Biosystems). Steady-state RNA expression was assayed from each isolated cDNA using Taqman probes directed against mouse Kcna1 (Mm00439977_s1, ThermoFisher Scientific) and using mouse Gapdh as an internal normalization control (Mm99999915_g1, ThermoFisher Scientific). Quantitative RT-PCR (qRT-PCR) reactions were prepared using Taqman Universal PCR mastermix (2X) (ThermoFisher Scientific) according to the manufacturer's protocol. Technical

replicates for all cDNA samples were performed in triplicate and average values used for data analyses. Gene efficiencies were calculated using the PCR miner algorithm (Zhao and Fernald, 2005). All data were normalized to internal Gapdh expression using the CFX Manager Software (Bio-Rad). In addition, all samples were normalized to a standard wild-type sample (of the same tissue type), re-assayed on each qRT-PCR plate. This ensured normalization consistency, as the number of replicate tissue samples required assaying over multiple qRT-PCR plates.

Mendelian distribution of progeny

Heterozygous crosses of Kv1.1 non-edited mice and heterozygous crosses of Kv1.1 edited mice were set up in multiple mouse housing facilities (MCNII Facility, on multiple floors, and the Barrier Facility) and the offspring tailed for genotyping. These offspring were generated for subsequent experimental analyses. Separate heterozygous crosses were set up for prenatal lethality analysis. Pregnant heterozygous female mice with embryos at E18.5 were anesthetized and euthanized.

Behavioral Testing

Initial behavioral characterization was performed using adult male non-edited [Kv1.1(I)] and edited [Kv1.1(V)] mice, and their wild-type littermates (Brooks and Dunnett, 2009). Grip strength was assessed with a force gauge (San Diego Instruments, San Diego, CA). The pole climb test involved placing the mice face upwards on the top of a vertical pole. The time to turn 180º and climb down the pole was measured for each animal.

Muscle endurance and motor coordination were assessed using an accelerating rotarod test (Ugo Basile, Comerio, Italy) on adult male mice: non-edited [Kv1.1(I)], edited [Kv1.1(V)], and their wild-type littermates (Brooks and Dunnett, 2009). Mice were placed on an accelerating rotating rod (rod diameter: 3.2 cm; acceleration: 5 to 40 revolution/minute over a 5-minute period). Latency to fall off the rod was measured by the device's automatic stopwatch. Mice that failed to walk on the rotarod were scored as fallen after two successive stationary rotations. Original unstressed trials were performed with the traditional rotarod paradigm: 3 trials per day for 3 days. A modified rotarod paradigm was performed for follow-up unstressed and stressed rotarod trials: trials were performed daily for 9 days with either control animals or mice that were stressed for 30 minutes by conical tube restraint immediately preceding the rotarod trial.

Gait analysis was assessed using the footprint test on adult male non-edited [Kv1.1(I)] mice, edited [Kv1.1(V)] mice, and their wild-type littermates (Carter et al., 2001). Forepaws and hindpaws were painted with non-toxic red or

blue paint, respectively, and mice were allowed to run through an opaque, plexiglass tunnel on standard legal paper (8.5 x 14 inches) to record the position of the paw prints. A light positioned above the entrance to the tunnel was used to motivate the mice to run to a dark, enclosed box at the end of the tunnel. Analysis of gait metrics included forelimb and hindlimb stride length, front and hind base width, and right and left overlap measurements. One group of mice performed the footprint test unstressed and another group were stressed for 30 minutes by conical tube restraint prior to the test.

The inverted screen task was performed on adult male non-edited [Kv1.1(I)] mice, edited [Kv1.1(V)] mice, and their wild-type littermates (Brooks and Dunnett, 2009). Prior to the task, mice were either unstressed or stressed by 30 minutes of conical tube restraint. Latency to fall from the inverted screen was measured, to a maximum of 60 s, and the task was repeated three times for the unstressed and stressed conditions.

The open-field task was performed to assess the locomotion and anxiety of adult male non-edited [Kv1.1(I)], edited [Kv1.1(V)], and their wild-type littermates (Brooks and Dunnett, 2009). Mice were tested under either the unstressed or stressed paradigm (30 minutes of conical tube restraint immediately prior the task), and then observed in the open field chamber for 30 minutes. Analysis of locomotion was achieved through measurements of distance traveled and velocity. Analysis of anxiety was achieved through measurements of center time, center entries, rearing counts, and grooming time.

Spontaneous Seizure Monitoring

Spontaneous seizures were analyzed by electroencephalogram (EEG) analysis. Preliminary studies were performed on adult male non-edited [Kv1.1(I)] mice, edited [Kv1.1(V)] mice, and their wild-type littermates by Alison Miller in the laboratory of Dr. Jennifer Kearney, which suggested that the non-edited [Kv1.1(I)] mice had abnormal recordings. Therefore, we performed an additional pilot study comparing a non-edited [Kv1.1(I)] mouse to a wild-type littermate, using cortical surface electrodes to allow for more precise measurements. Following isoflurane anesthesia, mice were implanted with cortical surface electrodes. Six positions were marked for electrode and screw placement- two positions above bregma on either side of the midline and four positions between lambda and bregma (two on either side of the midline). A microdrill was used to gently carve away an opening at each pre-marked position. Two screws were gently placed in the holes closest to lambda; these screws were used to anchor the prefabricated head mount. Surface electrodes attached to the head mount were gently threaded through the skull openings and secured with a small amount of cyanoacrylate. Electromyography (EMG) electrodes were placed in the muscle at the base of the skull. Following electrode placement, dental acrylic was used to seal and anchor the implant and the skin was sutured (sutures were later removed 10 to 14 days post-surgery). Ketoprofen was administered following surgery and once a day for 72 hours. Mice were returned to a singly housed holding cage that was maintained at a constant 39°C temperature during recovery with a Deltaphase isothermal pad (Braintree Scientific) placed under half of the cage. After

approximately 3 weeks of recovery, a continuous video-EEG recording was recorded for approximately 6 hours using Sirenia Acquisition software and data analyzed with Sirenia Seizure Basic software (Pinnacle Technology). Mice were returned to animal housing (singly housed) when not performing EEG analysis and euthanized within 2 months after initial EEG surgery.

Drug-induced Seizure Susceptibility

Flurothyl-induced seizures were performed by Alison Miller in the lab of Dr. Jennifer Kearney, comparing the seizure thresholds of adult non-edited [Kv1.1(I)] mice, edited [Kv1.1(V)] mice, and their wild-type littermates. Mice were individually placed in a clear plexiglass container and exposed to the volatile convulsant flurothyl (2,2,2-trifluroethyl ether) (Sigma-Aldrich), which was introduced via a syringe pump at a rate of 20 μL/min and allowed to volatize from a suspended platform. Latency to tonic-clonic seizure onset was measured as the seizure threshold.

Pentylenetetrazole (PTZ)-induced seizures were performed to compare the seizure threshold scores of the following genotypes using adult mice (mixed sex): non-edited [Kv1.1(I)], edited [Kv1.1(V)], V408A/+, and V408A/+ wild-type littermates. PTZ (Sigma-Aldrich) was dissolved in sterile saline (0.9% NaCl) and administered intraperitoneally at a volume of 0.1 mL/10 g mouse's body weight (De Sarro et al., 2004). Several doses were prepared by serial dilution to create a dose response curve based on previously determined seizure threshold data for

C57BL/6J mice in the literature: 0 mg/kg, 30 mg/kg, 60 mg/kg, 90 mg/kg, and 120 mg/kg (mg/kg= mg PTZ administered per kg of mouse's body weight) (De Sarro et al., 2004; Ferraro et al., 1999; Itoh and Watanabe, 2009). Mice were observed in isolated cages and video-monitored for 30 min, and scored for latency to hindlimb extension and for seizure severity using a modified Racine scale detailed in Table 2.1 (Racine 1972). Scoring of all exhibited behaviors was monitored and recorded on scoring sheets by two investigators during the experiment; following conclusion of the experiment, videos were reviewed by one investigator to ensure consistent scoring.

Table 2.1: Seizure threshold scale for scoring PTZ-induced seizures

stage	description
0	normal movement
1	hypoactivity with possible isolated small myoclonic jerks
2	recurrent partial clonus
3	generalized clonus without falling
4	generalized clonus with falling
5	tonic hindlimb extension

4-aminopyridine (4-AP)-induced seizures were assessed in two replicate trials. In the original 4-AP experiment, the seizure threshold scores of the following adult mice (mixed sex) were compared: non-edited [Kv1.1(I)], edited [Kv1.1(I)], V408A/+, and V408A/+ wild-type littermates. In the replicate 4-AP experiment the following adult mice (mixed sex) were compared: non-edited [Kv1.1(I)], edited [Kv1.1(I)], and the wild-type littermates of each. 4-AP (Sigma-

Aldrich) was dissolved in sterile saline (0.9% NaCl), the pH adjusted to 7 with HCl, and administered subcutaneously at a volume of 0.1 mL/10 g mouse's body weight (De Sarro et al., 2004). Several doses were prepared by serial dilution to create a dose response curve based on previously determined seizure threshold data for C57BL/6J mice in the literature: 0 mg/kg, 2 mg/kg, 6 mg/kg, 10 mg/kg, and 14 mg/kg (mg/kg= mg 4-AP administered per kg of mouse's body weight) (Chung et al., 2009; De Sarro et al., 2004; Dhir et al., 2011; Kim et al., 2001). Mice were observed in isolated cages and video-monitored for 1 hour and scored for latency to hindlimb extension and for seizure severity using a modified Racine scale detailed in Table 2.2 (Racine 1972). Scoring of all exhibited behaviors was monitored and recorded on scoring sheets by two investigators during the original experiment and 3 during the replicate experiment, however following the conclusion of the experiment videos were reviewed by one investigator to ensure consistent scoring. Additional precautions were taken in the replicate 4-AP experiment, where all investigators were blinded toward mouse genotype during the scoring and the final review of all the scores was performed by an investigator who was not part of the original test and who was unfamiliar with the original results.

Table 2.2: Seizure threshold scale for scoring 4-AP-induced seizures

stage	description
0	normal movement
1	hypoactivity with possible isolated small myoclonic jerks
2	recurrent partial clonus
3	episodes of generalized clonus without loss of righting ability
4	continuous generalized clonus with or without loss of righting ability and/or motoric control
5	tonic hindlimb extension

Hippocampal Slice Electrophysiology

We collaborated with Dr. Sam Centanni in the laboratory of Dr. Danny Winder to perform electrophysiological recordings of dentate granule cells in hippocampal slices of non-edited [Kv1.1(I)] mice and their wild-type littermates. Recordings were performed on mice which had either been unstressed or had been subjected to 30 minutes of conical tube restraint prior to brain isolation. Acute, 300 μm slices were obtained containing the hippocampus and recordings performed solely from dentate gyrus granule cells. The recordings were conducted using a potassium gluconate internal solution. All recordings were conducted in a current clamp configuration where the cell was injected with the necessary current required to keep the cell held at -70 mV. To analyze firing characteristics and intrinsic properties, current steps were applied for 1 second and increased in 25 pA increments (starting with -150 pA and going up to +350 pA).

Statistical analysis

Statistical tests were performed using Graphpad Prism (Graphpad Software). In experiments that have a single independent variable (genotype), one-way ANOVA was performed with Tukey's multiple comparisons test to determine genotype comparisons (grip strength, pole climb, and flurothyl-induced seizures). When two independent variables were present (genotype and type of brain region; genotype and stress), 2-way ANOVA was performed with Tukey's or Sidak's multiple comparisons test (type of multiple comparisons test was chosen based on recommendations by the Prism software) (qRT-PCR, gait analysis, inverted screen, open field, PTZ and 4-AP-induced seizures, and dentate granule cell electrophysiology). Rotarod data, which involved two independent variables (genotype and trial day), were analyzed by 2-way repeated measures ANOVA with Tukey's multiple comparisons test of the main effects, to determine genotype differences regardless of trial day. Deviations from normal Mendelian inheritance patterns were determined by $\chi 2$ analysis. Statistical significance was defined as $p \leq 0.05$.

Results

Characterization of Kv1.1 editing in wild-type mouse tissues

Previous studies have characterized the levels of Kv1.1 editing in human nervous and peripheral tissues, but only a few mouse and rat tissues were examined (Decher et al., 2010; Hoopengardner et al., 2003; Li et al., 2009). We confirmed and extended these previous characterizations, demonstrating that Kv1.1 RNA editing occurs most substantially in the nervous system and that distinct RNA editing profiles are observed when comparing different brain regions (Figure 2.3).

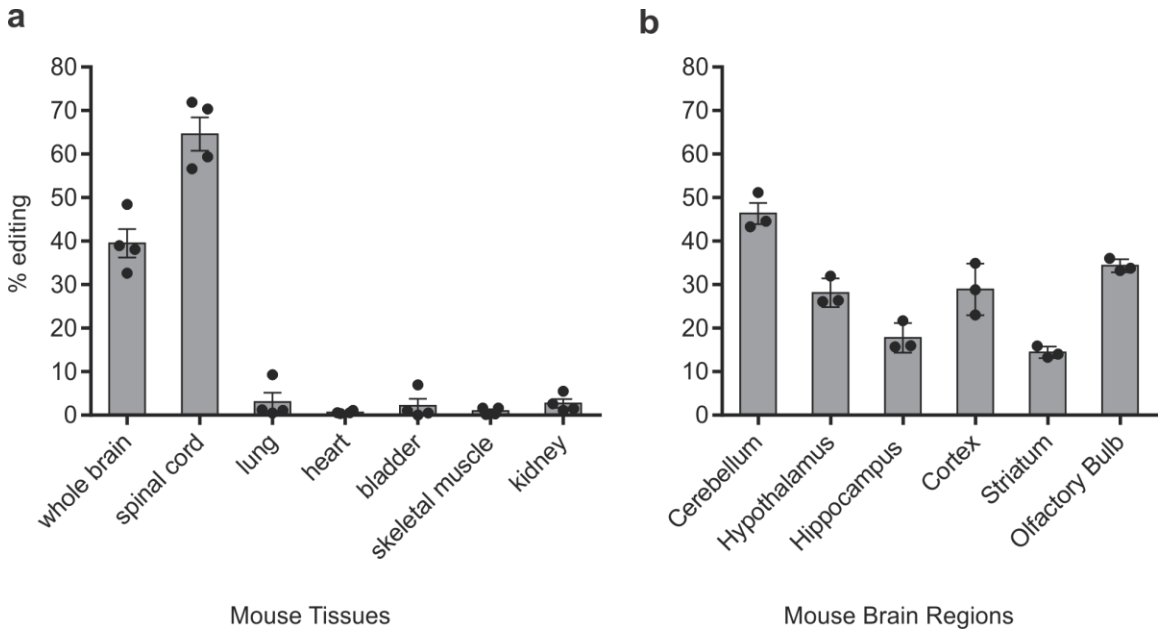

Figure 2.3. Quantitative analysis of Kv1.1 RNA editing (I/V site) in mouse. The extent of editing for Kv1.1 transcripts isolated from **(a)** mouse tissues or **(b)** dissected brain regions in adult animals was determined by high-throughput sequence analysis as described previously (Hood et al., 2014); data represent the analysis of 4 and 3 individual animals for tissue and brain regions, respectively (mean ± SEM).

Verification of non-edited [Kv1.1(I)] and edited [Kv1.1(V)] mutant mouse models

Although the function of the non-edited [Kv1.1(I)] and edited [Kv1.1(V)] isoforms of Kv1.1 have been studied in heterologous expression systems, no studies have been performed to examine the physiological significance of these editing-dependent changes *in vivo*. To address this issue, in collaboration with Dr. Robert Reenan, we have taken advantage of homologous recombination in C57BL/6J embryonic stem cells to generate genetically-modified mice that solely

expressed either the non-edited [Kv1.1(I)] or edited [Kv1.1(V)] subunit isoforms (Figures 2.1 and 2.2).

To confirm that mutant mice bearing modified Kv1.1 alleles expressed transcripts solely encoding the non-edited [Kv1.1(I)] or edited [Kv1.1(V)] isoform of the channel, cDNA was generated by RT-PCR amplification of cerebellar RNA and the resulting amplicons were sequenced directly. Sequences from wild-type animals exhibited overlapping adenosine/guanosine peaks in electropherogram traces resulting from a mixture of non-edited and edited Kv1.1 transcripts, as inosine base pairs similarly to guanosine during reverse transcription. As expected, sequences obtained from mutant animals showed only an adenosine or guanosine moiety, for the non-edited and edited transcripts, respectively (Figure 2.4).

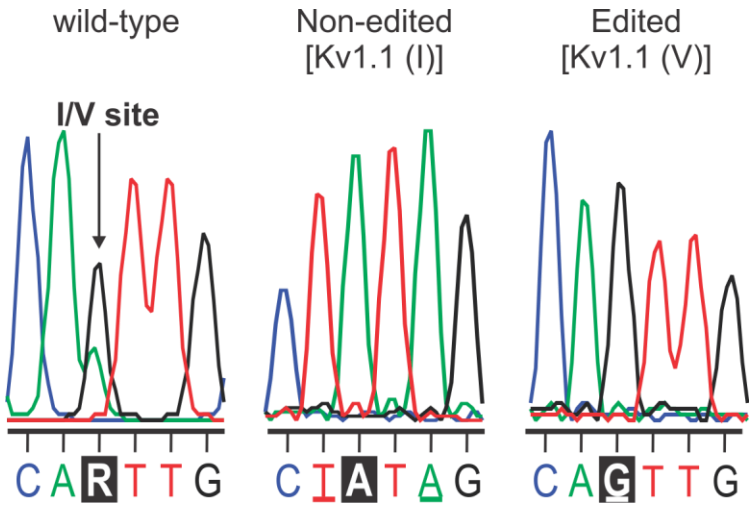

Figure 2.4. Confirmation of Kv1.1 isoform identity in mutant mice. Sequence analysis of Kv1.1 RNA isoforms in mutant mice. RNA was isolated from cerebella dissected from wild-type, non-edited [Kv1.1(I)], and edited [Kv1.1(V)] adult mice. A region spanning the editing site was amplified by RT-PCR and the amplicons were analyzed by Sanger sequencing. Electropherogram traces are shown with the editing site indicated in inverse lettering; mutant nucleotides introduced to produce the non-edited and edited isoforms are underlined.

Although the results in Figure 2.4 indicated that the expected Kv1.1 isoforms are being expressed in both mouse models, Sanger sequencing is qualitative by nature. To generate the edited [Kv1.1(V)] mouse model, the *Kcna1* gene was genomically altered at the editing site to a guanosine; this target cannot be altered by the adenosine-specific ADAR2 enzyme, and thus needed no further validation. In contrast, the non-edited [Kv1.1(I)] mouse model was generated by incorporating mutations around the editing site, relying on these synonymous mutations to sufficiently disrupt the Kv1.1 RNA duplex structure to prevent ADAR2 from recognizing and editing the RNA. As Sanger sequencing may not be sufficiently sensitive to determine whether low levels of editing may

have been occurring in the non-edited [Kv1.1(I)] mutant animals, we further examined Kv1.1 RNA expression using a high-throughput sequence strategy previously developed in our laboratory (Hood et al., 2014). We quantified RNA editing levels in the spinal cord, which contains one of the highest RNA editing levels, and thus would be the most likely of our tissue targets to display aberrant editing. Three mouse spinal cord samples were analyzed where isolated RNA was subjected to RT-PCR amplification and the resulting amplicons were sequenced by high-throughput sequence analysis (Hood et al., 2014). The mean RNA editing detected in the non-edited [Kv1.1(I)] spinal cord samples was 0.045 ± 0.0046 %, which corresponded to approximately 28 out of an average 60879 total reads.

After confirming that our mouse models solely expressed their intended RNA isoform, we sought to determine whether the isoform identity affected the steady-state RNA expression level encoding the Kv1.1 channel. We performed qRT-PCR to determine the relative expression of Kv1.1 RNA in six brain regions from non-edited [Kv1.1(I)], edited [Kv1.1(V)] and wild-type mice (Figure 2.5). Results from this analysis revealed no differences in steady-state Kv1.1 RNA expression between the non-edited [Kv1.1(I)], edited [Kv1.1(V)], and wild-type animals for all brain regions examined.

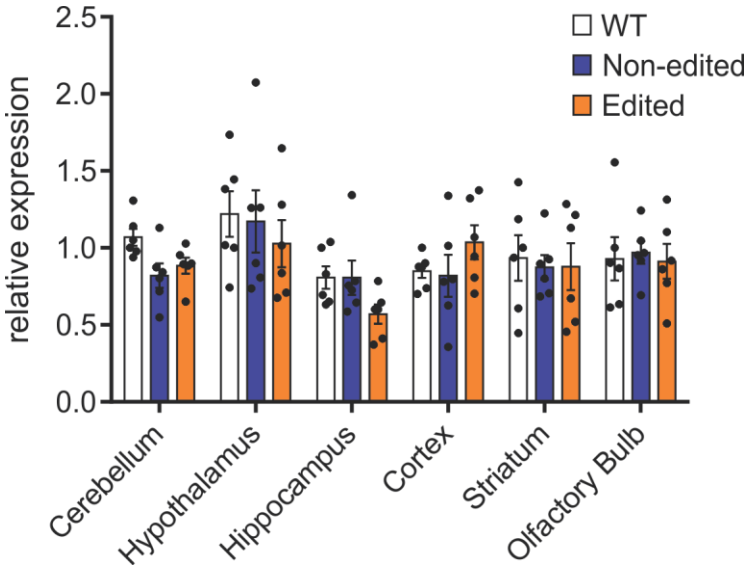

Figure 2.5. Steady-state Kv1.1 RNA expression is unchanged in non-edited [Kv1.1(I)] and edited [Kv1.1(V)] mutant mice compared to wild-type mice. Steady-state RNA expression was quantified by qRT-PCR. No genotype was significantly different from another in any brain region analyzed by 2-way ANOVA with Tukey's multiple comparisons test (mean ± SEM, n=6).

Mendelian distribution of progeny

The non-edited [Kv1.1(I)] and edited [Kv1.1(V)] mice were generated from heterozygous crosses of each mouse line to determine whether the ratio of offspring followed the expected Mendelian inheritance pattern of 1:2:1 for wild-type, heterozygous mutant and homozygous mutant animals, respectively (Tables 2.3 and 2.4). Interestingly, we discovered that the inheritance pattern varied based upon the animal facility in which the mice were being housed. In the original breeding location (MCNII animal facility), we observed a significantly diminished number of non-edited [Kv1.1(I)] and edited [Kv1.1(V)] homozygous mutant animals genotyped at the time of weaning (P21). By contrast, when

embryos from the original breeding location were genotyped at E18.5, immediately prior to birth, homozygous mutants from each mutant line did not differ from the expected Mendelian inheritance pattern. These results indicated that both strains demonstrate an incompletely penetrant postnatal lethality. However, when the mouse colony was moved to a new floor in the same facility, both mouse lines no longer exhibited the lethality observed for homozygous mutants. While undefined environmental factors such as background noise or access to the room by multiple investigators could produce stressors that affect the survival of mutant Kv1.1 homozygotes, we rederived both mouse lines into the pathogen-free barrier facility. Surprisingly, both lines regained the incompletely penetrant postnatal lethality. We observed fewer homozygous mutants at P21 in the original MCNII and Barrier facilities, yet genotype analyses of mice that died between P0 and P21 did not identify an overrepresentation of homozygous mutants which could be explained by the small sample size of mouse bodies that were found.

Non-edited: Kv1.1(I)/+ x Kv1.1(I)/+

genotype	E18.5 Original Obs (Exp)	P21 Original Obs (Exp)	P21 Barrier Obs (Exp)
Wild-type +/+	13 (12.25)	19 (17.75)	43 (34)
Heterozygous Kv1.1(I)/+	28 (24.5)	49 (35.5)	75 (68)
Homozygous Kv1.1(I)/Kv1.1(I)	8 (12.25)	3 (17.75)	18 (34)
total	49	71	136
p-value	p≤0.3641	p≤0.0002	p≤0.0049

Table 2.3. Conditional non-Mendelian distribution of non-edited [Kv1.1(I)] mutant offspring. Upon breeding heterozygous non-edited [Kv1.1 (I)] mice (Kv1.1(I)/+), either in the original facility or the barrier facility, offspring were genotyped at either E18.5 or by P21. Observed (Obs) progeny versus the expected (Exp) progeny were compared by $\chi 2$ analysis to determine significance.

Edited: Kv1.1(V)/+ x Kv1.1(V)/+

genotype	E18.5 Original Obs (Exp)	P21 Original Obs (Exp)	P21 Barrier Obs (Exp)
Wild-type +/+	12 (14.75)	46 (29)	55 (37.25)
Heterozygous Kv1.1(V)/+	34 (29.5)	60 (58)	67 (74.5)
Homozygous Kv1.1(V)/Kv1.1(V)	13 (14.75)	10 (29)	27 (37.25)
total	59	116	149
p-value	p≤0.4949	p≤0.0001	p≤0.0024

Table 2.4. Conditional non-Mendelian distribution of edited [Kv1.1(V)] mutant offspring. Upon breeding heterozygous edited [Kv1.1 (V)] mice (Kv1.1(V)/+), either in the original facility or the barrier facility, offspring were genotyped at either E18.5 or by P21. Observed (Obs) progeny versus the expected (Exp) progeny were compared by $\chi 2$ analysis to determine significance.

Behavioral characterization

We have used a variety of tasks to distinguish behavioral differences between the non-edited [Kv1.1(I)] and edited [Kv1.1(V)] mutant mouse models compared to their wild-type littermates (Brooks and Dunnett, 2009). Initial behavioral tasks showed that these mutant animals did not have deficits in grip strength, but that the edited [Kv1.1(V)] mice displayed enhanced motor coordination on the pole climb task (Figure 2.6). The locomotor coordination of the non-edited [Kv1.1(I)] and edited [Kv1.1(V)] mice was tested using the accelerating rotarod behavioral task, first using the traditional paradigm: three trials/day for three days (Figure 2.7). In preliminary studies, we compared non-edited [Kv1.1(I)] and edited [Kv1.1(V)] mutants to the performance of wild-type littermates, as well as their heterozygous mutant littermates [Kv1.1(I)/+ and Kv1.1(V)/+]. There were no significant differences between either type of mutant mice compared to the wild-type littermates or their respective heterozygous mutant mice (Figure 2.7). This lack of any impairment phenotype under normal conditions was similar to the EA1 mouse model (V408A/+), which only displays locomotor deficits under stressed conditions. All further behavioral tests were performed under control conditions (unstressed) as well as in response to a well characterized stressor involving 30 minutes of conical tube restraint immediately prior to the tests (Buynitsky and Mostofsky, 2009).

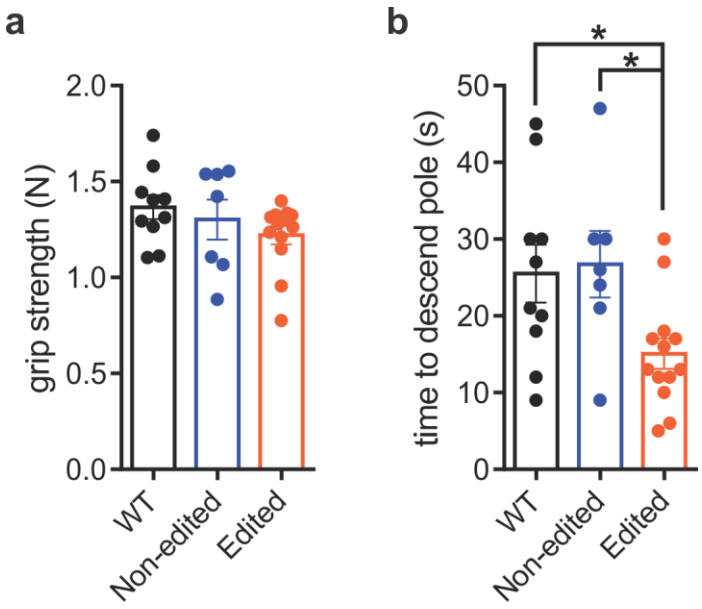

Figure 2.6. Initial behavioral analysis of non-edited [Kv1.1(I)] and edited [Kv1.1(V)] mice. Adult non-edited [Kv1.1(I)], edited [Kv1.1(V0], and wild-type littermate male mice were subjected to the **(a)** grip strength and **(b)** pole climb behavioral tests. No significant differences were found in the grip strength test, but the edited [Kv1.1(V)] mice were significantly faster to descend on the pole climb test compared to wild-type and non-edited [Kv1.1(I)] mice (mean ± SEM, n=7-13, *p<0.05, 1-way ANOVA with Tukey's multiple comparisons test).

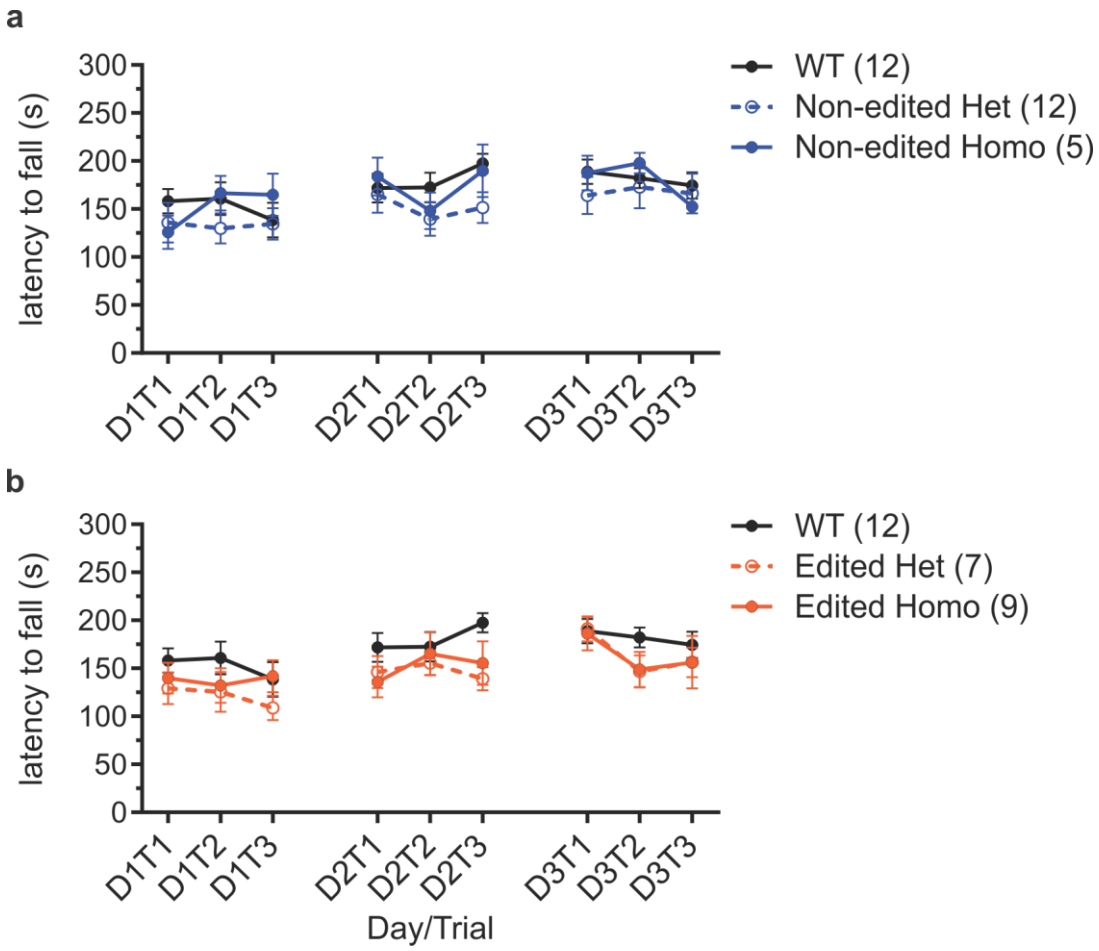

Figure 2.7. Non-edited [Kv1.1(I)] and edited [Kv1.1(V)] heterozygous and homozygous mutant mice do not display locomotor dysfunction under the unstressed traditional rotarod paradigm. Adult non-edited [Kv1.1(I)], edited [Kv1.1(V)], and wild-type littermate male mice were subjected to the traditional rotarod paradigm (3 rotarod trials per day over 3 days). Day and trial numbers are deliniated as D and T, respectively. **(a)** Non-edited homozygous [Kv1.1(I)/Kv1.1(I)] and non-edited heterozygous [Kv1.1(I)/+] mice were compared to wild-type mice and **(b)** Edited homozygous [Kv1.1(V)/Kv1.1(V)] and edited heterozygous [Kv1.1(V)/+] mice were compared to wild-type mice (mean ± SEM, n=5-12, indicated in parentheses in the legend). No significant differences were observed between genotypes (2-way ANOVA with Tukey's multiple comparisons of the main effects).

To incorporate a stressor paradigm in conjunction with the rotarod test, a modified rotarod paradigm was developed where mice were run on the rotarod one trial per day for nine days, with or without 30 minutes of conical tube restraint, immediately preceding the rotarod test. This modified rotarod paradigm was replicated in three unstressed replicate trials (Figure 2.8) and two stressed replicate trials (Figure 2.9). In the absence of a stressor, no differences were observed between the mutant and wild-type mouse lines, whereas, following 30 minutes of conical tube restraint, the non-edited [Kv1.1(I)] mice consistently underperformed compared to both the wild-type and the edited [Kv1.1(V)] mice. These studies were replicated and continued to show that homozygous mice solely expressing non-edited [Kv1.1(I)] underperformed compared to the wild-type and edited [Kv1.1(V)] lines.

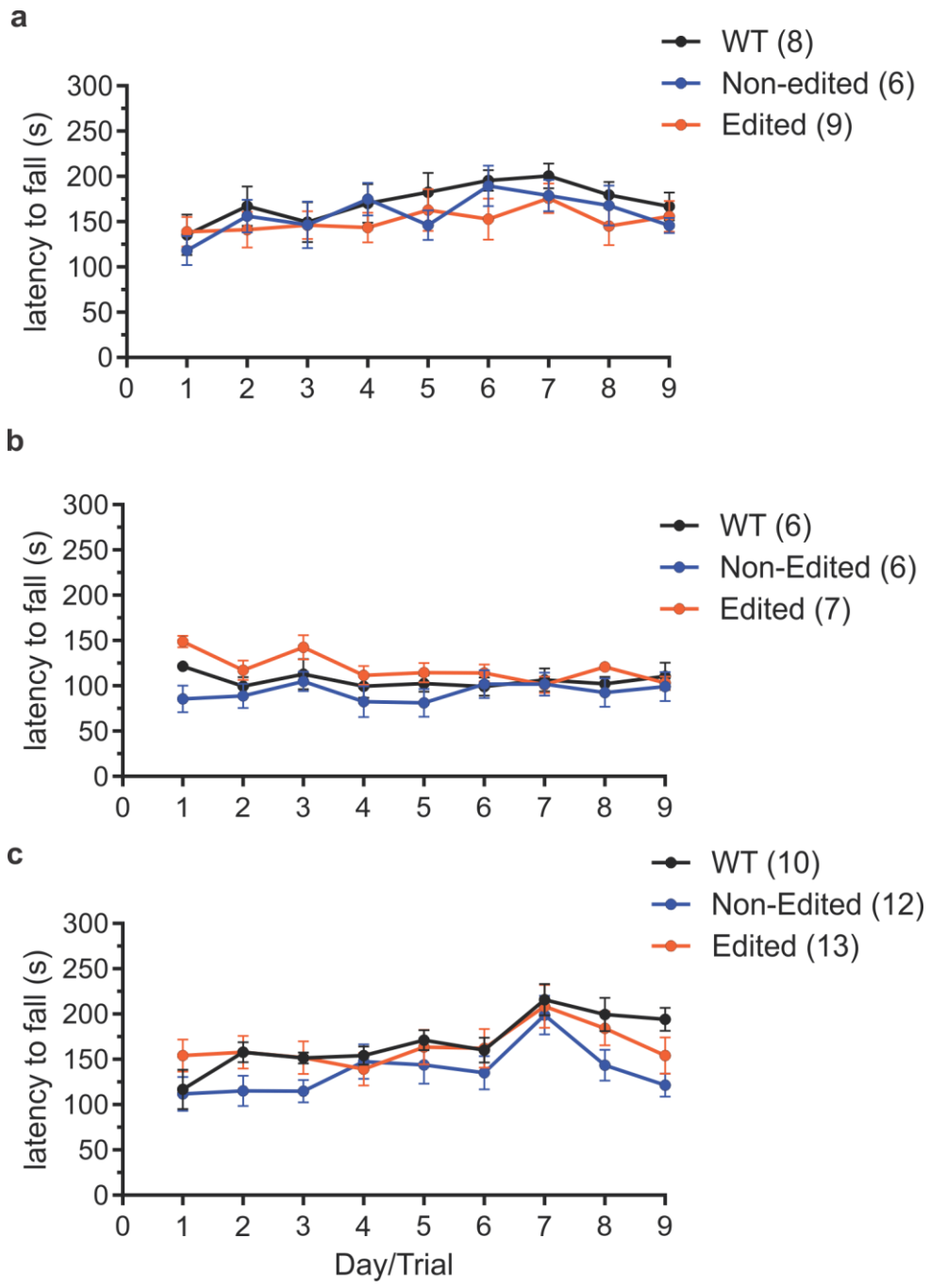

Figure 2.8. Non-edited [Kv1.1(I)] and edited [Kv1.1(I)] mutant mice do not display locomotor dysfunction under the unstressed modified rotarod paradigm. Adult non-edited [Kv1.1(I)], edited [Kv1.1(V)], and wild-type littermate male mice were subjected to the modified rotarod paradigm (1 rotarod trial per day over 9 days). **(a)** Unstressed trials I, **(b)** II, and **(c)** III were performed by three separate cohorts of mice (mean ± SEM, n=6-13, indicated in parentheses

in the legend). No significant differences were observed between non-edited [Kv1.1(I)], edited [Kv1.1(V)], or wild-type genotypes (2-way repeated measures ANOVA with Tukey's multiple comparisons of the main effects).

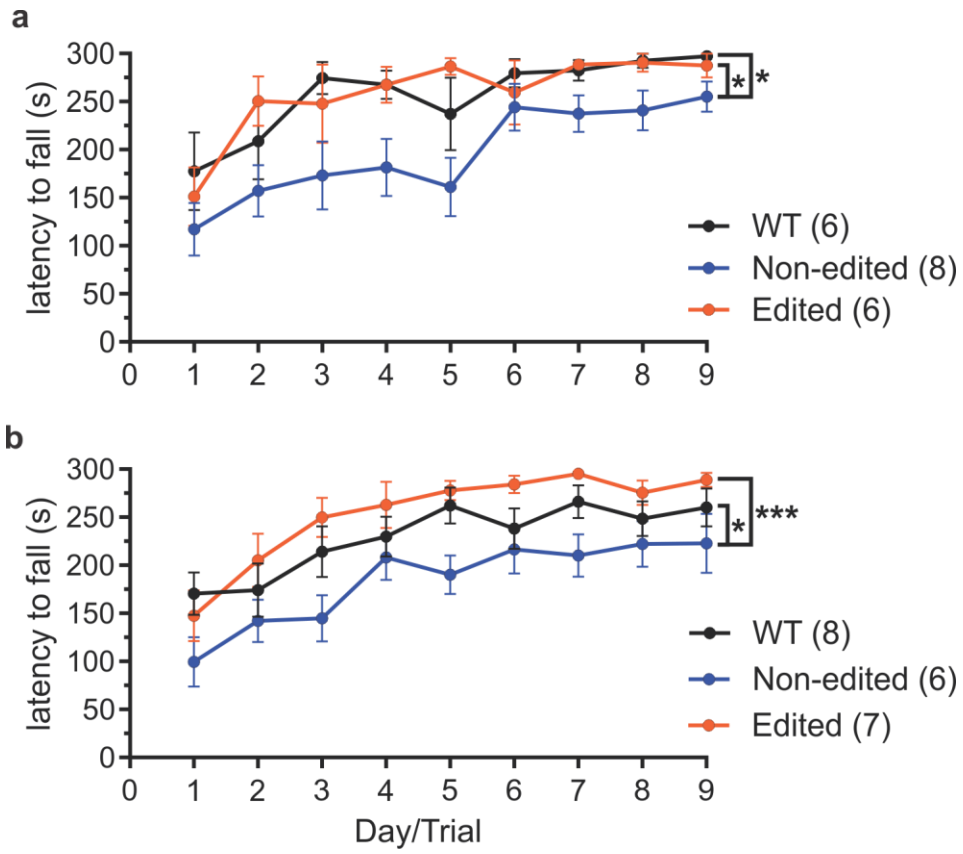

Figure 2.9. Non-edited [Kv1.1(I)] mutant mice display stress-induced locomotor dysfunction under the stressed modified rotarod paradigm. Adult non-edited [Kv1.1(I)], edited [Kv1.1(V)], and wild-type littermate male mice were subjected to a stressor (30 minutes of conical tube restraint) followed by the modified rotarod paradigm (1 rotarod trial per day over 9 days). **(a)** Stressed trials I, **(b)** II were performed by two separate cohorts of mice (mean ± SEM, n=6-8, indicated in parentheses in the legend). Significant differences were observed between the non-edited [Kv1.1(I)] mice and the edited [Kv1.1(V)] and wild-type genotypes (*p<0.05, ***p<0.001, 2-way repeated measures ANOVA with Tukey's multiple comparisons of the main effects).

To determine the underlying factors responsible for alterations in the rotarod task in response to stress, additional behavioral studies were employed to examine alterations in gait directly, similar to the deficits observed in EA1 patients. Alterations in gait were assessed using the footprint test, under unstressed or stressed conditions (30 min of conical tube restraint prior the task), and each condition was replicated twice using the same cohort of mice (Figure 2.10). No differences were seen between the replicate trials of either the unstressed or the stressed paradigm. In addition, no differences were found comparing the genotypes by the forelimb stride length and front base parameters. The hindlimb stride length, hind base, and right overlap parameters contained significant differences in one unstressed or stressed trial, but not both trials, suggesting that these differences were not replicable in our preliminary studies. In both stressed trials of the left overlap parameter, however, the non-edited [Kv1.1(I)] mice had a significantly smaller left overlap parameter as compared to wild-type littermates.

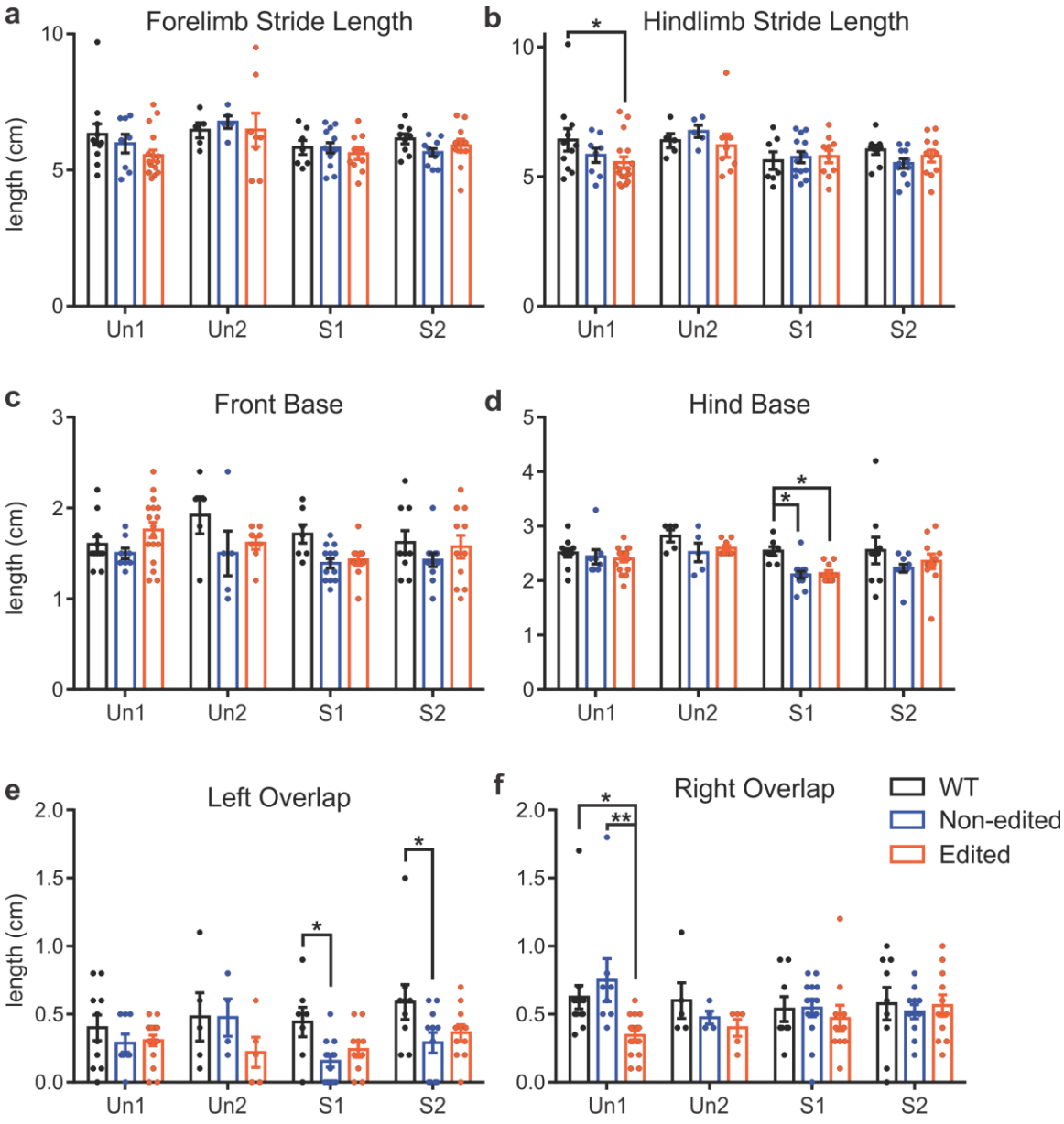

Figure 2.10. Non-edited [Kv1.1(I)] mice display reproducible stress-induced gait alterations. Adult non-edited [Kv1.1(I)], edited [Kv1.1(V)], and wild-type littermate male mice were subjected to either an unstressed or stressed paradigm (30 minutes of conical tube restraint) followed by footprinting gait analyses. Two trials were performed on the same cohort of mice (Un1=Unstressed trial 1, Un2=Unstressed trial 2, S1=Stressed trial 1, S2=Stressed trial 2). Several metrics were determined: **(a)** Forelimb Stride Length, **(b)** Hindlimb Stride Length, **(c)** Front Base, **(d)** Hind Base, **(e)** Left Overlap, and **(f)** Right Overlap. Several significant differences were observed (mean ± SEM, n=5-17, *p<0.05, **p<0.01, 2-way ANOVA with Tukey's multiple

comparisons test, comparing genotypes within each trial). Replicate trials were not different from each other by 2-way ANOVA wtih Sidak's multiple comparisons test.

Stressed effects to grip strength were determined by performing the inverted screen task, under the unstressed and stressed conditions (30 min of conical tube restraint prior the task) (Figure 2.11). Both the unstressed and stressed paradigms were replicated three times each. No significant differences were seen for the non-edited [Kv1.1(I)], edited [Kv1.1(V)], or the wild-type littermates, when comparing genotypes within the same trial.

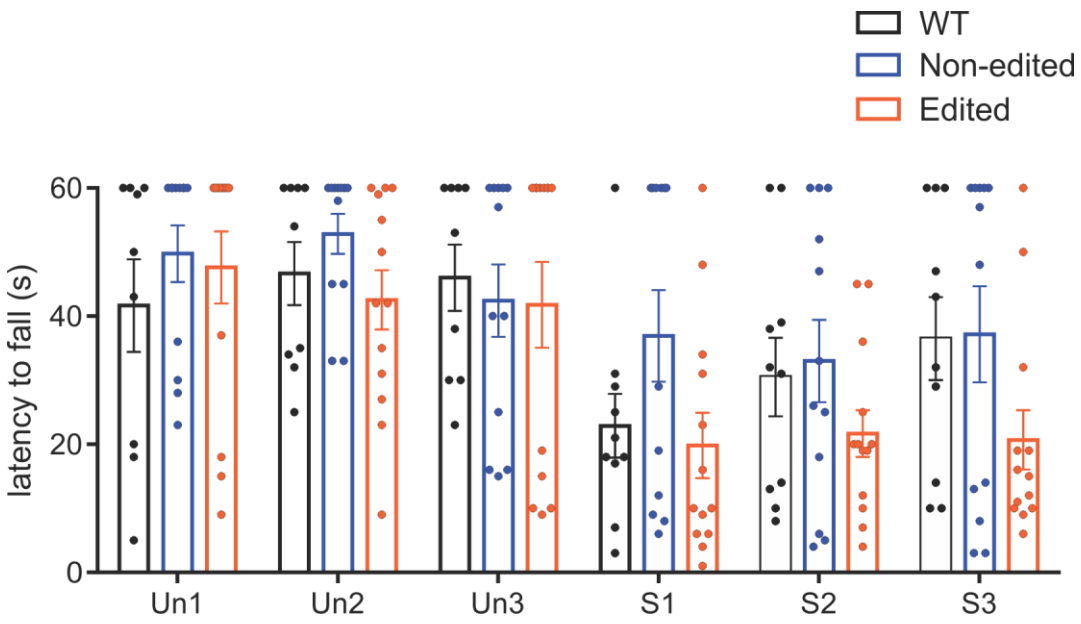

Figure 2.11. Non-edited [Kv1.1(I)] and edited [Kv1.1(V)] mice do not display stress-induced alterations by the inverted screen test. Adult non-edited [Kv1.1(I)], edited [Kv1.1(V)], and wild-type littermate male mice were subjected to either an unstressed or stressed paradigm (30 minutes of conical tube restraint) followed by the inverted screen test for a maximum of 60 s. Three trials were performed for the unstressed and stressed paradigms (Un1=Unstressed trial 1, Un2=Unstressed trial 2, Un3=Unstressed trial 3, S1=Stressed trial 1, S2=Stressed trial 2, S3=Stressed trial 3). No significant differences were observed between the genotypes within the same trial (mean ± SEM, n=9-13, 2-way ANOVA with Tukey's multiple comparisons test).

Finally, locomotion and anxiety were tested using an open field behavioral test under both unstressed and stressed conditions. Mice were observed for 30 min during the task and many parameters were observed (Figure 2.12). Although, many parameters were altered by stress when comparing each individual genotype (such as distance traveled, velocity, center time, center entries, and grooming time), differences between genotypes were rare. The only identified difference observed between genotypes was a decrease in thigmotaxis for non-edited [Kv1.1(I)] animals compared to wild-type mice.

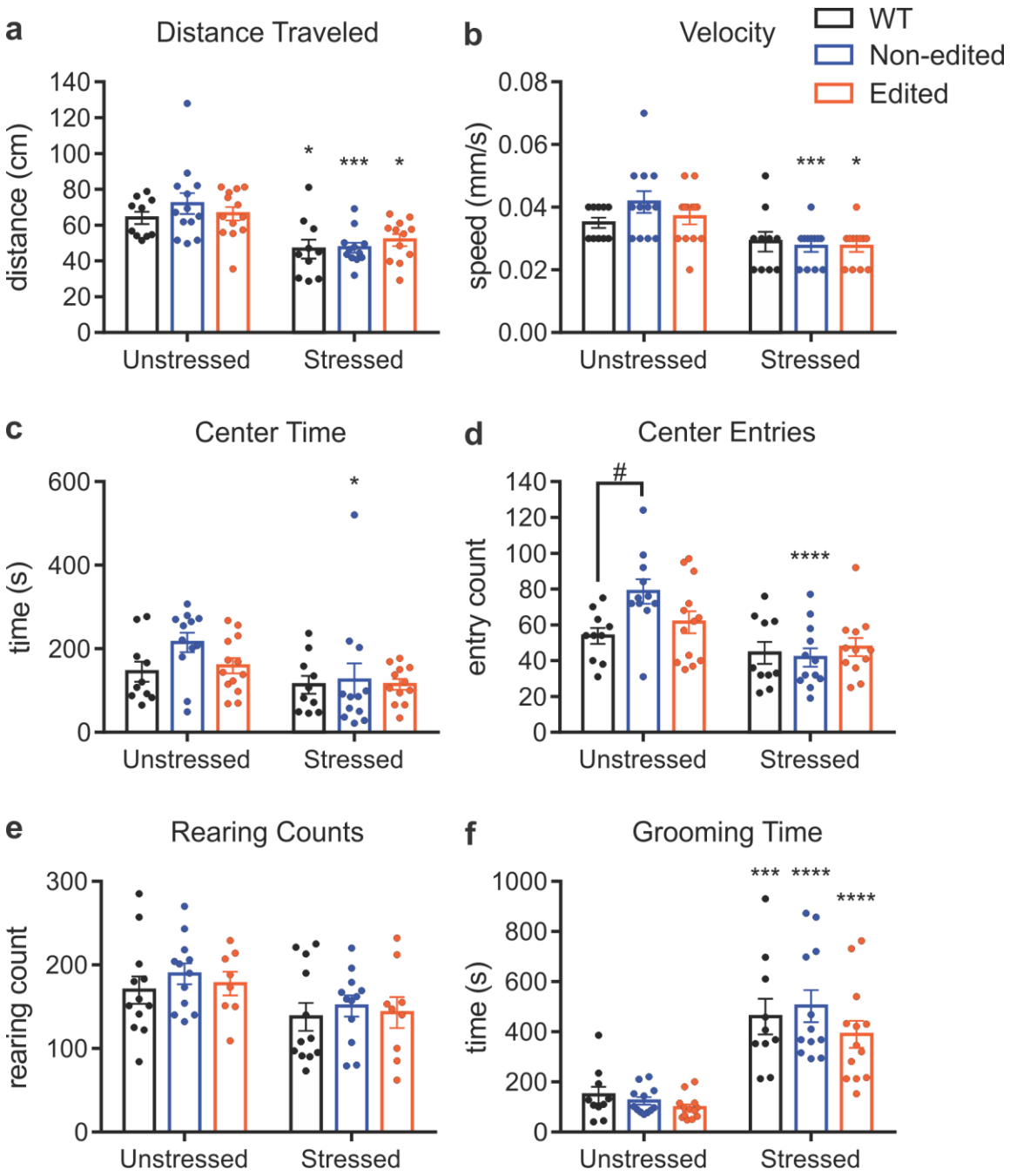

Figure 2.12. Open-field analysis of non-edited [Kv1.1(I)] and edited [Kv1.1(V)] mice. Adult non-edited [Kv1.1(I)], edited [Kv1.1(V)], and wild-type littermate male mice were subjected to either an unstressed or stressed paradigm (30 minutes of conical tube restraint) followed by 30 min of open-field analysis. Several metrics were determined: **(a)** Distance Traveled, **(b)** Velocity, **(c)** Center Time, **(d)** Center Entries, **(e)** Rearing Counts, and **(f)** Grooming Time. Several significant differences were observed between the Unstressed and

Stressed trials of the same genotype (mean ± SEM, n=8-13; *p<0.05, ***p<0.001, ****p<0.0001, 2-way ANOVA with Sidak's multiple comparisons test). When comparing genotypes within each trial, only the non-edited [KV1.1(I)] center entries were different from WT in (d) (#p<0.05, 2-way ANOVA with Tukey's multiple comparisons test).

Spontaneous Seizure Monitoring

Although collaborative EEG recordings, performed by Alison Miller in Dr. Jennifer Kearney's lab, qualitatively suggested abnormal activity in the non-edited [Kv1.1(I)] mutants, this data was not conclusive due to a high background in the collected data. To decrease the background for our EEGs, we performed a pilot study comparing a non-edited [Kv1.1(I)] mouse to its wild-type littermate using surface cortical electrodes, instead of screws, to decrease any noise that could be interfering with the measurements. The non-edited [Kv1.1(I)] mouse did not display any epileptiform activity visible in the EEG traces during six hours of recording, but video analysis revealed two tonic events in the non-edited [Kv1.1(I)] animal during sleep.

Drug-induced Seizure Susceptibility

Drug-induced seizure susceptibility was investigated using three different convulsant drugs: flurothyl, PTZ, and 4-AP in homozygous Kv1.1 mutant lines and wild-type mice. No differences were seen for flurothyl-induced seizures, however genotype-specific differences were observed in response to PTZ and 4-AP (Figure 2.13).

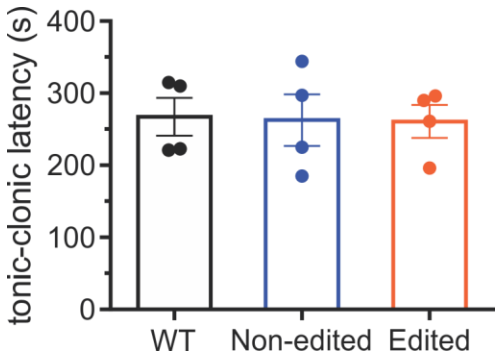

Figure 2.13. Flurothyl-induced seizures. Mice were individually exposed to the volatile convulsant flurothyl at a rate of 20uL/min. Latency to tonic-clonic seizure was measured. No genotypes were significantly different than another by 1-way ANOVA with Tukey's multiple comparisons test (mean ± SEM, n=4).

Upon administration of PTZ, the edited [Kv1.1(V)] mice displayed a damped seizure susceptibility, with significantly lower seizure scores at the 60 mg/kg PTZ dose than the wild-type and non-edited [Kv1.1(I)] animals (Figure 2.14). Additionally, no differences were found in seizure score when comparing male versus female mice of each genotype (Figure 2.15).No differences were found between genotypes when comparing the latency to hindlimb extension (HLE) (which corresponds to the maximal seizure score, which was not uniformly observed for all mice of any genotype) (Figure 2.16).

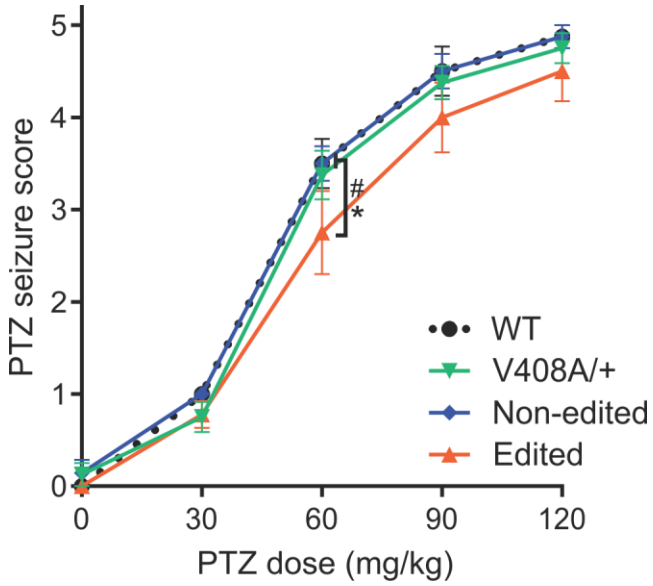

Figure 2.14. PTZ-induced seizure threshold scores. Mice were intraperitoneally administered increasing doses of PTZ, observed for 30 minutes, and scored for seizure severity on a scale from 0 to 5 (as described in the *Materials & Methods*). Non-edited [Kv1.1(I)], edited [Kv1.1(V)], and V408A/+ mice were compared to the wild-type littermates of the V408A/+ mice. Edited [Kv1.1 (V)] mice differed significantly from wild-type and non-edited [Kv1.1 (I)] animals at the 60mg/kg PTZ dose by 2-way ANOVA with Tukey's mulitple comparisons test (mean ± SEM, n=7-9 mice for each genotype per dose; Edited to WT: *$p<0.05$; Edited to Non-edited: #$p<0.05$).

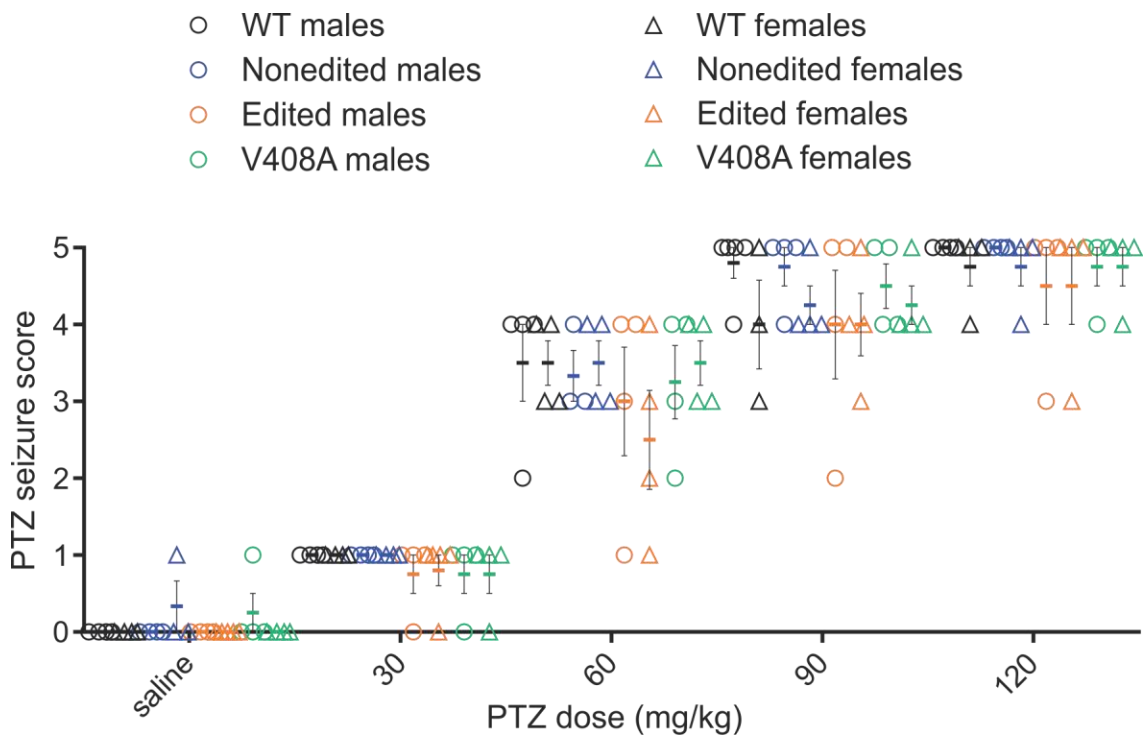

Figure 2.15. Male versus female comparison of PTZ-induced seizure threshold scores. Mice were intraperitoneally administered increasing doses of PTZ, observed for 30 minutes, and scored for seizure severity on a scale from 0 to 5 (as described in the Materials & Methods). Male non-edited [Kv1.1(I)], edited [Kv1.1(V)], V408A/+ mice, and the wild-type littermates of the V408A/+ mice were compared to their respective female counterparts within each dose. No comparisons were significant by 2-way ANOVA with Tukey's mulitple comparisons test (mean ± SEM, n=3-5 mice for each genotype per dose and per sex).

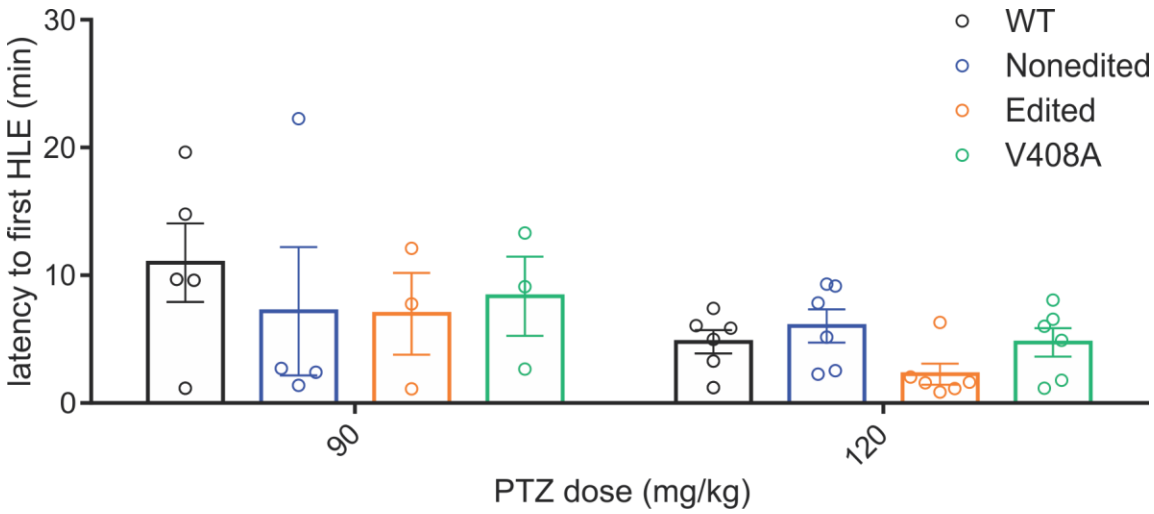

Figure 2.16. Latency to hindlimb extension following PTZ-induced seizures. Mice were subcutaneously administered increasing doses of 4-AP, observed for 1 hour, measuring the latency to first hindlimb extension (HLE), if it occurred. Non-edited [Kv1.1(I)], edited [Kv1.1(V)], and V408A/+ mice were compared to the wild-type littermates of the V408A/+ mice (mean ± SEM, n=7-9 mice for each genotype per dose; not every mouse reached HLE). No statistical comparisons were significant by 2-way ANOVA with Tukey's multiple comparisons test.

In the original 4-AP-induced seizure threshold test, the non-edited [Kv1.1(I)] mice displayed an increased seizure susceptibility, displaying higher scoring seizures at the 6mg/kg 4-AP dose, compared to all other genotypes (Figure 2.17a). Due to experimental limitations, the PTZ and original 4-AP seizure threshold tests used wild-type littermates from the V408A/+ mice as control animals. To ensure consistency however, the 4-AP seizure threshold test was replicated with the appropriate wild-type littermates for non-edited [Kv1.1(I)] and edited [Kv1.1(V)] mice (Figure 2.17b). In the replicate 4-AP analysis, the non-edited [Kv1.1(I)] mice demonstrated a significantly higher score at the 6 mg/kg 4-AP dose compared to wild-type animals, yet edited [Kv1.1(V)] mice

showed a significantly lower score. Furthermore, the edited [Kv1.1(V)] mice had a significantly dampened seizure susceptibility compared to the non-edited [Kv1.1(I)] mice at the higher (6 mg/kg and 10 mg/kg) 4-AP doses. Although male versus female differences were observed in both 4-AP trials, replicate tests did not agree on the type of sex differences, and likely were not biologically significant (Figure 2.18). The non-edited [Kv1.1(I)] mice, of both replicate trials, had a significantly shorter latency to HLE at the 10 mg/kg dose compared to all the other genotypes (Figure 2.19). In addition, many non-edited [Kv1.1(I)] mice exhibited HLE at the 6 mg/kg dose in both replicate trials (though not enough individuals of the other genotypes exhibited HLE for statistical analysis at this dose).

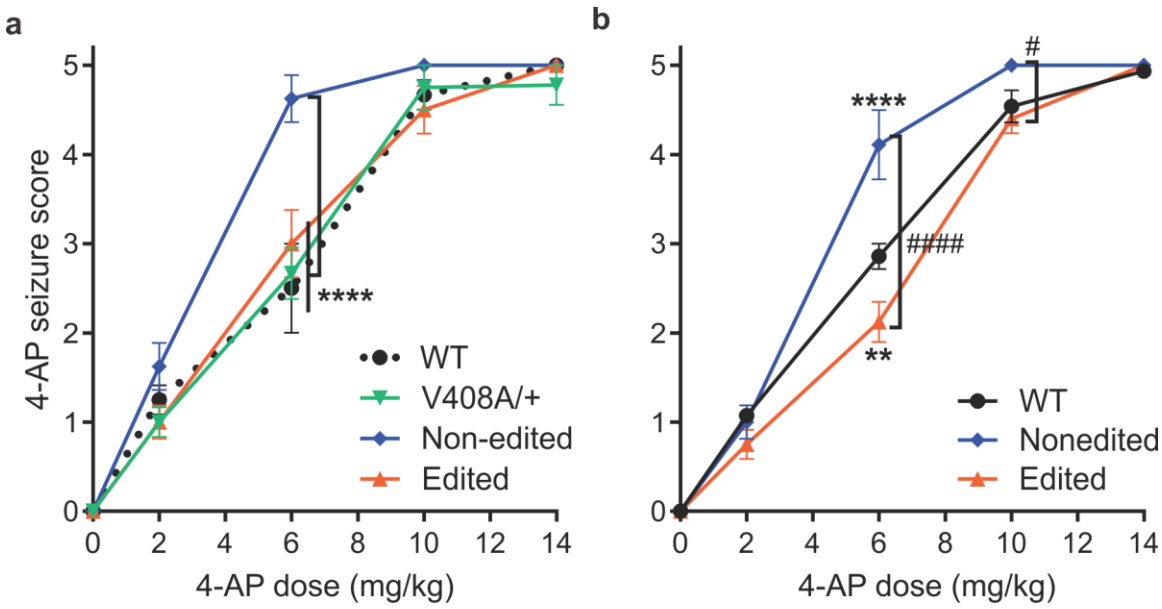

Figure 2.17. 4-AP-induced seizure threshold scores. Mice were subcutaneously administered increasing doses of 4-AP, observed for 1 hour, and scored for seizure severity on a scale from 0 to 5 (as described in the *Materials & Methods*). **(a,b)** Two trials were performed. **(a)** Non-edited [Kv1.1(I)], edited [Kv1.1(V)], and V408A/+ mice were compared to the wild-type littermates of the V408A/+ mice. Non-edited mice had a significantly higher score at the 6 mg/kg 4-AP dose compared to all other genotypes by 2-way ANOVA with Tukey's multiple comparisons test (mean ± SEM, n=7-10 mice for each genotype per dose; ****p<0.0001). **(b)** Non-edited [Kv1.1(I)] and edited [Kv1.1(V)] mice were compared to their wild-type littermates (mean ± SEM, n=8-16 mice for each genotype per dose). Non-edited mice and edited mice were significantly different than wild-type at the 6 mg/kg 4-AP dose by 2-way ANOVA with Tukey's multiple comparisons test (compared to WT: **p<0.01, ****p<0.0001). Non-edited and edited mice were significantly different than each other at the 6 mg/kg and 10 mg/kg 4-AP doses by 2-way ANOVA with Tukey's multiple comparisons test (#p<0.05, ####p<0.0001).

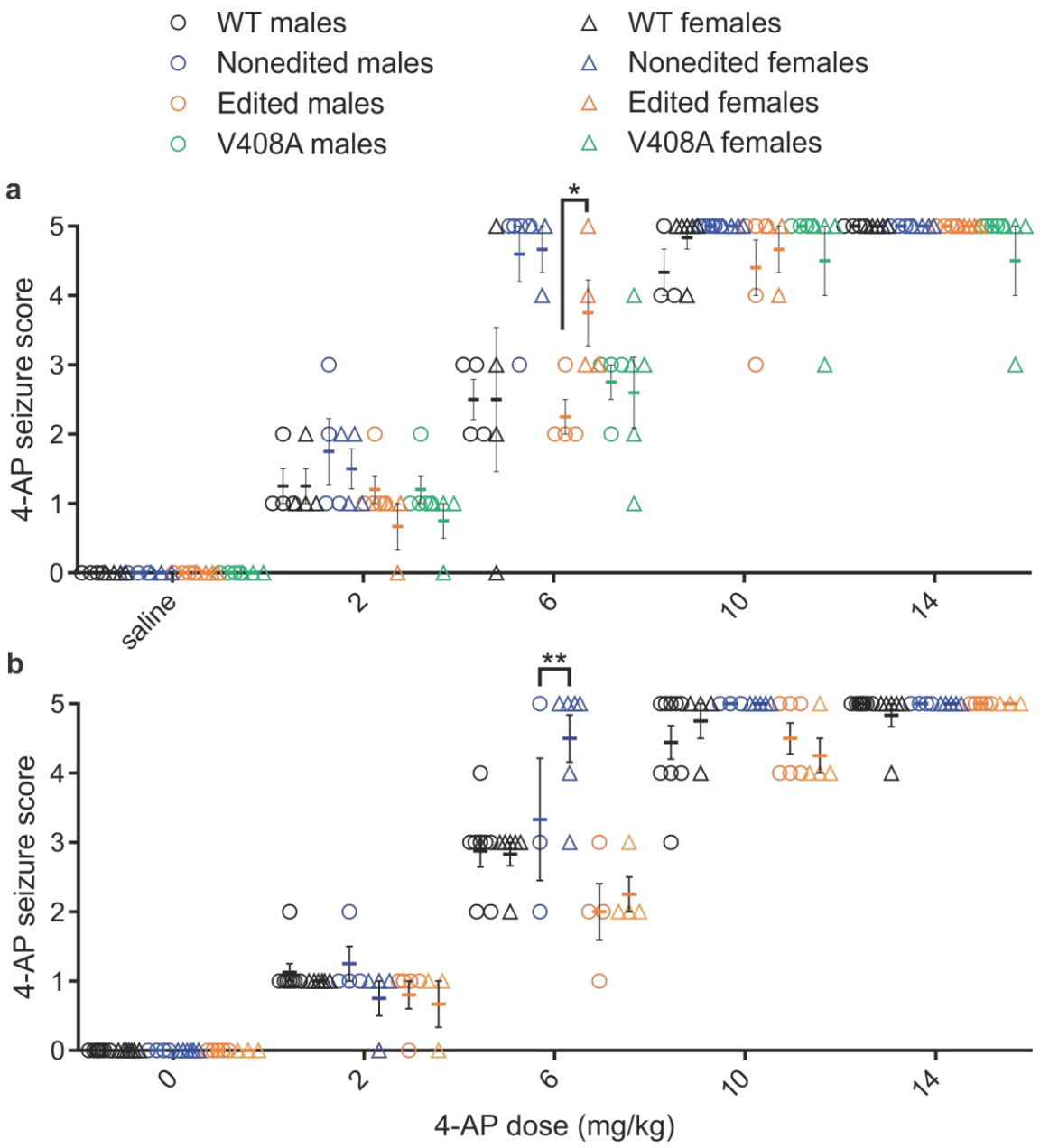

Figure 2.18. Male versus female comparison of 4-AP-induced seizure threshold scores. Mice were subcutaneously administered increasing doses of 4-AP, observed for 1 hour, and scored for seizure severity on a scale from 0 to 5 (as described in the Materials & Methods). (a,b) Two trials were performed. (a) Male non-edited [Kv1.1(I)], edited [Kv1.1(V)], V408A/+ mice, and the wild-type littermates of the V408A/+ mice were compared to their respective female counterparts within each dose. At the 6 mg/kg 4-AP dose, edited [Kv1.1(V)] male mice were significantly different than the respective female mice by 2-way ANOVA with Tukey's multiple comparisons test (mean ± SEM, n=3-6 mice for each genotype per dose and per sex; *p<0.05). (b) Male non-edited [Kv1.1(I)],

edited [Kv1.1(V)], and their wild-type littermate mice were compared to their respective female counterparts within each dose. At the 6 mg/kg 4-AP dose, non-edited [Kv1.1(I)] male mice were significantly different than the respective female mice by 2-way ANOVA with Tukey's multiple comparisons test (mean ± SEM, n=3-9 mice for each genotype per dose and per sex; **p<0.01).

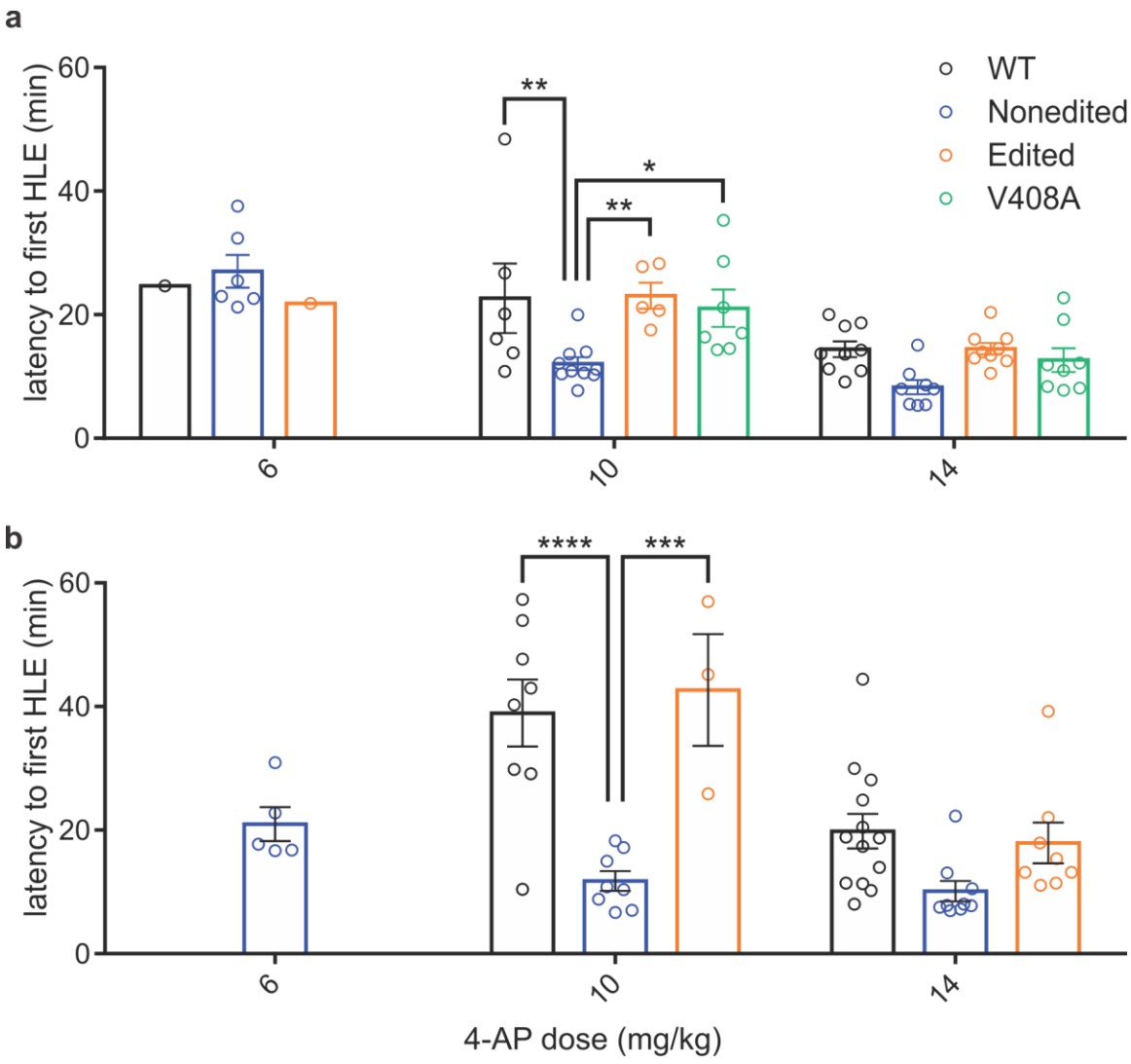

Figure 2.19. Latency to hindlimb extension following 4-AP-induced seizures. Mice were subcutaneously administered increasing doses of 4-AP, observed for 1 hour, measuring the latency to first hindlimb extension (HLE), if it occurred. (a,b) Two trials were performed. (a) Non-edited [Kv1.1(I)], edited [Kv1.1(V)], and V408A/+ mice were compared to the wild-type littermates of the V408A/+ mice (mean ± SEM, n=7-10 mice for each genotype per dose; not every mouse reached HLE). No statistical comparisons were possible at the 6 mg/kg 4-AP dose, because only the non-edited [Kv1.1(I)] mice had more than one individual mouse reaching HLE. Non-edited [Kv1.1(I)] mice had a significantly shorter latency to HLE at the 10 mg/kg 4-AP dose compared to all other genotypes by 2-way ANOVA with Tukey's multiple comparisons test (*p<0.05,**p<0.01). (b) Non-edited [Kv1.1(I)] and edited [Kv1.1(V)] mice were compared to their wild-type littermates (mean ± SEM, n=8-16 mice for each genotype per dose; not every mouse reached HLE). No statistical comparisons were possible at the 6 mg/kg 4-AP dose, because only the non-edited [Kv1.1(I)]

mice had mice reaching HLE. Non-edited [Kv1.1(I)] mice had a significantly shorter latency to HLE at the 10 mg/kg 4-AP dose compared to all other genotypes by 2-way ANOVA with Tukey's multiple comparisons test (***p<0.001, ****p<0.0001).

Preliminary Electrophysiological characterization

Due to the observed alterations in drug-induced seizure susceptibility, we collaborated with Dr. Sam Centanni in the laboratory of Dr. Danny Winder to perform a pilot study of slice electrophysiology in homozygous non-edited [Kv1.1(I)] mutant mice. We focused our pilot recordings on dentate granule cells in the hippocampus of non-edited [Kv1.1(I)] mice compared to wild-type littermates because of a recent study which observed a dramatic upregulation of Kv1.1 in these neurons in a model of temporal lobe epilepsy (Kirchheim et al., 2013). Results from this analysis showed no differences between non-edited [Kv1.1(I)] and wild-type animals, comparing the intrinsic properties and single action potential firing characteristics of dentate granule cells. Since we observed phenotypic differences only in non-edited [Kv1.1(I)] mice following conical tube restraint, Dr. Centanni also performed recordings on mice that had just undergone conical tube restraint and again, there were no significant differences in any signaling parameters between the genotypes (Figure 2.20).

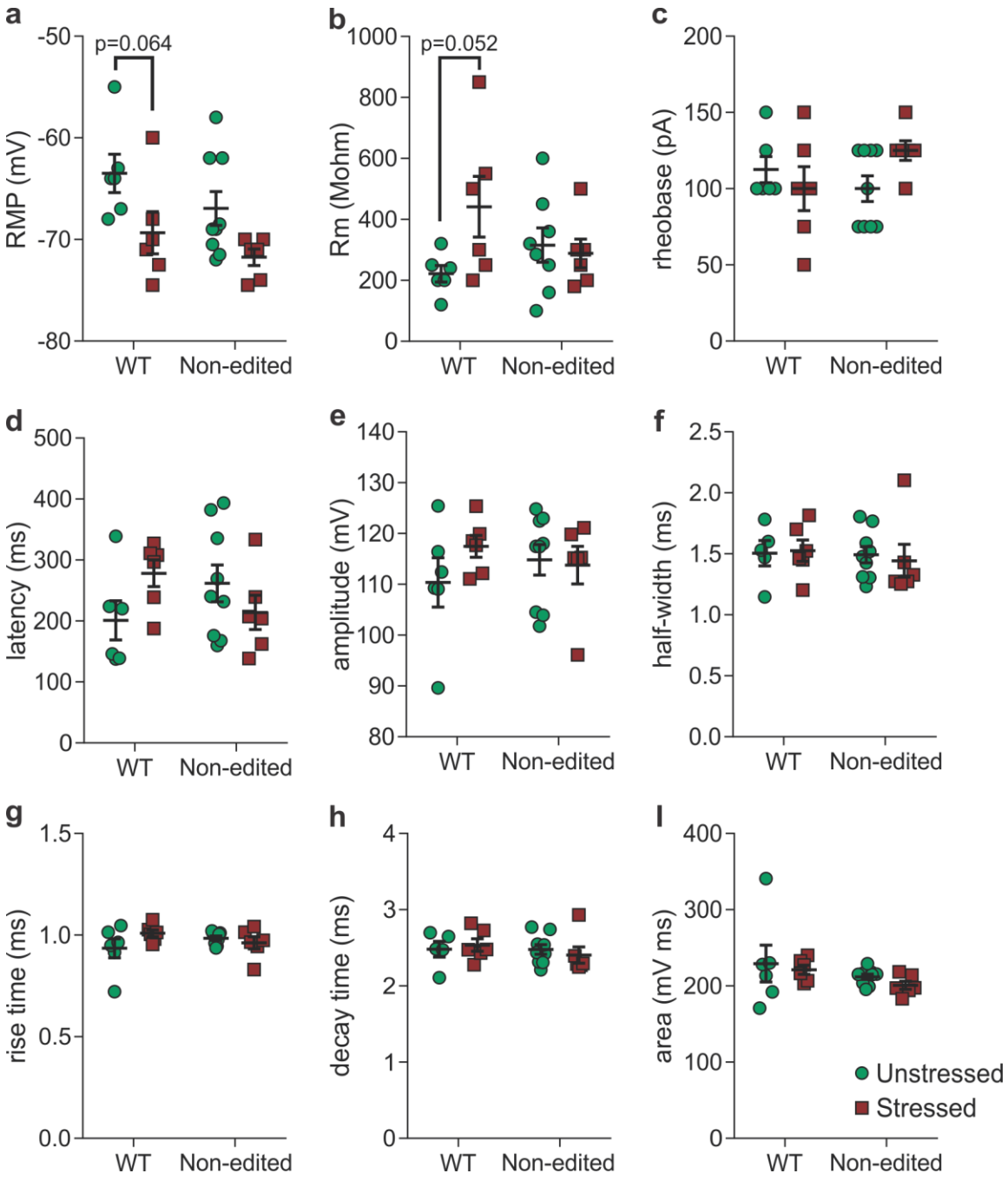

Figure 2.20. Electrophysiological characterization of dentate gyrus granule cells of non-edited [Kv1.1(I)] and wild-type mice. Dentate gyrus granule cells were recorded from hippocampal slices obtained from non-edited [Kv1.1(I)] and wild-type littermates. Prior to hippocampal isolation the mice were either unstressed or stressed by 30 minutes of conical tube restraint. Electrophysiological parameters recorded from dentate gyrus granule cells included: **(a)** resting membrane potential (RMP), **(b)** membrane resistance (Rm), **(c)** rheobase, **(d)** action potential (AP) latency, **(e)** AP amplitude, **(f)** AP half-

width, **(g)** AP rise time, **(h)** AP decay, **(i)** AP area. No significant differences were found between genotypes or unstressed versus stressed conditions, though p-values close to 0.05 are marked (mean ± SEM, n=5-9, 2-way ANOVA with Sidak's multiple comparisons test).

Discussion

Characterization of Kv1.1 editing in wild-type mouse tissues

Our studies extending characterization of Kv1.1 editing in wild-type mouse tissues highlight the importance of Kv1.1 regulation throughout the nervous system. We did not see substantial Kv1.1 editing in any peripheral tissues examined, however these dissections were of large tissues and do not discount a small subset of cells that might still undergo RNA editing, which could have been diluted out in our broad studies. The specific and reproducible levels of Kv1.1 editing characterized in each of the brain regions tested may indicate that regulating expression of the non-edited versus edited Kv1.1 transcripts allows for unique signaling properties for each tissue type. Further studies will be required on single cells to determine whether the RNA editing levels we observed occur across multiple cell types or whether the level of editing in a subset of the cellular populations drives the average.

In general, the levels of RNA editing that we observed in these mouse tissues were comparable to the levels other investigators have seen in mice, rats, and humans, especially considering the known variation in editing between

different wild-type mouse strains (Morabito et al., 2010). One notable exception was Decher *et al.* (2010), where a high level of editing in human striatum was observed (approximately 65%), whereas levels of editing in mouse striatum were approximately 14%. These results suggest that mouse and human Kv1.1 editing profiles could vary more in the striatum as compared to other tissues. It is also important to note that RNA editing levels are necessarily more precise in mouse lines, which are genetically identical, compared to wide variability in human RNA editing. This variability has been previously characterized for Kv1.1 in human tissues obtained from patients undergoing surgery for mesial temporal lobe epilepsy with hippocampal sclerosis (MTLE+HS) (Krestel et al., 2013). Krestel *et al.* (2013) observed normal Kv1.1 RNA editing levels in control human hippocampal RNA at 23% and 20%, respectively, representing commercially available human hippocampal RNA (pooled sample from 19 individuals) and from autopsy controls (pooled from 5 individuals). Conversely, their samples from MTLE+HS patients varied widely, with Kv1.1 RNA editing ranging from 0% to approximately 47%. The variability of editing levels in epilepsy patients could result from their underlying disorder or might represent normal variability between individuals, whereas the controls were pooled samples that could artificially mask the population's variability. A second interpretation is that the dissections are not of comparable regions of the striatum. In Decher *et al.* (2010), human brain RNA was obtained commercially and consisted of pooled RNA from 100 to 200 individuals. Unfortunately, no detail is given for which part of the striatum was obtained, whether a particular region or a homogenate of the entire brain region,

or whether the RNA was obtained from clinically healthy humans or from patients with an underlying disorder. In a similar manner, the wide variability in MTLE+HS patients also could stem from differences in which part of the hippocampus was surgically removed. For these reasons, we can only speculate as to whether the difference in editing frequency between mouse and human striatum is biologically consequential or an experimental artifact. Future research is needed to describe the normal human variation in Kv1.1 RNA editing, in order to understand if it is as variable as observed in MTLE+HS tissue samples, and if this variability could underlie a risk factor for seizures or whether variability is a resulting consequence of seizures (Krestel et al., 2013). This could particularly be studied by comparing Kv1.1 RNA editing in focal tissue versus the surrounding/non-focal tissue from epileptic patient samples. Our high-throughput sequencing method would be key to detecting accurate measurements of RNA editing, as other studies of human variation of RNA editing have lacked robustness, with low read levels covering the editing site (O'Neil and Emeson, 2012).

Verification of non-edited [Kv1.1(I)] and edited [Kv1.1(V)] mutant mouse models

Our mutant mouse lines can serve as important model systems to assess the consequences resulting from editing dysregulation of Kv1.1 transcripts, including alterations in survival, behavior, seizure-susceptibility, and electrophysiological properties of Kv1.1-expressing neurons in their native

environment. However, to make meaningful assertions regarding the roles of the non-edited [Kv1.1(I)] and edited [Kv1.1(V)] isoforms, we needed to first validate that our mouse models only differed in Kv1.1 isoform identity, not steady-state Kv1.1 mRNA levels. First, we confirmed that the intended isoform was being expressed and not altered at the RNA level by qualitative Sanger sequencing of RT-PCR amplicons generated from cerebellar RNAs from the wild-type, non-edited [Kv1.1(I)], and edited [Kv1.1(V)] mouse lines. Editing of the Sanger sequenced WT cerebellum sample in Figure 2.4 appears to be greater than the editing determined by high-throughput sequence analysis in Figure 2.4; for a comparative analysis of editing quantification by Sanger versus high-throughput sequencing, see *Appendix A* and Figure A.1.

Additional verification was performed for non-edited [Kv.1.1(I)] mice to ensure that the mutations introduced around the editing site were sufficient to prevent RNA editing from occurring. Although a low level of RNA editing was detected for the non-edited [Kv1.1(I)] mice in RNAs isolated from spinal cord (0.045 ± 0.0046 %), it is likely to have little physiological significance. These edited reads are likely the outcome of the low level of erroneous nucleotide incorporation, arising from the error rate of the polymerase during RT-PCR amplification, as well as the error rate for accurate detection on the Illumina sequencing platform. Two contributing factors to the error profiles using Illumina sequencing are the presence of the motif GGC (or GCC when sequencing the reverse strand) within 10 bases of the sequence specific error (SSE) as well as the presence of inverted repeats in the vicinity of the SSE (Nakamura et al.,

2011). Interestingly, there are two GCC motifs within 10 bases downstream of the editing site and the editing site naturally resides within an extended inverted repeat. These type of errors also are heavily influenced by the sample preparation method as well as primers used, with different motifs influencing the types of errors that occur (Schirmer et al., 2015). They also noted that amplicon-based sequencing is more prone to motif-based errors due to the high degree of similarity in sequenced reads. Our high-throughput sequencing technique is able to limit the effects of errors by excluding reads containing any errors that differ from the reference sequence, but cannot differentiate necessarily between G-to-A and A-to-G sequencing errors at the editing site. This represents a small amount of error with little effect on the overall editing percentage, but can explain the very small number of edited reads found in spinal cord RNA isolated from non-edited [Kv1.1(I)] mice.

To make accurate conclusions about our mouse models, we also needed to verify whether our efforts to express a fixed Kv1.1 isoform led to alterations in steady-state Kv1.1 RNA expression. Quantitative RT-PCR experiments validated that isoform identity did not alter Kv1.1 RNA levels for either isoform from that observed in wild-type mice. These controls further support the idea that any variation in phenotype that we might observe would result from restricting Kv1.1 expression to a single edited isoform, either non-edited [Kv1.1(I)] or edited [Kv1.1(V)], and not due to unpredicted isoform expression or alterations in Kv1.1 RNA expression levels.

Mendelian distribution of progeny

We have observed that both homozygous non-edited [Kv1.1(I)] and edited[Kv1.1(V)] mutant alleles can result in early postnatal lethality with incomplete penetrance, but that such postnatal lethality may be dependent on environmental factors such as stress. Mice were bred in both a traditional (MCNII) and pathogen-free Barrier facility to assess whether the observed postnatal lethality in homozygous mutant mice resulted from an external pathogen. However, both facilities demonstrated lethality for a subset of the homozygous mutants. Although we cannot rule out that there was a difference in the gut microbiota of the two breeding colonies in the different floors of the MCNII facilities, prior studies of gut microbiota variability have demonstrated that raising mice in individually ventilated cages in separate rooms of the same facility led to mice with statistically similar cecal microbiomes (Hufeldt et al., 2010). Because mutations in Kv1.1 underlie the etiology of EA1, which involves stress-induced symptoms, it is possible that there are stress-induced environmental factors that lead to the difference in survival. Such environmental factors might include a difference in animal care technicians, levels of noise, and/or levels of activity in each room. Informal characterization of the two MCNII rooms indicates that one had a higher level of noise and activity because it contained a commonly used procedural hood. When we genotyped the corpses of dead pups found in the breeding facilities, we did not see an overrepresentation of homozygous mutants for any genotype. There are several possibilities for why we never observed the postnatal lethality. One possibility is that the offspring are dying sometime after

birth, triggered by an environmental stressor, at an early enough stage that the mother can cannibalize the dead pup without leaving any trace. Another possibility is that some of the homozygous pups are dying during the stress of birth, followed by maternal cannibalization. Finally, environmental stressors could be affecting the mother rather than the pup, leading to selective maternal cannibalism of the homozygous mutants. Although it seems unlikely that the mothers are using some unknown differentiating factor to distinguish homozygous mutants versus heterozygotes and wild-type littermates, this has been previously documented in the literature for other homozygous mutant animals (Kastner et al., 1996; Lohnes et al., 1993; Lugt et al., 1994). More detailed video monitoring and cross-fostering analyses will be required to determine when these homozygous mutant animals are lost and what the underlying factors could be (Kuroda and Tsuneoka, 2013; Weber et al., 2013).

Behavioral characterization

We observed that the non-edited [Kv1.1(I)] mice show locomotor deficits under stressed conditions, similar to those observed in the human disorder, EA1. While rotarod results for all animals were within the range of normal literature values obtained from C57BL/6J mice, the mice of some unstressed trials did not appear to increase their improvement on the task (Figure 2.8b) (Matsuo et al., 2010). This apparent lack of learning in one of the unstressed trials likely results from random sampling and increasing the number of animals used in the trial

could better display this trend. Local maxima are seen before the last trial day for the first and third trials, but this is in agreement with studies by Matsuo *et al.* (2010), which also observed this kind of trend for data with smaller animal numbers, whereas when they increased their sample size from 13 to 1087 animals, the curve smoothed to a steady plateau.

We observed a statistical difference between left overlap parameters of the non-edited [Kv1.1(I)] mice compared to the wild-type littermates in gait analyses, though not in any other parameters. This result could be indicative of a stress-induced gait difference, though it is generally held that decreases in the paw overlap indicate improvements in motor coordination rather than impairments (Carter et al., 1999; Carter et al., 2001). However, there are several examples of mouse models with locomotor deficits in the rotarod task that do not display an ataxic gait by footprinting analysis (Jayabal et al., 2015; Kayakabe et al., 2014). Furthermore, the observed decrease in left paw overlap could potentially lead to dysfunction because it is an unbalanced change not reflected in the right overlap.

Importantly, all behavioral tasks where we observed stress-mediated differences were performed on mice originating from the second MCNII facility, where no lethality was observed for either mutant genotype. As we have hypothesized that the conditional lethality of the original MCNII and barrier facilities may be associated with an environmental stressor, using mice from these facilities could result in inadvertently selecting for mutants that are hardened to stress, which could confound our interpretation. In contrast, by using

mice from the facility with no observed lethality, we avoided this possible selection.

Unfortunately, additional studies of grip strength, motor coordination by the pole climb test, inverted screen, and open field analysis did not indicate dysfunction for homozygous non-edited [Kv1.1(I)] mice. The results of open field analysis also indicate that the non-edited [Kv1.1(I)] mice do not have increased anxiety, although direct assessments of anxiety-like behavior (e.g. elevated plus maze) were not employed. The rotarod task may be uniquely suited to promoting the stress-induced ataxia because it is a more strenuous task than the other behavioral studies used for these animals.

The interaction between stress and genotype is complex and leads to further questions about how stress is leading to genotype differences. Stress appears to increase performance for all genotypes, but also reveals a differential genotypic effect of stress between different trial days. To compare the effects of stress, the data described in Figures 2.8 and 2.9 were combined; this was done in order to minimize the differences due to each trial being performed at a different time on separate, naive cohorts (trials would need to be simultaneous for all groups for the most accurate comparisons) (Figure 2.21). Stress led to significant increases in rotarod performance for all genotypes, when comparing the performance over the entire test (significant main effects indicated by # symbols in Figure 2.21). Significant differences comparing among the unstressed genotypes or among the stressed genotypes followed the insignificant and significant trends described for the individual cohort data in Figures 2.8 and 2.9,

respectively (significant main effects indicated by + symbols in Figure 2.21). Interestingly, when the significance was tested for each trial day separately, the edited [Kv1.1(V)] and wild-type stressed groups performed significantly longer than the corresponding unstressed edited or wild-type groups starting on days 2 and 3, respectively (indicated by * symbols in Figure 2.21). In contrast, the non-edited [Kv1.1(I)] stressed group was not significantly increased compared to the non-edited [Kv1.1(I)] unstressed group until day 6. This indicates that the non-edited [Kv1.1(I)] mice gain less from the stressed performance enhancement compared to the other genotypes and the stress performance enhancement begins later.

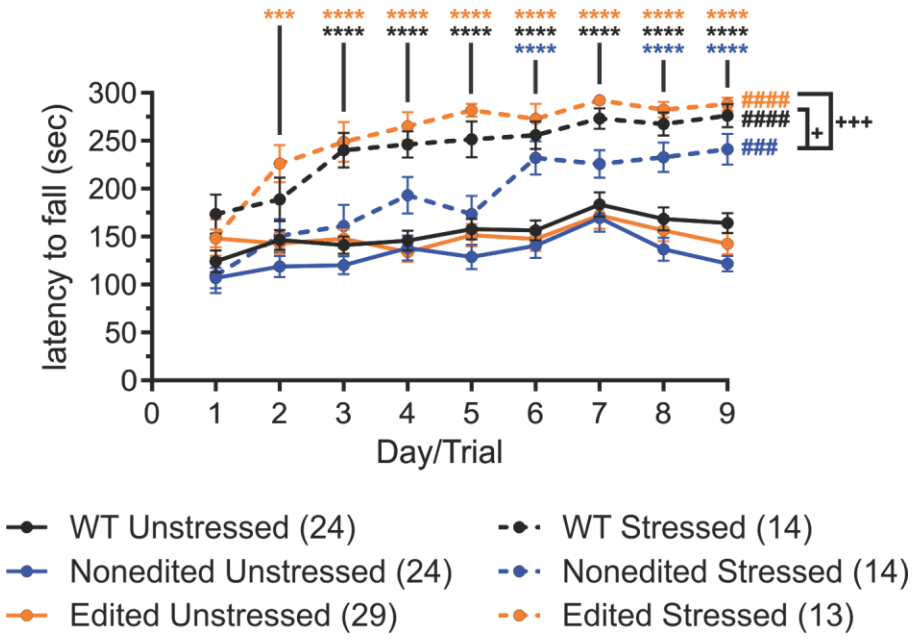

Figure 2.21. Stress-enhancement of rotarod performance. Adult male mice were subjected to the unstressed or stressed condition (stress: 30 minutes of conical tube restraint) followed by the modified rotarod paradigm (1 rotarod trial per day over 9 days). Data described above were composed of the combined data of multiple naive cohorts, tested at different times, described in Figures 2.8 and 2.9 (mean ± SEM, n=13-29, indicated in parentheses in the legend). Significant differences were observed between the unstressed versus stressed groups within each genotype (###p<0.001, ####p<0.0001 (color-coded for genotype), 2-way repeated measures ANOVA with Tukey's multiple comparisons of the main effects). No differences were found between unstressed groups as in Figure 2.8, but similar differences were found between the stressed groups as is reported in Figure 2.9 (+p<0.05, +++p<0.001, 2-way repeated measures ANOVA with Tukey's multiple comparisons of the main effects). In addition, significant differences were observed on individual trial days between the unstressed versus stressed groups within each genotype (***p<0.001, ****p<0.0001 (color-coded for genotype), 2-way repeated measures ANOVA with Tukey's multiple comparisons).

Finally, our data also lead to another question, whether the enhancement over the test period could be related to habituation to the stressor. If habituation were occurring, we would expect to see the non-edited [Kv1.1(I)] mice performing more divergently only when the stressor was novel and that performance would

not differ as the mice became habituated to the stressor. As the non-edited [Kv1.1(I)] unstressed versus stressed mice do not significantly differ until day 6, this could indicate a delay in habituation compared to the other genotypes (Figure 2.21). Unfortunately, for the comparisons between genotypes in Figures 2.8 and 2.9, the statistics were limited to main effects, because comparisons at individual trials were underpowered for most trial days (though in the combined data in Figure 2.21, the non-edited [Kv1.1(I)] mice were significantly decreased compared to the edited [Kv1.1(V)] mice on days 2, 3, 4, 5 and 7). Thus, in order to determine significance between genotypes at each trial day in data consisting of a single cohort, a mixed-model should be developed for more precise statistical comparisons. An important caveat to the rotarod paradigm is that the maximum run time for the mice is 300 s, thus the apparent plateau in rotarod performance over time is likely an artifact of this ceiling effect, which could confound statistical tests at the later trial days, and future experiments should increase the maximum time to determine the exact latency to fall value. In order to specifically address any stressor habituation, a follow-up study could be performed, using a chronic unpredictable stress protocol (Monteiro et al., 2015). Varying the stressor may reveal additional deficits, possibly leading to further decreases in rotarod performance for the non-edited [Kv1.1(I)] mice compared to the unstressed paradigm or the other genotypes. Although a chronic unpredictable stress paradigm may provide additional insights into genotypic differences, the nature of EA1 as a paroxysmal stimulus-induced disorder suggests that patients do not habituate to the triggering stressors, and using a

chronic unpredictable stress may reveal no more information than only using the conical tube restraint stressor (Dreissen and Tijssen, 2012).

Spontaneous Seizure Monitoring and Drug-induced Seizure Susceptibility

Initial EEG analyses did not reveal epileptiform activity, though the homozygous non-edited [Kv1.1(I)] mouse exhibited two tonic events during sleep. These abnormal movements could not be classified as seizures, because there were no concurrent alterations in the EEG traces, yet they suggested that the non-edited [Kv1.1(I)] mutants may have underlying signaling deficits that could lead to altered seizure-susceptibility. Additional studies are required to discern if this observed activity was consistent for this genotype.

Subsequent studies assessed whether Kv1.1 mutant animals displayed differences in drug-induced seizure susceptibility using the pro-convulsant drugs, flurothyl, PTZ, and 4-AP. These convulsants were chosen due to their widespread use, as well as prior use in Kv1.1 studies in the literature. PTZ has been shown to alter the voltage dependence and decrease the maximal current of Kv1.1, when exogenously expressed in *Xenopus* oocytes, and Kv1.1 editing has been implicated in reducing the 4-AP-seizure susceptibility (Madeja et al., 1996; Madeja et al., 1994; Streit et al., 2011). These drugs each have different mechanisms of action, therefore it is not surprising that one has no effect (flurothyl) and the others have opposite effects (PTZ and 4-AP) on homozygous Kv1.1 mutant animals.

The mechanism of action for flurothyl is not well understood, so the lack of a genotype difference is less informative. It has been previously demonstrated that Kv1.1-null mice experience flurothyl-induced seizures 60% faster than their wild-type littermates (Smart et al., 1998). In contrast, we found no difference in the onset of flurothyl-induced seizures between our mutant mouse lines, indicating that any effect of flurothyl is independent of Kv1.1 editing. The loss of Kv1.1 in null mice might lead to an increase in seizure susceptibility by increasing the expression of Kv1.x channels at the plasma membrane (since Kv1.1 can lead to greater internalization of heterotetrameric Kv1.x channels) (Manganas and Trimmer, 2000). Our characterization of the steady-state levels of Kv1.1 RNA indicates similar expression of either isoform in mutant lines compared to wild-type mice, so an expression-dependent flurothyl effect would not be expected to alter seizure-susceptibility. We did not follow up with a larger cohort study because power analyses (at 80% power and 5% type-I error rate) predicted that we would need to test 2472 non-edited [Kv1.1(I)] and 1185 edited [Kv1.1(V)] animals in order to see significant differences compared to wildtype (using the average standard deviation derived from our flurothyl data described above). By contrast, it is interesting that 4-AP and PTZ are each able to reveal differences between the homozygous non-edited [Kv1.1(I)] and edited[Kv1.1(V)] mutant mice, respectively.

PTZ is proposed to weaken $GABA_A$ receptor mediated inhibition and PTZ has been shown to alter the voltage-dependence of Kv1.1 in exogenously expressing *Xenopus* oocytes (Madeja et al., 1994; Ramanjaneyulu and Ticku,

1984). We observed that the edited [Kv1.1(V)] mice displayed a dampened seizure-susceptibility towards PTZ-induced seizures. The main biophysical difference between the non-edited [Kv1.1(I)] and edited[Kv1.1(V)] mutant channels is the speed of the recovery from fast-inactivation. Whereas faster recovery from inactivation is epileptogenic for sodium channels (R1460H mutation in SCN1A) (Alekov et al., 2000), we have observed that the edited [Kv1.1(V)] isoform is resistant to PTZ-induced seizures, indicating that faster recovery from inactivation for potassium channels is anti-epileptogenic. The opposing effects of faster recovery from inactivation for the sodium channel mutant and potassium channel edited isoform mentioned above may alter the frequency and shape of the repetitive firing of action potentials. Faster recovery from inactivation for a sodium channel may overall lead to greater sodium influx and hyperexcitability, whereas faster recovery for a potassium channel may lead to less potassium efflux and hypoexcitability. Our studies indicating that the edited channel confers dampened seizure susceptibility also are consistent with studies indicating that drugs, which open potassium channels or prevent β-inactivation, counteract PTZ-induced seizures (Lu et al., 2008; Pozo et al., 1990).

4-AP is a known Kv channel blocker with high-affinity for the Kv1 channel family (Decher et al., 2010; Grissmer et al., 1994). It was hypothesized that homozygous non-edited [Kv1.1(I)] mice would have a greater 4-AP-induced impairment, given that 4-AP efficiently blocks the non-edited [Kv1.1(I)] isoform, but not the edited [Kv1.1(V)] isoform when exogenously expressed in *Xenopus* oocytes (IC_{50}: nonedited= 98 μM; edited= 6.7 mM) (Decher et al., 2010).

Recordings from entorhinal slices from chronic epileptic rats, observed to have increases in Kv1.1 RNA editing, revealed a resistance to 4-AP-induced seizure-like events (Streit et al., 2011). Thus our results, demonstrating that the homozygous non-edited [Kv1.1(I)] mutant mice were more susceptible to 4-AP-induced seizures agrees well with previous studies. The 4-AP experiment was replicated twice and the increase in seizure susceptibility was still observed, though interestingly our second experiment, using the wild-type littermates of the non-edited [Kv1.1(I)] and edited [Kv1.1(V)] mice demonstrated further differences that were not seen in the original experiment using the wild-type littermates of the V408A/+ mice. The latency to HLE did differ between genotypes for the 4-AP-induced seizures, unlike the results with PTZ (in which genotype had no effect on seizure latency). This difference in the seizure latency was only observed for the non-edited [Kv1.1(I)] mice, which exhibited faster maximal seizure onset (HLE) than the other genotypes. The presence of edited channels in the edited [Kv1.1(V)], wild-type, and V408A/+ mice may have a dominant effect on seizure latency, which all displayed similar seizure latency, whereas the complete lack of edited channels in the non-edited [Kv1.1(I)] mice led to faster and more severe seizures.

It is noteworthy that the wild-type littermates had an intermediate 4-AP seizure-susceptibility curve between the non-edited [Kv1.1(I)] and edited [Kv1.1(V)] mice, especially given the lower rates of editing in the hippocampus in particular (approximately 18%). This could also indicate that the edited [Kv1.1(V)] isoform exerts a dominant effect, even when it is expressed at a lower ratio

compared to the non-edited [Kv1.1(I)] channel. This interpretation is consistent with studies by Decher *et al.* (2010), which demonstrated that edited [Kv1.1(V)] exerts dominant effects on drug and fatty acid binding when in tetramers with non-edited [Kv1.1(I)] as well as in tetramers with other Kv1.x family members. Another possible explanation is that a small subset of neurons has a high expression of edited [Kv1.1(V)] and these neurons set the epileptic tone of the predominantly nonedited [Kv1.1(I)] isoform expressing tissue. This is possible but is less likely, given that editing has been quantified in CA1 pyramidal neurons and these neurons had low levels of editing (7%), similar to the average of region (Decher et al., 2010).

Preliminary Electrophysiological characterization

Collaborations with the Winder lab performed the first electrophysiological characterization of the homozygous non-edited [Kv1.1(I)] mutant mice. We chose to focus on the non-edited [Kv1.1(I)] animals to probe whether these mice have altered signaling properties which could explain the heightened seizure-susceptibility seen in the 4-AP experiments. In addition, recordings were performed under stressed conditions, due to the observed stress-induced motor discoordination of non-edited [Kv1.1(I)] mutant animals upon conical tube restraint. Kv1.1 has been implicated in alterations in dentate granule cells' signaling, as Kv1.1 was upregulated in dentate granule cells in a model of temporal lobe epilepsy (Kirchheim et al., 2013). When Kv1.1 was reversibly

knocked down by antisense oligonucleotides, electrophysiological recordings of dentate granule cells revealed action potential broadening and an abolished hyperpolarization phase, though no alterations in other parameters were observed, such as the resting membrane potential and action potential amplitude (Kirchheim et al., 2013; Meiri et al., 1997). Unfortunately, our studies did not identify any differences between the homozygous non-edited [Kv1.1(I)] mice and their wild-type littermates. This outcome may result from our choice of recording in the hippocampus where wild-type mice express approximately 80% non-edited Kv1.1 transcripts, which could explain why the signaling in the hippocampus of non-edited [Kv1.1(I)] mutant animals was very similar to that observed in control mice. The lack of a difference in signaling for the non-edited [Kv1.1(I)] mice may indicate that the presence or absence of the edited [Kv1.1(V)] isoform may be more informative for understanding Kv1.1 editing effects *in vivo*.

Summary

Until now, characterization of Kv1.1 editing has been restricted to heterologous expression systems. Our newly developed mouse models allow for phenotypic contrasting of the non-edited [Kv1.1(I)] and edited [Kv1.1(V)] mice and the opportunity to observe the electrophysiological changes upon solely expressing either isoform *in vivo*. Our characterization has revealed that disrupting the normal ratios of Kv1.1 editing has surprising effects on postnatal lethality that are related to environmental factors. Furthermore, our phenotypic

characterization has indicated that the non-edited [Kv1.1(I)] mouse shares similarities with the V408A EA1 mouse model, posing new questions as to how these two mouse models are similar and whether altered Kv1.1 editing could be a contributing factor in the V408A/+ mouse model as well.

CHAPTER III

INTERACTIONS BETWEEN KV1.1 RNA EDITING AND EPISODIC ATAXIA TYPE-1 MUTATIONS

The contents of this chapter were adapted from the published work, "Mutations underlying Episodic Ataxia type-1 antagonize Kv1.1 RNA editing," in the journal *Scientific Reports* in February 2017, under a Creative Contributions Attribution v4.0 International License (Ferrick-Kiddie et al., 2017).

Introduction

At least three EA1-associated mutations (V404I, I407M, and V408A) have been identified within the duplex region required for editing of Kv1.1 RNAs (Adelman et al., 1995; Eunson et al., 2000; Imbrici et al., 2006; Maylie et al., 2002; Tomlinson et al., 2013; Zerr et al., 1998). Due to the proximity of the mutant amino acids to the editing site (I400V), we sought to determine whether such EA1 mutations affect the editing profiles for Kv1.1 transcripts and to determine the resultant biophysical properties of edited, mutant channels.

Our studies reveal an antagonistic relationship between these EA1 mutations and RNA editing. Each EA1 mutation decreased the rate of RNA editing using an *in vitro* editing system and the V408A mutation decreased the extent of editing in a previously characterized mouse model of EA1. Furthermore,

we show that editing can have a variable effect on each type of EA1 mutant protein, altering voltage sensitivity, activation and deactivation, and inactivation with a Kvβ subunit. Not only do our studies demonstrate that EA1 mutations can impede RNA editing and alter resulting protein function, but also represent the first examples of existing disease-associated human mutations which act to disrupt *cis*-regulatory elements required for RNA editing.

Materials & Methods

Kv1.1 and Kvβ1.1 constructs

A 463 bp-region encompassing the duplex required for Kv1.1 editing was amplified by PCR from human genomic DNA using sense (5'-GC-GAAGCTTCCTCTTCATCGGGGTCATCCT-3') and antisense (5'-GCGGCGGCCGCAGTTTTGGTTAGCAGTGG-3') oligonucleotide primers in exon 2. To aid in subcloning, the primers incorporated Hind III and Not I restriction sites on their 5'-ends for the sense and antisense primers, respectively. The PCR amplicon was subcloned into the mammalian expression vector, pRc-CMV (Thermo Fisher) to generate a wild-type Kv1.1 minigene. To generate the V404I, I407M, and V408A minigenes, the wild-type Kv1.1 construct was mutagenized using the QuikChange II Site-Directed Mutagenesis kit (Agilent Technologies), where the PCR reactions were supplemented with 5% DMSO. Full-length mouse Kv1.1 (Addgene) and mouse Kvβ1.1 (Thermo Scientific)

cDNAs were subcloned into the *Xenopus* expression vector, pGEM HE (Liman et al., 1992). The following full-length constructs were created by PCR mutagenesis from the full-length mouse non-edited [Kv1.1(I)] cDNA and validated by sequence analysis: wild-type edited [Kv1.1(V)] and V404I, I407M, and V408A mutant Kv1.1 (non-edited [Kv1.1(I)] and edited [Kv1.1(I)]) cDNAs.

In vitro analysis of RNA editing

RNAs were transcribed *in vitro* from the wild-type Kv1.1 minigene, as well as corresponding minigenes harboring the V404I, I407M, and V408A mutations using the MAXIscript kit (Ambion) with T7 RNA polymerase according to manufacturer's instructions. Nuclear extracts were prepared from transiently transfected HEK293 cells expressing rat ADAR2, as described previously, and stored at -80º C until required (Schreiber et al., 1989; Stefl et al., 2010). Immediately prior to *in vitro* editing analysis, nuclear extracts were diluted 1:10 in dialysis buffer [20 mM HEPES, 1 mM EDTA, 1 mM EGTA, 10% glycerol, 300 mM NaCl, 1 mM PMSF, 1 mM DTT, 1X complete, EDTA-free protease inhibitor cocktail (Roche)], before a 2-hour incubation at 30°C with RNase inhibitors and RNA substrates varying in concentration from 0.125 to 2 nM. Nuclear extracts represented one-third of the total 50 μL reaction volume which was diluted with the RNA substrate and water to reduce the glycerol concentration into a range necessary for ADAR2 activity. The incubation time was determined empirically by time-course analyses to ensure that editing of the wild-type Kv1.1 minigene was

within the linear range of the reaction (Figure 3.1). In Figure 3.1, editing was determined by Sanger sequencing electropherogram peak height analysis (see *Appendix A* for additional description of the accuracy of Sanger compared to high-throughput sequencing analyses). By the limitations of this technique, very low editing levels were undetectable, especially at the 1 hour time point for the mutant duplexes (and editing was undetectable for all RNA duplexes in pilot trials at 20 minutes (*data not shown*)). Reactions were terminated by the addition of TRIzol (Ambion) and RNA was extracted according to the manufacturer's protocol. RNA was reverse-transcribed with random primers using the High Capacity cDNA Reverse Transcription kit (Applied Biosystems) and the extent of RNA editing was quantified by high-throughput multiplexed sequence analysis as described previously (Hood et al., 2014). The editing rate was calculated as the fmol RNA converted to the edited isoform divided by the duration of the reaction.

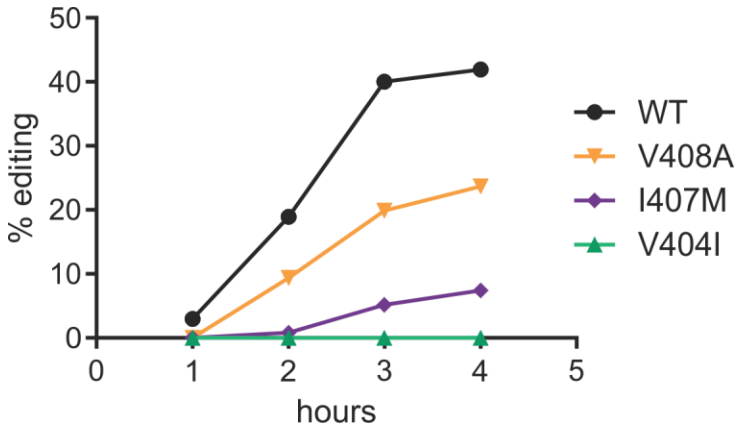

Figure 3.1. Time course analysis to determine the linear range for the *in vitro* RNA editing rates. Wild-type (WT) and mutant Kv1.1 RNA minigenes, encompassing the duplex region required for editing, were *in vitro* transcribed and incubated between 1 and 4 hours with nuclear extracts prepared from HEK293 cells transiently expressing rat ADAR2. The extent of editing was quantified by the relative A and G peak heights derived from Sanger sequence analysis, used to calculate the approximate editing rate.

In vivo analysis of RNA editing

All animal care and experimental procedures involving mice were approved by the Vanderbilt University Medical Center Institutional Animal Care and Use Committee and were performed in accordance with relevant guidelines and regulations. Mice harboring the heterozygous V408A mutation (V408A/+) were generously provided by Dr. James Maylie (Oregon Health & Science University) (Herson et al., 2003). At approximately 6 weeks of age, male V408A/+ and wild-type littermates were euthanized by cervical dislocation under anesthesia followed by decapitation. Six brain regions (cerebellum, hippocampus, hypothalamus, cortex, striatum, olfactory bulb) and spinal cord were dissected from each mouse. Tissues were flash-frozen in liquid nitrogen and RNA was isolated by sonication in TRIzol (Ambion) according to the

manufacturer's instructions. RNA was reverse-transcribed and Kv1.1 editing was quantified by high-throughput sequence analysis as described for *in vitro* RNA editing analyses.

Electrophysiological recording in Xenopus oocytes

All animal care and experimental procedures involving *Xenopus laevis* were approved by the University of Puerto Rico Institutional Animal Care and Use Committee. Kvβ1.1 and full-length, wild-type, V404I, I407M, and V408A Kv1.1 RNAs were transcribed *in vitro*, capped, and polyadenylated using the T7 mScript Standard mRNA Production System (CELLSCRIPT). Ovary sections containing several hundred oocytes were removed from adult specimens of *Xenopus laevis* obtained from Xenopus Express (Brooksville, FL). Oocytes were dispersed with type II collagenase and manually defolliculated. Stage V and VI oocytes were then selected by manual inspection for subsequent RNA injection. On day 1, oocytes were injected with 38.6 nL of one of the eight full-length Kv1.1 RNAs encoding non-edited [Kv1.1(I)] and edited [Kv1.1(V)] isoforms of wild-type, V404I, I407M, and V408A channels, with or without the Kvβ1.1 RNA. Injection concentrations were optimized individually for each construct, with greater concentrations required for the I407M and V408A RNAs due to protein expression differences previously described in the literature (Tomlinson et al., 2013; Zerr et al., 1998). Each α-subunit was injected at a concentration from 2 ng/μL to 1 μg/μL and co-injected with Kvβ1.1 when applicable; concentrations for

the Kvβ1.1 constructs were 10-fold more than each α-subunit, up to a maximum injection concentration of 500 ng/μL. Electrophysiological analysis of oocytes were performed between day 3-5 post-injection using the cut-open oocyte voltage-clamp technique (Stefani and Bezanilla, 1998). The external solution consisted of: 20 mM K-glutamate, 100 mM L-glutamate, 2.5 mM $MgCl_2$, 2.5 mM $CaCl_2$, 10 mM HEPES, pH 7.4. The internal solution consisted of: 120 mM K-glutamate, 2.5 mM EGTA, 10 mM HEPES, pH 7.4. The pH of the solutions was adjusted using N-methyl-D-glucamine, as an alternative to NaOH, to limit the introduction of sodium ions into the solutions. To gain electrical access to the oocyte interior, the internal solution was supplemented with 0.3% saponin and used for a brief permeabilization prior to recording. The oocyte membrane potential was controlled using a CA-1B High Performance Oocyte Clamp (Dagan Corporation). Analog current signals were digitized at 100 kHz using an SBC6711 A/D D/A board (Innovative Integration, Simi Valley CA) and filtered at 5 kHz. To avoid errors introduced by series resistance, only traces exhibiting less than 10 μA were used for analysis. GPATCH M software, kindly provided by Dr. F. Bezanilla (University of Chicago), was used for data collection and clamp control. Leak currents were subtracted using a linear P/4 procedure. Data were analyzed using ANALYSIS software, also provided by Dr. F. Bezanilla, for fitting data with exponential functions and measuring current amplitudes. In addition, single exponential curves were fitted to recovery from the inactivation data using Graphpad Prism (Graphpad Software) to determine the rate constant, τ. As the channels encoded by edited V408A transcripts closed too rapidly for

measurements of tail current amplitude, conductance (G) was calculated using Ohm's law (Equation 3.1),

$$G = \frac{I}{V - V_r} \qquad (3.1)$$

where I represents the maximal current at the test potential (V) and V_r signifies the reversal potential, determined empirically. In primary traces displayed, points arising from brief capacity transients were removed for clarity.

Statistical analysis

Statistical comparisons for *in vitro* and *in vivo* editing analyses were determined by 2-way ANOVA with Tukey's multiple comparisons test (Figures 3.3 and 3.4). Boltzmann functions were fitted using non-linear regression to model conductance-voltage curves and to determine $V_{1/2}$ and k values associated with each replicate. Two-sample Student's t-tests were used to compare the voltage-dependent parameters, long pulse characterization with and without Kvβ1.1, and recovery from inactivation τ values (Tables 3.2 and 3.3; Figures 3.9 and 3.11). The above analyses were conducted using Graphpad Prism (Graphpad Software). To maintain the type I error rate for each experiment at 5%, a Bonferroni correction was applied to each test based on the number of comparisons within each experiment and statistical significance for any pair of

treatment comparisons was redefined according to these adjusted p-values. For Table 3.2 and Table 3.3, 10 comparisons were made and the significance was adjusted to $p \leq 0.005$. For Figure 3.9b, 42 comparisons were made and the significance was adjusted to $p \leq 0.0012$. For Figures 3.9c and 3.11b, 30 comparisons were made and the significance was adjusted to $p \leq 0.0017$. Analysis of activation and deactivation, and inactivation kinetics (Figures 3.6, 3.8, and 3.10) were performed with linear mixed models using the natural log of the acquired data to better meet model assumptions (developed by Dan Ayers). Individual group comparisons for p-values were based on the Wald tests of model-based predicted (least square) means and appropriate standard errors (and reported in *Appendix B*). Because these data indicate that the measurements of activation, deactivation, and β-inactivation were dependent on voltage, comparisons were made only between values obtained at the same voltage. Data are presented with their original scale to allow for easier interpretation and comparison with the existing EA1 literature. All statistical tests were two-sided and statistical significance was defined as $p \leq 0.05$. Unless specified, no adjustments for multiple comparisons were performed.

Results

EA1-associated mutations alter RNA editing in vitro

Three known EA1-associated mutations, V404I, I407M, and V408A, are encoded within the predicted 114-bp RNA duplex, which represents the minimum sequence required for site-specific editing of Kv1.1 transcripts by ADAR2 (Figure 3.2) (Bhalla et al., 2004). Using an RNA-folding algorithm (mfold) (Zuker, 2003), we examined whether any of these mutations were predicted to grossly alter the structure of the duplex region. Results from this analysis revealed that each individual mutation predicted a single-nucleotide mismatch within the duplex at each mutation site, with no further perturbations to the predicted RNA secondary structure and only minimal alterations in the free-energy (ΔG) calculations for each duplex (Table 3.1) (SantaLucia, 1998).

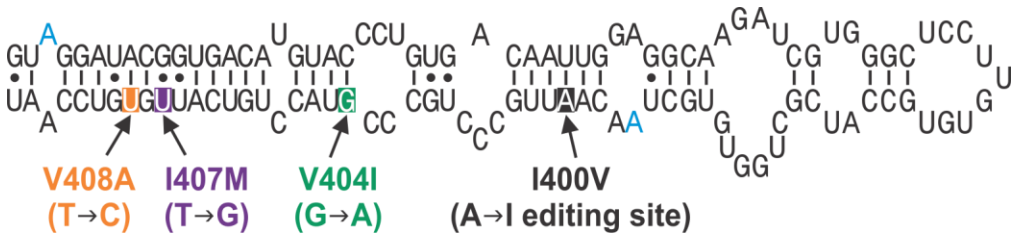

Figure 3.2. The proximity of the Kv1.1 editing site compared to the EA1 mutations responsible for V404I, I407M, and V408A. The predicted secondary structure for a portion of the wild-type (WT) human Kv1.1 pre-mRNA is indicated with the positions of the A-to-I editing site (I400V) and three non-synonymous mutations associated with EA1 shown with inverse lettering. The locations of two human versus mouse sequence differences are indicated in blue (which are both G in the mouse sequence).

Table 3.1. Free energy calculations of wild-type and EA1 human mutant duplexes

Duplex type	ΔG
Wild-type Kv1.1	-42.6
V404I	-39.3
I407M	-41.7
V408A	-38.5

To test whether these mutations affected the rate of editing for Kv1.1 RNAs, each of the EA1-associated mutations was incorporated separately into constructs encompassing a 463-bp region of human Kv1.1, centered on the known editing site. RNA transcripts were transcribed *in vitro* using these minigenes as a template and a range of concentrations for each RNA was subjected to an *in vitro* editing assay using ADAR2 protein derived from nuclear

extracts isolated from HEK293 cells transiently expressing ADAR2 (Stefl et al., 2010). The extent of editing was quantified by high-throughput sequence analysis as described previously and used to calculate the rate of editing (Figure 3.3) (Hood et al., 2014). Results from these studies clearly demonstrated that introduction of any of these EA1-associated point mutations into the wild-type sequence was sufficient to decrease the editing rate for Kv1.1 transcripts *in vitro*. Furthermore, the magnitude of this rate decrease corresponded to the proximity of the mutation to the editing site (I400V), with the most severe deficit observed for the V404I mutation (81% rate reduction at 2 nM RNA), and a 58% and 17% reduction in editing rate for the I407M and V408A mutations, respectively.

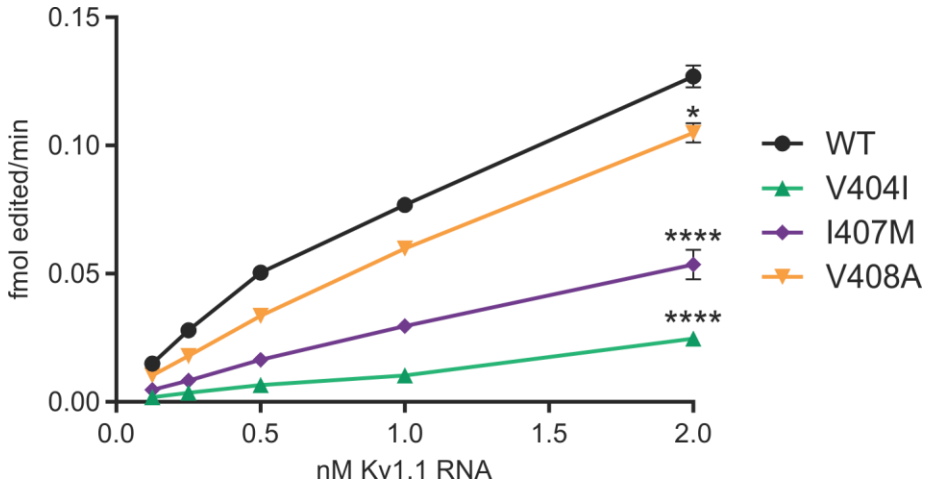

Figure 3.3. Quantitative analysis of *in vitro* RNA editing rates for wild-type and mutant Kv1.1 transcripts. Wild-type (WT) and mutant human Kv1.1 RNA minigenes, encompassing the duplex region required for editing, were *in vitro* transcribed and incubated with nuclear extracts prepared from HEK293 cells transiently expressing rat ADAR2. The extent of editing was quantified by high-throughput sequence analysis and used to calculate the editing rate, as described previously (Hood et al., 2014). Statistical differences were determined for replicates at the 2 nM RNA concentration by 2-way ANOVA with Tukey's multiple comparisons test (mean ± SEM, n=4 replicate reactions, *p ≤ 0.05; ****p ≤ 0.0001). Small error bars were obscured by the data symbol for the V404I 2nM data point.

A mouse model of EA1 (V408A/+) alters RNA editing in vivo

To date, only one mouse model of EA1 has been developed (Herson et al., 2003). Mutant mice homozygous for the V408A allele die between E3 and E9, whereas V408A/+ heterozygotes are characterized by stress-induced ataxia as well as attenuated cerebellar Purkinje signaling, which has been attributed to action potential broadening at basket cell boutons leading to increased GABA release (Begum et al., 2016; Herson et al., 2003). To determine whether the presence of the V408A mutation inhibited Kv1.1 editing *in vivo*, we isolated RNA

from multiple dissected brain regions and spinal cord of wild-type and V408A/+ mutant animals to determine RNA editing profiles by high-throughput sequence analysis of Kv1.1 transcripts. Since this deep-sequencing approach generates sequence reads covering both the V408A mutation and the editing site, it was possible to quantify allele-specific editing profiles in V408A/+ heterozygotes. Results from this analysis indicated that the extent of editing for the wild-type allele in V408A/+ mutant mice was similar to that observed in wild-type animals. Editing for the mutant V408A allele showed a 59% reduction in site-specific editing efficiency in all tissues examined when compared to either wild-type littermates or the V408A/+ wild-type allele (Figure 3.4).

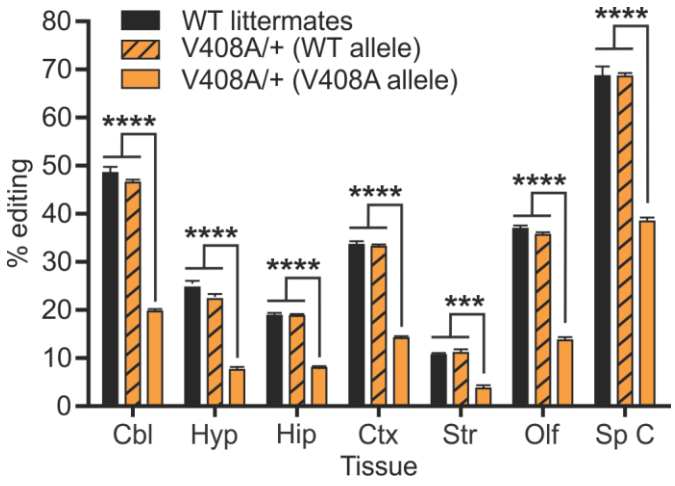

Figure 3.4. Quantitative analysis of allele-specific Kv1.1 editing in V408A mutant mice. The extent of editing for the wild-type and mutant alleles in heterozygous V408A adult mice (V408A/+), compared to wild-type littermates, was determined for RNA isolated from dissected brain regions and spinal cord by high-throughput sequence analysis. Significance was determined by 2-way ANOVA with Tukey's multiple comparisons test (mean ± SEM, n=4, ***p ≤ 0.001, ****p ≤ 0.0001). Cbl, cerebellum; Hyp, hypothalamus; Hip, hippocampus; Ctx, cortex; Str, striatum; Olf, olfactory bulb; Sp C, spinal cord.

Gating properties are altered between non-edited and edited Kv1.1 channels harboring EA1 mutations

We now have demonstrated that these three EA1 mutations can affect the rate of editing *in vitro* and the V408A allele can reduce the extent of editing *in vivo*. Although editing and EA1 mutations separately have been shown to alter the biophysical properties of Kv1.1 channels, it is unknown whether editing may cause unique effects when paired with these EA1-associated mutations. Similarly, it is unclear whether the phenotypic alterations observed in patients bearing the V404I, I407M, or V408A mutations result from changes in channel function mediated by these missense mutations alone or in concert with their affects upon editing. To address these questions, *Xenopus* oocytes were injected with *in vitro* transcribed RNAs encoding either the non-edited [Kv1.1(I)] (N) or edited [Kv1.1(I)] (E) isoforms of the wild-type, V404I, I407M, or V408A mouse Kv1.1 subunits, expressed as homotetramers.

The voltage dependence of activation for each channel subtype was analyzed to determine editing-dependent changes, and representative traces for each channel are shown in Figure 3.5. The relationship between macroscopic conductance and voltage was quantified for each channel type. For most constructs, this was derived from normalized tail current measurements; however, V408A E closed too quickly for accurate measurements of tail currents so conductance was measured using outward currents (*see Equation 3.1 in Materials & Methods*). Conductance (G) versus voltage (V) curves were fit to a Boltzmann function (Equation 3.2),

$$G = \frac{1}{1 + e^{\frac{V_{1/2} - V}{k}}} \qquad (3.2)$$

to estimate the midpoint of channel activation ($V_{1/2}$) and the relative voltage sensitivity (k) (Table 3.2). Consistent with previous reports for I407M N channels(Tomlinson et al., 2013), we observed a 30 mV positive shift in the $V_{1/2}$, but this change was not influenced by editing (Figure 3.5 and Table 3.2). By contrast, V404I also caused a positive shift, but it was more pronounced for the non-edited channel (a shift of 22.1 mV for the non-edited channel, 14.2 mV for the edited channel). Thus, editing partially ameliorated the alteration in channel function caused by the V404I mutation. V408A channels did not exhibit altered voltage-dependence for either the non-edited or edited isoforms. Editing had little effect on voltage sensitivity for any of the wild-type or mutant homotetrameric channels.

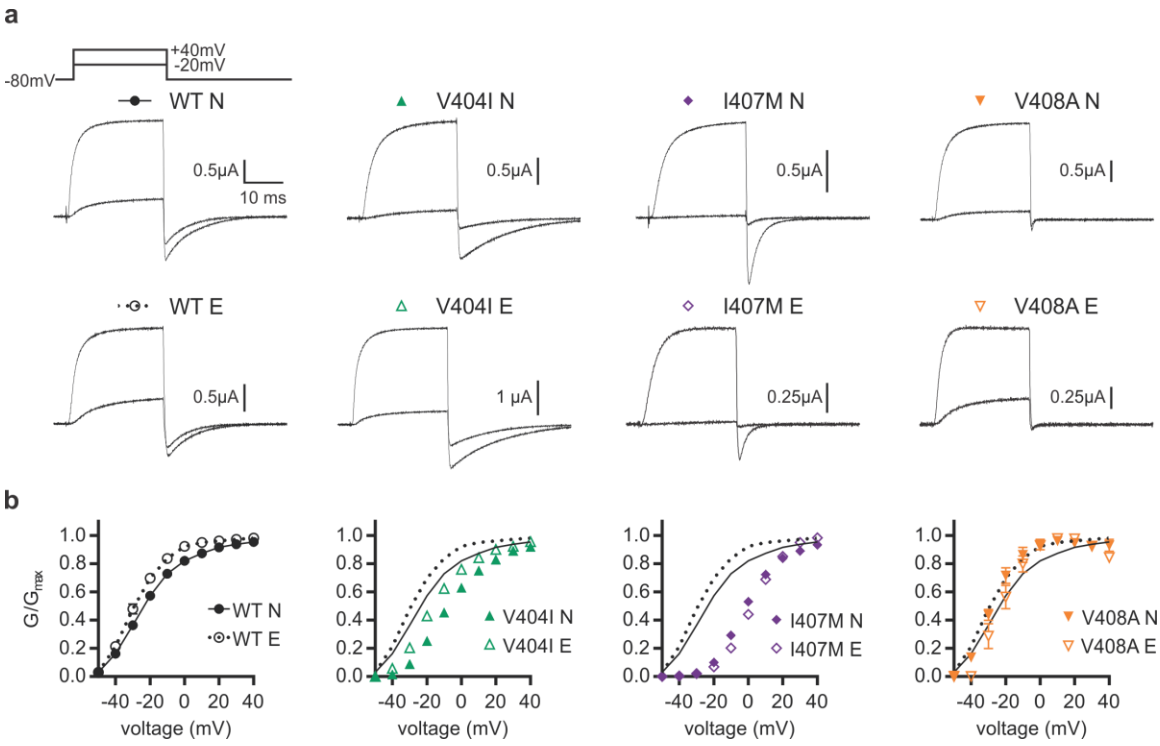

Figure 3.5. Voltage-dependence of non-edited compared to edited mutant channels. Whole-cell K+ currents were recorded from oocytes expressing either the non-edited (N) or edited (E) isoforms of homotetrameric wild-type (WT), V404I, I407M, or V408A mouse Kv1.1 channels. Test potentials were elicited in 10 mV voltage steps from -50 to 40 mV, from a holding potential of -80mV. **(a)** Representative activating traces at -20 and 40 mV are shown for each construct. **(b)** Conductance (G) versus voltage plots are shown where data has been normalized to the maximal conductance (Gmax), demonstrating shifts in voltage dependence for I407M and V404I. Normalized conductance was measured from tail current amplitude for all channel types except for V408A E, which exhibited tail currents too fast to measure and was derived by Ohm's Law (Equation 3.1), as described in the *Materials and Methods*. Conductance (G) versus voltage plots were normalized to the maximal conductance (Gmax) (mean ± SEM, n = 4-8 oocytes). Small error bars may be obscured by the data symbols in some cases.

	$V_{1/2}$ (mV)	k (mV)
WT N	-31.6 ± 1.7	16.0 ± 0.9
WT E	-34.5 ± 2.3	12.3 ± 1.4
V404I N	-9.5 ± 1.4 **** +++	14.7 ± 1.1
V404I E	-20.3 ± 1.5 ***	14.2 ± 0.9
I407M N	-1.9 ± 0.8 ****	10.7 ± 0.2 *** ++
I407M E	2.5 ± 1.1 ****	9.4 ± 0.2
V408A N	-29.4 ± 0.9	9.1 ± 1.0 ***
V408A E	-23.6 ± 3.4	8.1 ± 0.4

Table 3.2. Voltage-dependence of activation. Voltage-dependence of activation was determined by fitting data to a Boltzmann function (Equation 3.2), to determine the mid-point of channel activation (V1/2) and relative voltage sensitivity (k). All data are represented as mean ± SEM, n=4-8 oocytes for each channel type. Non-edited (N) and edited (E) isoforms of the mutant channels were compared to WT E and WT N channels, respectively: ***p≤0.001; ****p<0.0001. All types of N channels were compared to their respective E channels: ++p≤0.005; +++p≤0.001. Significance was determined by two-sample t-tests; due to multiple comparisons, significance was set at p≤0.005.

To examine how editing affected channel opening kinetics, the time to reach half-maximal activation across a range of voltages was determined (Figure 3.6). The only editing-dependent change was observed for the I407M mutation. Both I407M channels opened more slowly than their wild-type counterparts, but the slowing was more severe for I407M E channels, leading to channels with an exacerbated slow opening phenotype. In addition, I407M E and V408A E channels demonstrated non-linearity in their voltage dependence for outward currents (Figure 3.7). This was particularly evident at very positive voltages, where I407M E and V408A E channels reached peak current amplitudes at 50 and 40 mV respectively, with further voltage steps resulting in decreasing current amplitudes.

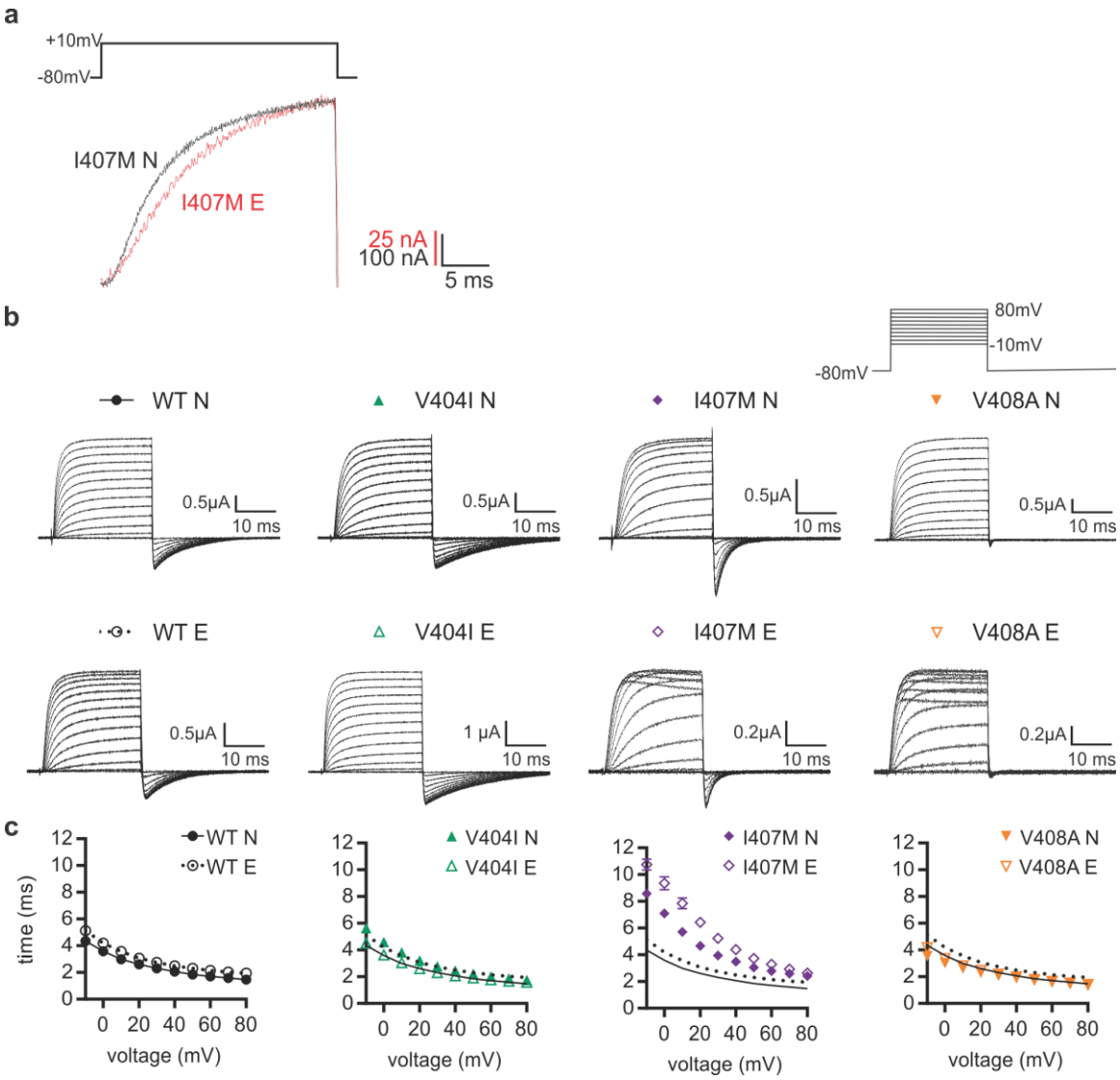

Figure 3.6. Editing alters opening (activation) kinetics of I407M channels. **(a)** Example trace overlay of I407M editing dependent alteration of opening kinetics at the 10mV activating pulse **(b)** Representative activation traces, depicting whole-cell currents, were recorded from oocytes expressing either a non-edited (N) or edited (E) isoform of the wild-type (WT) or mutant mouse Kv1.1 channel. Test potentials were elicited in 10 mV voltage steps from -10 to 80 mV, from a holding potential of -80 mV. **(c)** Opening kinetics were measured as the time to reach half-maximal current amplitude and individual group comparisons for p-values were based on the Wald tests of model-based predicted (least square) means (mean ± SEM, n=3-7 oocytes). I407M N and I407M E channels were significantly slowed in their time to half-activation compared to each other, in the voltage range -10 to 70 mV ($0.05 > p \geq 0.0008$). I407M N was significantly slower than WT N at all voltages ($p \leq 0.0001$) and I407M E was significantly

slower than WT E at all voltages (0.01 > p ≥ 0.0001). Small error bars were obscured by the data symbols in some cases.

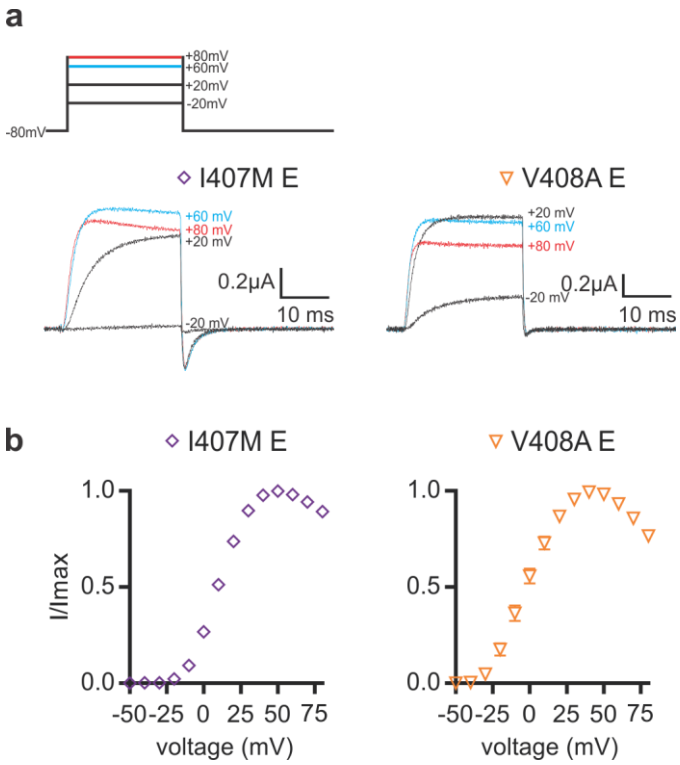

Figure 3.7. I407M E and V408A E channels display decreased currents at the most positive voltages. Whole-cell K+ currents were recorded from oocytes expressing either the I407M E or V408A E mouse Kv1.1 channel. Test potentials were elicited in 10 mV voltage steps from -50 to 80 mV, from a holding potential of -80 mV. **(a)** Representative traces for I407M E and V408A E channels are shown, indicating loss of current amplitude at the highest voltages. Voltages at 60mV (blue) and 80mV (red) are colored for clarity. **(b)** Current (I) versus voltage plots, normalized to the maximal current (Imax), are shown; note the unusual bell-shaped curves. Data points represent mean ± SEM (N=7-8 oocytes). Small error bars were obscured by the data symbols in some cases.

Closing (deactivation) kinetics were measured by fitting single exponential curves to tail current traces to obtain estimates of tau (τ), the reciprocal of the closing rate constant (Figure 3.8). Editing resulted in wild-type channels closing slightly faster. In addition, the I407M and V408A mutations greatly increased closing speeds on their own. The editing of I407M channels had only a small effect on deactivation kinetics, while the edited V408A channels closed so quickly that the closing rate could not be accurately measured. Unlike the other mutations, however, V404I led to slower closing speeds and editing partially ameliorated this phenotype.

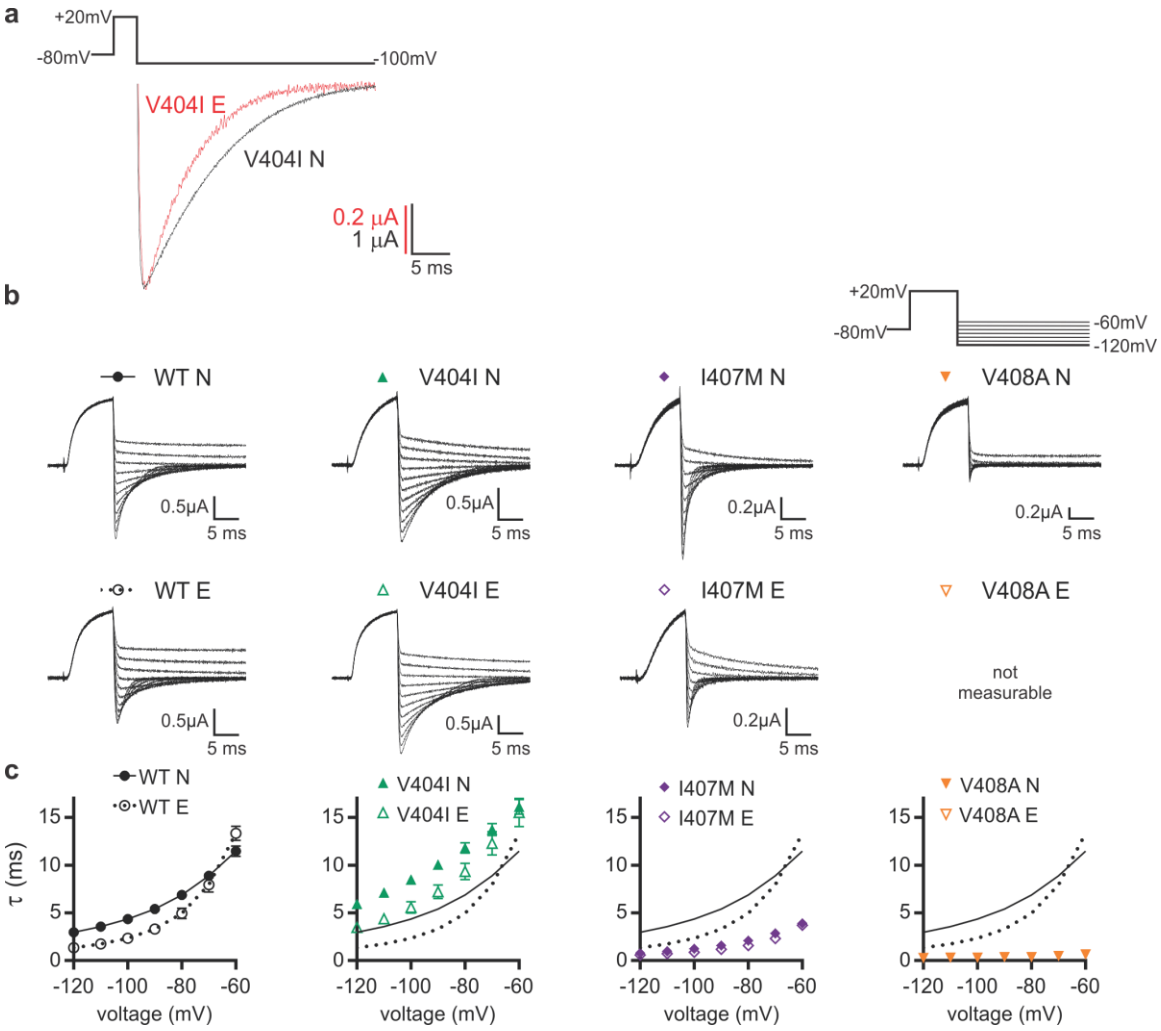

Figure 3.8. Editing alters closing (deactivating) kinetics of V404I channels. **(a)** Example trace overlay of V404I editing dependent alteration of closing kinetics at the -100mV deactivating pulse **(b)** Representative tail current traces, depicting whole-cell K+ currents, were recorded from oocytes expressing either a non-edited (N) or edited (E) isoform of the wild-type (WT) or mutant mouse Kv1.1 channel. Following a holding potential of -80 mV and a depolarizing pulse to 20 mV, test potentials were elicited in 10 mV voltage steps from -120 to -60 mV. **(c)** Closing kinetics were determined by fitting the tail currents with single exponential curves to determine the associated τ value; individual group comparisons for p-values were based on the Wald tests of model-based predicted (least square) means (mean ± SEM, n = 3-6 oocytes). WT N and WT E channels closed significantly slower than each other from -120 to -80 mV ($0.05 > p \geq 0.0002$). V404I N channels closed slower than V404I E from -120 to -100 mV ($0.05 > p \geq 0.0066$). V404I N channels closed slower than WT N at all voltages ($p < 0.0001$) and V404I E channels closed significantly slower than WT E channels from -120 to -80 mV ($0.01 \geq p \geq 0.0005$). I407M E channels closed significantly

faster than I407M N channels from -120 to -80 mV ($0.05 > p \geq 0.0036$). I407M N and I407M E channels closed significantly faster than their WT counterparts at all voltages tested (N: $p \leq 0.0001$; E: $0.01 > p \geq 0.0001$). V408A E channels closed too quickly for measurement, but V408A N channels closed significantly faster than WT N channels at all voltages ($p \leq 0.0001$). Small error bars were obscured by the data symbols in some cases.

Slow inactivation (C-type) was examined by analyzing channel function under conditions of long depolarizations. The I407M E and V408A E channels demonstrated editing-dependent dysfunction, with a prominent fast component of their inactivation appearing alongside the slow component. Thus, while a single exponential function was sufficient to describe the inactivation for the majority of the channels, I407M E and V408A E required a double exponential fit (Figure 3.9a). Both the fast and slow components of the I407M E and V408A E channels were fast compared to their non-edited counterparts (Figure 3.9b). By contrast, the extent of inactivation was predominantly mutation-driven, except for the V408A mutation, in which editing decreased the extent of inactivation, bringing it closer to wild-type levels (Figure 3.9c).

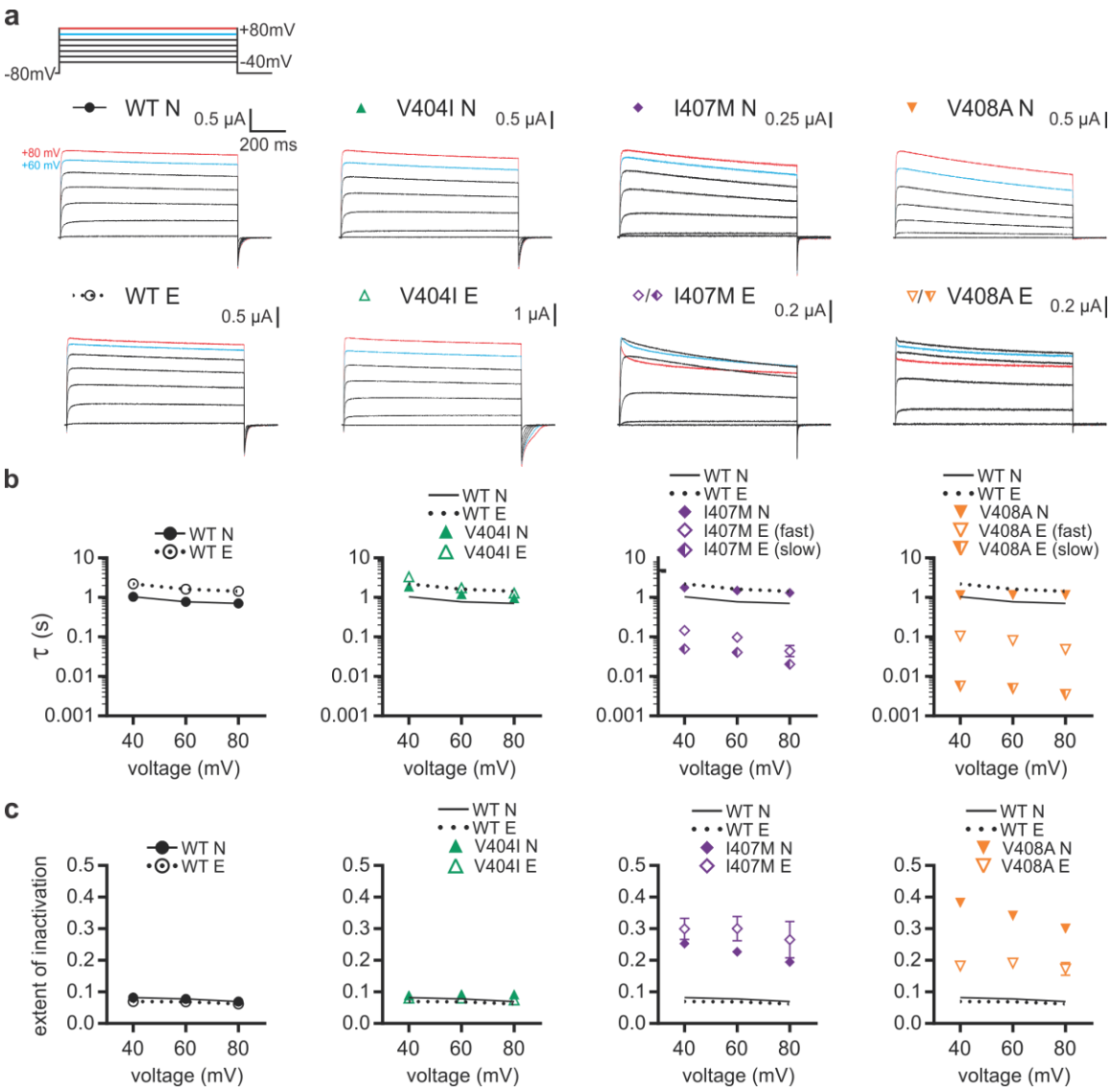

Figure 3.9. Long pulse characterization of WT and EA1 channels. (a) Representative traces, depicting whole-cell K+ currents, were recorded from oocytes expressing either a non-edited (N) or edited (E) isoform of the wild-type (WT) or mutant mouse Kv1.1 channel. Test potentials were elicit-ed in 20 mV voltage steps from -40 to 80 mV for 1 s, from a holding potential of -80 mV. Voltages at 60mV (blue) and 80mV (red) are colored for clarity. **(b)** The slow inactivation was predominantly measured by fitting single exponential curves to the test pulse currents to determine τ values, however the I407M E and V408A E channels were best fit by double exponential curves with fast and slow τ values (mean ± SEM, n=6-7 oocytes). Both the fast and slow τ values of I407M E were significantly faster than I407M N channels at all voltages tested. I407M N channels were significantly different from WT N from 60 to 80mV (though within

the range of WT E). Both the fast and slow τ values of V408A E were significantly faster than V408A N channels at all voltages tested. **(c)** Extent of inactivation was measured by dividing the amplitude of inactivation by the total amplitude (mean ± SEM, n=3-7 oocytes). I407M N channels had significantly greater inactivation that WT N channels at all voltages tested. V408A N channels had significantly increased inactivation compared to V408A E at all voltages tested. V408A N had significantly greater inactivation that WT N at all voltages tested and V408A E was significantly different from WT E channels from 40 to 60mV. Significance was determined by two-sample t-tests; due to multiple comparisons, significance was set at $p \leq 0.0012$ for **(b)** and $p \leq 0.0017$ for **(c)**. Small error bars were obscured by the data symbols in some cases.

Inactivation kinetics are altered between non-edited and edited EA1 mutant proteins

Previous characterization of non-edited and edited wild-type Kv1.1 channels found that the most profound difference was a change in the rate of recovery from channel inactivation, presumably by altering interactions with an inactivating Kvβ subunit (Bhalla et al., 2004). To determine the effect of EA1 mutations on this biophysical property, non-edited and edited isoforms of the wild-type, V404I, I407M, and V408A channels were co-expressed with Kvβ1.1 to measure N-type, fast inactivation kinetics and recovery from inactivation.

Oocytes expressing each channel subtype, along with Kvβ1.1, were subjected to short depolarizing pulses to different voltages and the resulting fast inactivation traces were fit to a single exponential (Figure 3.10). These studies identified a previously uncharacterized difference in wild-type channels where editing modestly slowed the rate of channel inactivation. V404I N and E channels inactivated within the wild-type range, without exhibiting any editing-dependent

changes. Inactivation for non-edited isoforms of the I407M and V408A mutants resembled edited, wild-type channels, however, editing of I407M and V408A resulted in drastically slower rates of inactivation for both channels. This effect was most extreme and apparent at all voltages for I407M E, whereas slowing was only observed for V408A E with shallow depolarizations. Interestingly, the V404I N channels also exhibited a low extent of inactivation where inactivation could not be measured in over half the oocytes tested. This variability in the extent of inactivation for the mutant channels is consistent with previous studies demonstrating that the extent of inactivation could be manipulated by varying the aliphatic amino acid residues at the position of the editing site (Gonzalez et al., 2011).

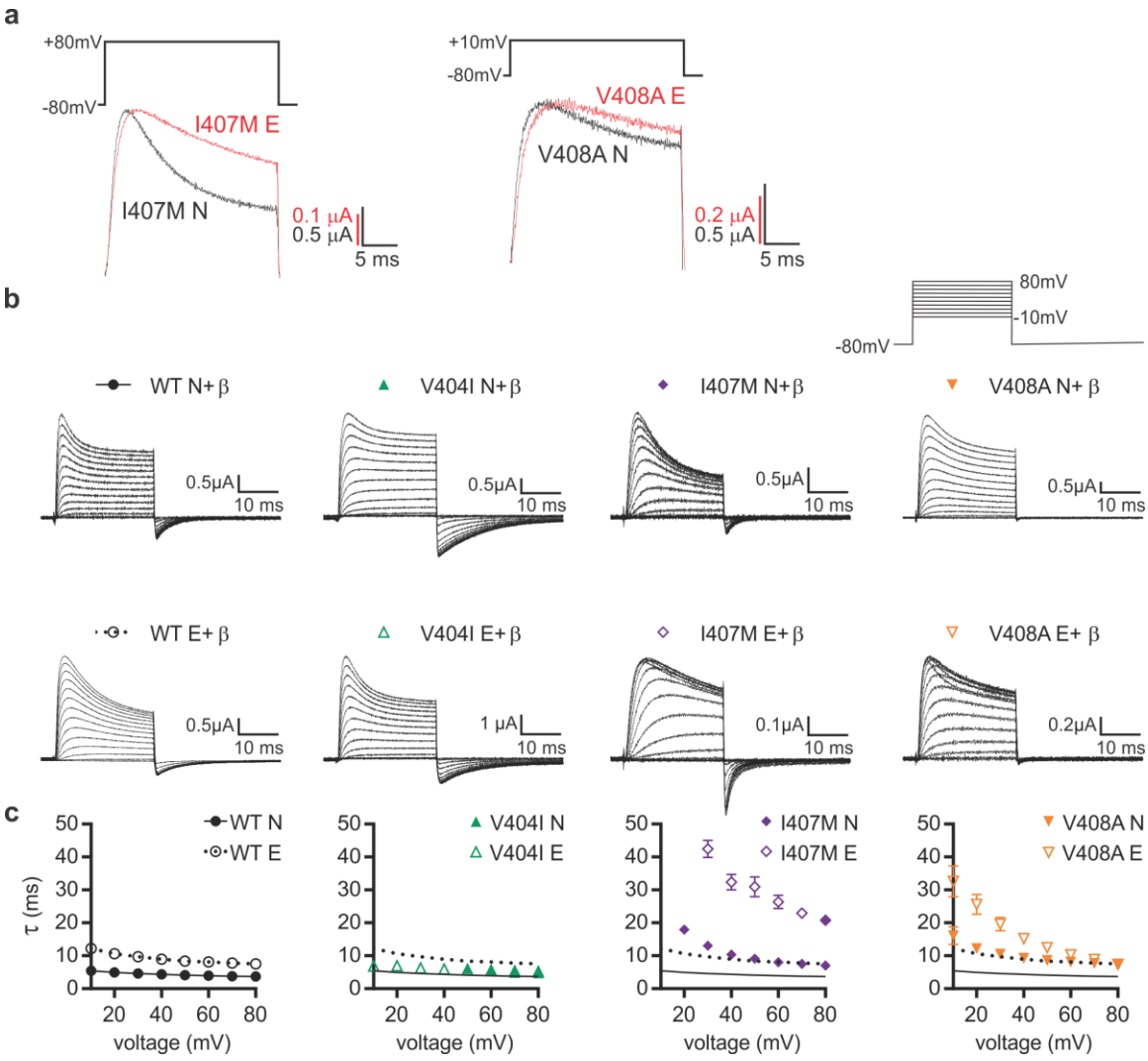

Figure 3.10. Editing slows Kvβ1.1-induced inactivation kinetics of I407M and V408A channels. (a) Example trace overlays of I407M and V408A editing-dependent alterations of Kvβ1.1-inactivation kinetics at the 80 and 10 mV activating pulses, respectively **(b)** Representative Kvβ1.1-inactivation traces, depicting whole-cell currents, were recorded from oocytes expressing either a non-edited (N) or edited (E) isoform of the wild-type (WT) or mutant mouse Kv1.1 channel, co-expressed with mouse Kvβ1.1. Test potentials were elicited in 10 mV voltage steps from 10 to 80 mV, from a holding potential of -80 mV. **(c)** Inactivation kinetics were measured by fitting single exponential curves to the test pulse currents, to determine the associated τ value; individual group comparisons for p-values were based on the Wald tests of model-based predicted (least square) means (mean ± SEM, n=3-6 oocytes). WT E channels were significantly slower than WT N channels at every voltage ($p \leq 0.0001$). V404I N and V404I E were not significantly different from each other, though

each was significantly different from their respective WT counterpart (N: $0.05 > p \geq 0.0052$; E: $0.01 > p \geq 0.0002$). I407M E channels were significantly slower to inactivate than I407M N channels at every voltage ($p \leq 0.0001$) and both I407M N and I407M E channels were slower than WT N and WT E channels, respectively, at every voltage ($p \leq 0.0001$). V408A E channels were significantly slower than V408A N channels from 10 to 50mV ($0.05 > p \geq 0.0005$). V408A E channels were slower than WT E channels from 10 to 60mV ($0.05 > p \geq 0.0001$). V408A N channels were significantly slower than WT N channels at all voltages ($p \leq 0.0001$). Small error bars were obscured by the data symbols in some cases.

Long depolarizing pulses were measured to determine the fast and slow components of Kv1.1 channels when co-expressed with Kvβ1.1 (Figure 3.11). Double exponential curves were fit to the inactivating traces, to determine the fast and slow τ values and the relative amplitude of the fast component of the inactivation (compared to the slow component). The fast and slow τ values largely corresponded to the results described for the β-inactivation of the short pulses and the slow inactivation of the long pulses without Kvβ1.1 (*data not shown*). In wild-type channels, editing led to an increase in the relative amplitude of the fast component of inactivation. An editing-dependent change also was observed for the V404I channels, where editing brought the relative amplitude of the fast component closer to that of the wild-type channel.

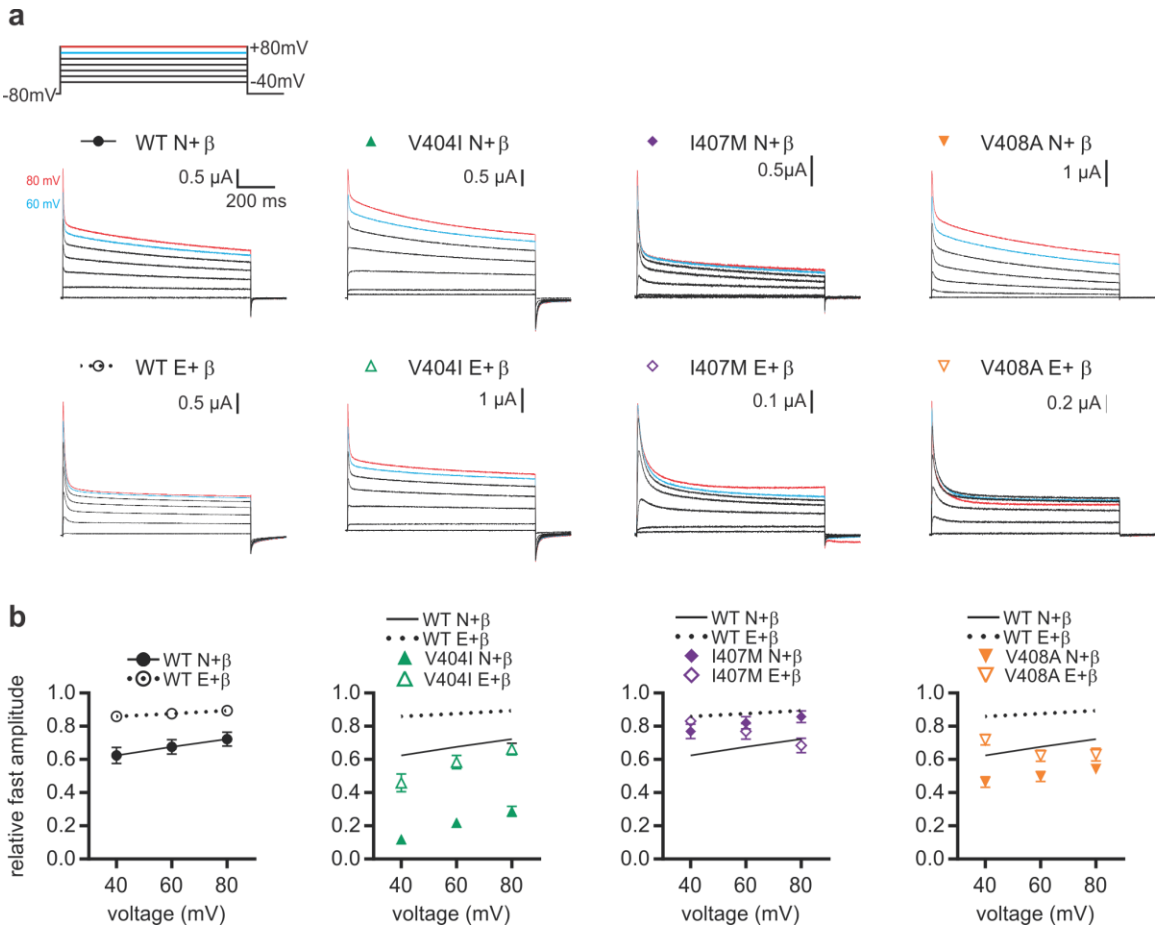

Figure 3.11. Long pulse characterization of Kvβ1.1-inactivation of WT and EA1 channels. (a) Representative Kvβ1.1-inactivation traces, depicting whole-cell K+ currents, were recorded from oocytes expressing either a non-edited (N) or edited (E) isoform of the wild-type (WT) or mutant mouse Kv1.1 channel, co-expressed with mouse Kvβ1.1. Test potentials were elicit-ed in 20 mV voltage steps from -40 to 80 mV for 1 s, from a holding potential of -80 mV. Voltages at 60mV (blue) and 80mV (red) are colored for clarity. **(b)** The slow and fast inactivation was measured by fitting double exponential curves to the test pulse currents to determine the relative amplitude of the fast component of the inactivation (fast amplitude as a ratio of the total inactivation amplitude) (mean ± SEM, n=5-7 oocytes). Significance was determined by two-sample t-tests; due to multiple comparisons, significance was set at $p \leq 0.0017$. WT E channels were significantly slower than WT N channels from 40 to 60mV. V404I N and V404I E were significantly different from each other at every voltage tested, as well as compared to their respective WT counterpart. I407M N and I407M E channels were not significantly different from each other, though I407M E was significantly lower than WT E at 80mV. V408A N and V408AE channels only differed from one another at 40mV, and V408A E channels differed from WT E at 60 and 80mV. Small error bars were obscured by the data symbols in some cases.

Finally, the rate of recovery from fast inactivation was measured using a two-pulse protocol, where the fractional recovery at specific time intervals was assessed after the onset of inactivation. A representative experiment for oocytes expressing either I407M N or E channels is presented in Figure 3.12a. As previously reported in Bhalla *et al.* (2004), editing increased the rate of recovery when comparing non-edited and edited isoforms of the wild-type channel (Figure 3.12b) (Bhalla et al., 2004). All edited isoforms of the mutant channels exhibited a significantly faster rate of recovery than their respective non-edited counterparts (Figure 3.12b and Table 3.3). Recovery from inactivation for the V404I E channel was significantly slower than that of the WT E channel, whereas for the I407M N, I407M E, and V408A N channels it was faster compared to its corresponding wild-type channel. Although the extent of the effect differed for each mutation, editing resulted in a unique and substantial contribution to the rate of recovery from fast-inactivation for each channel type.

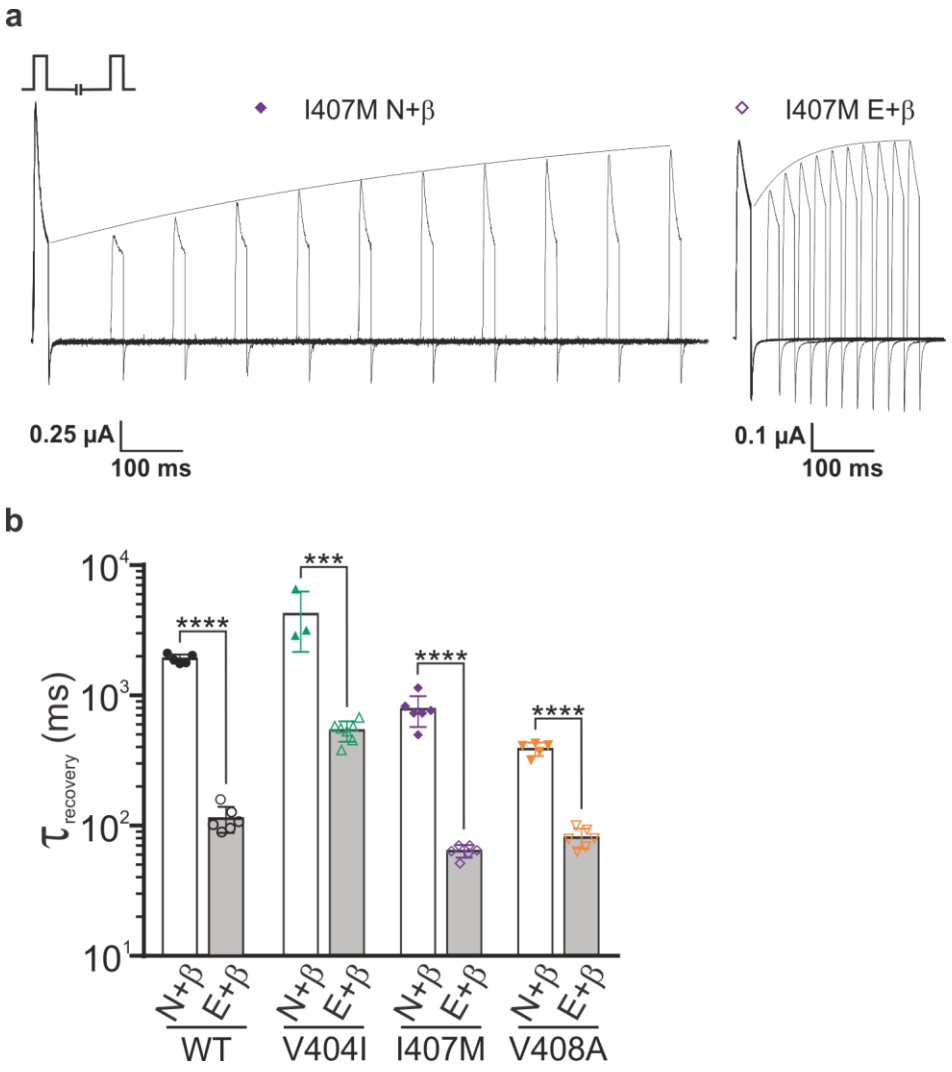

Figure 3.12. Editing alters the recovery from Kvβ1.1-induced inactivation in V404I, I407M, and V408A channels. Whole-cell K+ currents were recorded from oocytes co-expressing the mouse Kvβ1.1 subunit and either a non-edited (N) or edited (E) isoform of the wild-type (WT) or mutant mouse Kv1.1 channel. **(a)** Representative I407M N and I407M E recovery traces are overlaid to depict the increased rate of recovery from β-inactivation, typical of an E isoform. A two-pulse protocol was used, eliciting a depolarizing pulse to 80 mV followed by a variable interpulse duration at -80 mV before a final depolarizing pulse at 80 mV. Recovery from β-inactivation was plotted as the time for the second pulse to regain the current amplitude of the first pulse. **(b)** τ values were determined by fitting single exponential curves to the recovery plots (mean ± SEM, n=3-7 oocytes, ***p ≤ 0.001, ****p ≤ 0.0001).

	τ (ms)		fold change N vs. E
WT N+β	1912 ± 68.55	++++	16.8
WT E+β	113.6 ± 10.46		
V404I N+β	4218 ± 1189	+++	7.8
V404I E+β	538.0 ± 36.29****		
I407M N+β	783.2 ± 85.15****	++++	12.3
I407M E+β	63.82 ± 2.887***		
V408A N+β	388.4 ± 20.20****	++++	3.3
V408A E+β	80.83 ± 5.709		

Table 3.3. Kinetics of recovery from Kvβ1.1 inactivation. All data represent mean ± SEM, n=3-7 oocytes for each channel type. Mutant N and E channels were compared to their WT N and E channels, respectively: ***p ≤ 0.001; ****p ≤ 0.0001. All types of N channels were compared to their respective E channels: +++p ≤ 0.001; ++++p ≤ 0.0001. Significance was determined by two-sample t-tests; due to multiple comparisons, significance was set at p ≤ 0.005.

Discussion

Proof of concept that existing mutations alter RNA editing

The conversion of A-to-I by RNA editing has been shown to represent an important post-transcriptional modification by which to modulate the function of numerous proteins critical for nervous system function (Hood and Emeson, 2012). Previous studies have shown that site-selective editing of transcripts encoding the Kv1.1 channel can affect the rate of recovery from channel inactivation, the binding of drugs and highly unsaturated fatty acids, the regulation of homotetrameric Kv1.1 channel trafficking, and seizure-susceptibility in chronic epileptic rats (Bhalla et al., 2004; Decher et al., 2010; Gonzalez et al.,

2011; Streit et al., 2011; Streit et al., 2014). While numerous EA1-associated mutations have been identified throughout the *KCNA1* coding region, several of these mutations (V404I, I407M, and V408A) are within close proximity to the Kv1.1 editing site (I400V) and also are predicted to disrupt the critical RNA duplex structure required for this post-transcriptional modification.

To our knowledge, the present studies represent the first demonstration that disease-associated mutations can disrupt critical *cis*-regulatory elements to change their gene's RNA editing profile, by altering the RNA structure required for site-selective A-to-I conversion. It is well established that artificially incorporating mutations in an RNA duplex can abolish editing by disrupting duplex pairing; indeed, this technique was used to experimentally verify the RNA duplex responsible for Kv1.1 editing (Bhalla et al., 2004; Dawson et al., 2004). However, this is the first evidence that existing human mutations in an RNA can disrupt its own editing and represents a unique advancement in our understanding of the mutational consequences of human disorders involving RNA editing targets. Results using both *in vitro* and *in vivo* model systems have shown significant reductions in the extent and rate of editing for Kv1.1 transcripts harboring specific EA1 mutations (Figures 3.3 and 3.4). Importantly, because the wild-type allele RNA was unchanged in the V408A/+ mouse model, it is likely that the observed changes in the editing of the V408A allele-derived RNA were solely due to the V408A mutation and not due to any developmental, compensatory changes. These *in vitro* and *in vivo* data serve as a proof of concept that even single nucleotide changes in an RNA can alter its RNA editing potential.

Furthermore, our studies suggest that both synonymous and non-synonymous duplex-disrupting mutations and single nucleotide polymorphisms within Kv1.1 and other edited RNA targets may also affect the expression of their specific edited isoforms, thus altering the activity of the encoded protein products. And more broadly, the mutations we studied affect Kv1.1 RNA interactions with the editing enzyme and dsRNA-binding protein, ADAR2, and could indicate that mutational consequences in other genes should be studied not only for the amino acid changes, but also for their alterations on RNA-binding protein interactions.

Edited Isoforms of EA1 mutants alter electrophysiological properties

These studies also have revealed that the effects of EA1 mutations on Kv1.1 function are far more complex than originally anticipated, as each mutation produces channels with unique biophysical properties that depend on the I400V amino acid identity, mediated by RNA editing. The V404I mutation altered several electrophysiological parameters on its own, but the edited isoform demonstrated less drastic changes than the non-edited isoform, as observed for channel voltage sensitivity, closing kinetics, and the amplitude of β-inactivation (Figures 3.5, 3.8, and 3.11). Although it is tempting to speculate that editing could dampen the defects in channel function resulting from this point mutation, it also should be noted that this mutation largely prevents the RNA from being edited in the first place (Figure 3.3). Thus, it is anticipated that edited V404I isoforms

contribute little to the electrophysiological properties of Kv1.1 channels in those tissue where they are expressed.

Unlike the V404I channel, however, editing combined with the I407M or V408A mutations led to more severe channel dysfunctions than the non-edited isoforms. Edited isoforms of both I407M and V408A exhibited unusually slow β-dependent inactivation kinetics (Figure 3.10) and severe defects in activation at higher voltages (Figure 3.7). The current-voltage curves of I407M E and V408A E were bell-shaped, resembling the 'rapid' delayed rectifier activation kinetics typical of Kv11.1 (hERG) channels, though reaching peak amplitudes at markedly higher voltages than Kv11.1 (Figure 3.7) (Sanguinetti et al., 1995). These defects could possibly be caused by a significantly faster entry into, or slower recovery from, C-type inactivation (Figure 3.9) (Sanguinetti et al., 1995). In addition, while the I407M mutation slowed the kinetics of channel opening, the effect was greater for the edited isoform (Figure 3.6). These studies also extended the characterization of the I407M mutation, as previous studies of the non-edited I407M channel reported only alterations in expression and voltage-sensitivity, while the present study also shows changes in kinetics (Tomlinson et al., 2013).

Although our studies suggest that edited isoforms of mutant channels represent a smaller portion of the total Kv1.1 population, they may still exert functional effects, particularly in tissues with higher editing levels (such as cerebellum and spinal cord) (Figure 3.4). This is supported by previous studies, which have shown that incorporating even one edited subunit into a Kv1.x

heterotetramer was sufficient to alter its sensitivity to open-channel blocking molecules (Decher et al., 2010). Alternatively, despite the many functional differences observed between edited isoforms of the mutant channels, all recovered from fast inactivation significantly faster than their non-edited counterparts (Figure 3.12). As these EA1 mutations reduced their own isoform editing, it is predicted that the overall recovery from fast inactivation *in vivo* will be comparatively slow, possibly resulting in unanticipated effects that could prevent normal neuronal signaling.

Incorporating RNA editing into the complex interactions involved in the EA1 disorder

While no clear correlation has been established between the diverse clinical phenotypes of EA1 patients and specific mutations within Kv1.1 (Graves et al., 2014; Graves et al., 2010), part of the observed variability in symptoms might be explained by differences in RNA editing. These phenotypic differences could arise from EA1 mutations that disrupt the editing duplex, or from overall changes in Kv1.1 editing regulation. Although the mechanisms regulating Kv1.1 RNA editing are largely unknown, recent studies have demonstrated that inducing rats with chronic epilepsy led to a 4-fold increase in Kv1.1 editing in the entorhinal cortex (Streit et al., 2011). Interestingly, once Kv1.1 editing was increased, recordings in isolated rat brain slices demonstrated that these animals had a decreased sensitivity to 4-AP-induced seizure-like events, suggesting that

increasing editing might dampen seizure susceptibility. Similarly, analyses of patients undergoing surgery for mesial temporal lobe epilepsy revealed that having increased levels of Kv1.1 RNA editing was negatively correlated with the period of years that the patients had experienced epileptic activity (Krestel et al., 2013), suggesting that decreased Kv1.1 editing may represent a risk factor for long-term seizures. Graves *et al*. (2010) clinically surveyed two families containing the same EA1 mutation (F414S), and found that one family exhibited seizures while the other did not, raising the possibility that additional factors, such as differences in editing regulation, could represent an explanation for these phenotypic differences (Graves et al., 2010). As previous studies have shown that open-channel blocking drugs interact less with edited Kv1.1 homo- and heterotetramers (Decher et al., 2010), a precise therapeutic strategy for the treatment of Kv1.1-dependent seizures may require not only a knowledge of the specific mutation(s) involved, but also the editing profiles of Kv1.1 transcripts.

CHAPTER IV

CONCLUSIONS

Significance

Kv1.1 is an important voltage gated α-subunit and human mutations have revealed that its misregulation contributes to epilepsy and the EA1 disorder. Although Kv1.1 RNA editing is known to be regulated differentially in the brain, until now, its impacts were mainly proposed from exogenous expression studies within cell lines and *Xenopus* oocytes. This work has begun the process of understanding the role of Kv1.1 RNA editing within the context of normal physiology, as well as its implications for the EA1 disorder.

By utilizing two newly developed mouse models, we have characterized the effects of solely expressing either the non-edited [Kv1.1(I)] or edited [Kv1.1(V)] isoforms in mice. We have observed that our editing mouse models share similarities with previously characterized Kv1.1 and Kvβ mouse models, relating to ataxia and seizure-susceptibility. The non-edited [Kv1.1(I)] mouse displays EA1-like stress-induced ataxia, similar to the V408A/+ mouse (Herson et al., 2003). This is particularly salient because our EA1 experiments have demonstrated that the V408A mutation leads to decreased editing *in vivo*; thus ataxia might have a multifaceted onset arising from either mutant Kv1.1 or

editing-deficient Kv1.1. The non-edited [Kv1.1(I)] and edited [Kv1.1(V)] mice display diverging susceptibilities to 4-AP-induced seizures, where the non-edited [Kv1.1(I)] mice required a smaller concentration of drug for seizure symptoms compared to the wild-type littermates and the edited [Kv1.1(V)] mice required a greater concentration. This is in agreement with the studies of Streit *et al.* (2011), which compared the 4-AP susceptibility of rats with higher versus lower Kv1.1 RNA editing. Importantly, we have also observed that the dampening of seizure susceptibility observed in the edited [Kv1.1(V)] mice is translatable to PTZ seizure induction as well, indicating that Kv1.1 RNA editing may have a protective effect against seizures arising from disparate pathways of initiation and propagation. Although no changes in signaling were observed upon electrophysiological characterization of dentate granule cells of the hippocampus, interestingly other mouse models of Kv1 and Kvβ alterations also do not show overt changes in electrophysiology, such as the intrinsic membrane properties of the Kv1.1-null mice.

Our characterization of the complex interplay between RNA editing and EA1 mutations have revealed new mechanisms of channel dysfunctions to factor into our broader understanding of this human disorder. First, we have demonstrated that at least three documented EA1 mutations contain the ability to inhibit Kv1.1 RNA editing *in vitro*, and confirmed that the V408A mutation inhibits editing *in vivo*. We observed that the *in vivo* decreases in editing were more severe than would be predicted by our *in vitro* editing assay- indicative of the presence of further regulatory factors that mediate the rate of editing *in vivo*.

Unfortunately, little is known about the regulation of RNA editing, though particular nucleotide motif biases and structural determinants play a dominant role in setting the rates (Dawson et al., 2004). It was surprising that only single-nucleotide changes in the Kv1.1 duplex were necessary to impair editing to such a high degree, as well as that the level of editing impairment was related to the proximity to the editing site (with the closest mutation,V404I, leading to the greatest impairment in editing). This may be indicative that the Kv1.1 duplex is particularly susceptible to mutation-driven decreases in RNA editing because it is a relatively poor ADAR2 substrate; this is supported by data which shows that Kv1.1 editing is low compared to other ADAR2 substrates sequences isolated from the same tissue dissections, across development and in adult mice (ex. GluA2 Q/R site and the $5HT_{2C}$ D site) (Hood et al., 2014; Jacobs et al., 2009). In addition, we experimentally observed that the wild-type Kv1.1 duplex was a poorer substrate compared to the $5HT_{2C}$ RNA duplex, which was used as a positive control for the *in vitro* editing assay (*data not shown*). The susceptibility of mutations leading to RNA disruptions signifies that other mutations, including silent mutations or single-nucleotide polymorphisms within the Kv1.1 duplex may also be able to disrupt Kv1.1 editing.

And, finally, edited isoforms of EA1 mutant proteins were shown to have altered electrophysiological properties compared to their non-edited counterparts. The type and severity of the defects were unique to each mutation. The edited V404I mutant channels seemed to normalize the biophysical properties that were dysfunctional in the non-edited V404I channels. In contrast, the edited I407M and

V408A mutant channels often displayed more severe defects compared to their non-edited counterparts. The role of editing on setting the fast rate of recovery from β-inactivation was noticeably similar between wild-type and mutant channels, indicating that the I400V amino acid has a particularly important role in this capability, regardless of mutations. However, the expression of these edited channels will depend on each mutation's disruption of normal RNA editing. If RNA editing is decreased substantially in patients with duplex mutations, then the altered edited mutant channels may have little effect on overall physiology. In contrast, the editing-dependent fast rate of the recovery from β-inactivation would be prominently lost if editing is lowered substantially. As the EA1 disorder is a multifaceted disorder with incomplete penetrance, additional factors, including the presence of edited mutant isoforms, may be able to explain the clinical and genetic heterogeneity in symptom severity.

Future Directions

Utilizing the newly developed mouse models of Kv1.1 editing

Although our studies have brought new insights into the role of Kv1.1 RNA editing for normal physiology and in the context of EA1, new questions can now be raised in response. First of all, we have developed new mouse models of Kv1.1 editing, the non-edited [Kv1.1(I)] and edited [Kv1.1(V)] mice, which should continue to be characterized in-depth. And our studies of the implications of

Kv1.1 RNA editing on the complexity of EA1 provide a new avenue for investigating this multifaceted disorder.

Our mouse models offer a unique opportunity to study the impacts of the non-edited [Kv1.1(I)] and edited [Kv1.1(V)] isoforms *in vivo*, starting with a detailed study of each isoform's localization and heterotetrameric assembly in the brain. Immunohistochemistry of non-edited [Kv1.1(I)], edited [Kv1.1(V)], and wild-type brain slices can be performed to determine whether editing alters Kv1.1 localization in different brain regions, as well as the impacts on other Kv1 family members and β-subunits. In addition, subcellular localization may be determined by differential centrifugation strategies to isolate different membrane protein fractions. Alterations in localization at the plasma membrane versus the ER could be determined by Western blot analysis and performed in concert with Kv1.1-pull-down studies to probe for other Kv1.x and β-subunits (particularly for co-assembly with Kv1.2, Kv1.4, Kvβ1, Kvβ2). These studies will be important for determining whether localization and heterotetrameric assembly differs for non-edited and edited Kv1.1.

Although we have performed many behavioral tests to compare the non-edited [Kv1.1(I)] and edited [Kv1.1(V)] mice, there are several others that could give important insights. Kv1.1 has known roles in mechanosensation and nociception (Clark and Tempel, 1998; Galeotti et al., 1997; Hao et al., 2013), and editing effects on these signaling pathways could be tested by observing alterations between the non-edited [Kv1.1(I)] and edited [Kv1.1(V)] mice in von Frey filament stimulation and thermal stimulation (such as the hotplate test).

Alterations in ananamide effects would be interesting to study, given the known differential in anandamide block for the non-edited [Kv1.1(I)] versus edited [Kv1.1(V)] isoforms (Decher et al., 2010) and the locomotor deficits and antinociception observed following anandamide administration (Stein et al., 1996). The non-edited [Kv1.1(I)] and edited [Kv1.1(V)] mice could be administered anadamide and monitored for alterations in locomotion and nociception, in order to determine whether editing has a role in regulation of these anadamide responses. For testing prolonged effects of anandamide, these experiments could be done in mutants crossed with fatty acid amide hydrolase (FAAH) knock-out mice, as FAAH is the enzyme responsible for hydrolyzing anandamide, and FAAH-null mice display magnified anandamide effects (Cravatt et al., 2001). Finally, the role of Kv1.1 editing on metabolic function could be probed, as Kv1.1 has been implicated in contributing to glucose-induced insulin release, with islets isolated from both *mceph/mceph* and Kv1.1-null mice secreting greater insulin upon glucose challenge (Ma et al., 2011). Ma *et al.* (2011) detail that, while there are discrepancies in the literature concerning detecting Kv1.1 in islets, their expression analyses and electrophysiological characterization supports functional expression in mouse β-cells, and expression was further confirmed in rat and human islets (Ma et al., 2011; MacDonald and Wheeler, 2003). In addition, ADAR2 expression has been shown to be upregulated in pancreatic islets following a high-fat diet, leading to an increase in GluA2 RNA editing (unfortunately Kv1.1 expression was undetectable in this study) (Gan et al., 2006). First, editing should first be fully characterized in

pancreas and islets from normal and type-2 diabetic mice (we have preliminary studies that Kv1.1 editing might be affected, however these preliminary studies need to be replicated to determine precise quantification). Following this, the non-edited [Kv1.1(I)] and edited [Kv1.1(V)] mice could be subjected to metabolic studies starting with glucose tolerance tests, compared to wild-type littermates, to see whether editing alters glucose homeostasis.

The altered seizure susceptibility to PTZ and 4-AP-induced seizures has indicated that editing plays a role as a contributing factor in seizure severity. While we did not observe spontaneous seizures in either mouse model, the alteration in seizure-susceptibility suggests that, although editing may not be an originating cause for seizures, it can act as a downstream modifier to heighten or dampen seizures. Now that we have characterized this function by drug-induced seizures, seizure-susceptibility could be further investigated in chronically induced-seizure models (such as the kainic acid model) or by genetic mechanisms- breeding non-edited [Kv1.1(I)] and edited [Kv1.1(V)] mice with genetic mouse models of epilepsy to see if editing status can affect seizure susceptibility and resistance. A relevant epilepsy mouse model to begin with could be breeding the non-edited [Kv1.1(I)] or edited [Kv1.1(V)] mice with Kv1.2-null mice, which are postnatal lethal from P16 to P19 and coincide with spontaneous seizures (Brew et al., 2007). The severe phenotype of the Kv1.2-null mouse is in sharp contrast to the mild phenotypes of other knock-out models of Kv1 family members, which have normal life spans and no (Kv1.3-null and Kv1.5-null) or limited seizures (Kv1.4-null) (Archer et al., 2001; London et al.,

1998; Xu et al., 2003). Unexpectedly, hypoactivity and larger K+ currents were observed in auditory neurons of the medial nucleus of the trapezoid body (MNTB) in the brainstem of Kv1.2-null mice (hyperexcitability was found in the same neurons of Kv1.1-null mice) (Brew et al., 2007; Brew et al., 2003). As the brainstem is a location of high levels of Kv1.1 RNA editing (60% in mice, 80% in humans) (Decher et al., 2010; Hoopengardner et al., 2003), this could be an indication that Kv1.1 editing may serve a more dominant role in Kv1.2-null mice.

Knowing that editing can dampen seizure-susceptibility also begs the question: how can this knowledge be utilized in a pharmacological approach to treat epilepsy (or at least dampen its severity)? The predominant biophysical difference noted between the non-edited [Kv1.1(I)] and edited [Kv1.1(V)] channels is that the edited isoform promotes rapid recovery from β-subunit inactivation. Thus, a non-edited [Kv1.1(I)] channel could be pharmacologically similar to an edited [Kv1.1(V)] channel if the inactivation domain of the β-subunit was prevented from interacting. Interestingly, studies of this topic have already been performed and fit well with the editing-modifier effects on seizures that we have observed (Lu et al., 2008; Pozo et al., 1990). In particular, Lu *et al.* (2008) performed in-depth drug screens looking for drugs that could disrupt β-inactivation while not altering interactions responsible for the assembly of the β-subunit with the Kv1 T1 domain (while leaving Kv1.4 inactivation intact). Drugs discovered in this screen were then administered prior to PTZ-induced seizures. Three drugs dampened seizure-susceptibility, indicating that decreasing β-inactivation pharmacologically could dampen seizure susceptibility (Lu et al.,

2008). These drugs could be further tested with our mice to determine whether editing-dependent alterations mediating the β-interaction are involved in mediating this dampened seizure-susceptibility.

Finally, a key reason for developing our non-edited [Kv1.1(I)] and edited [Kv1.1(V)] mouse models was to allow for electrophysiological characterization of neurons in slices. Our initial studies in dentate granule cells of the non-edited [Kv1.1(I)] mutants should be compared next to signaling dynamics of the same cells in edited [Kv1.1(V)] mice. In addition, as Kv1.1 editing is regulated during embryonic development, our mice could be used as controls for a study of alterations in Kv1.1 editing during adult neurogenesis of dentate granule cells following seizure-induction in wild-type mice. Alterations in signaling in immature versus mature dentate granule cells may correlate with the Kv1.1 editing status, and our non-edited [Kv1.1(I)] and edited [Kv1.1(V)] mice may serve as important controls. As the non-edited [Kv1.1(I)] mice display stress-induced motor dyscoordination, cerebellar recordings of basket cells and Purkinje neurons will be important for determining if editing in basket cells is altering the GABA release, controlling the rate of Purkinje neuron firing. Since MNTB neurons have already been described in Kv1.1-null and Kv1.2-null mice, characterizing the excitability of these neurons in our mouse models may be able to differentiate whether editing is a key contributor to the normally low excitability of these neurons (Brew et al., 2007; Brew et al., 2003). Peripheral nerve studies can also be performed, particularly investigating whether the non-edited [Kv1(I)] or edited [Kv1.1(V)] mutants have similarities to the Kv1.1-null mice, which have

temperature-sensitive neuromuscular transmission (Zhou et al., 1998). Particular attention should be devoted to probing for the type of altered signaling dynamics that have been observed in other Kv1-related mouse models, not only assessing passive membrane properties and action potential shape. This could include probing for alterations in repetitive firing properties such as the frequency of stimulus-induced pulse trains (*mceph/mceph* mice) and the presence of frequency-dependent spike broadening (Kvβ1.1-null mice) (Giese et al., 1998; Petersson et al., 2003).

Recording from neurons in slices also offers a convenient model for epileptic drug administration, using drugs we have already determined to have an effect (4-AP and PTZ) as well as other widely used pharmacological agents, such as picrotoxin (Gonzalez-Sulser et al., 2012; Marsh et al., 1999; Piredda et al., 1985). We expect that experiments using these drugs will give comparable results consistent with our seizure studies as well as the previous findings using 4-AP to induce seizure-like events in slices from chronic epileptic rats (which displayed higher editing levels) (Streit et al., 2011). We predict that seizure-like events will be observed to the greatest extent in the slices from non-edited [Kv1.1(I)] mice, absent in the edited [Kv1.1(V)] mice, and intermediate in severity in the wild-type mice (or possibly similar to the non-edited mice). Finally, aside from incorporating a stressor prior to hippocampal slice isolation (as is described in the electrophysiology of Chapter 2), other methods of stressing the slices during recording could include oxygen-glucose deprivation, hypo- and hyper-osmotic challenges, and incubation with corticosterone (Alfarez et al., 2002;

Karst et al., 1993; Lipski et al., 2006; Risher et al., 2009). These stressor experiments could help define mechanisms for the stress-vulnerability for the non-edited [Kv1.1(I)] mice.

Continuing the study of RNA editing effects on EA1

We have identified that RNA editing is impacted by the presence of EA1 mutations and that edited EA1 isoforms have altered homotetrameric properties. However, additional experiments are needed to further understand the role of EA1 RNA editing in heterotetramers. The V408A/+ mice can also be further studied for *in vivo* effects of EA1 altered RNA editing.

Further characterizations of edited EA1 mutant channels could help us better understand their physiological defects *in vivo*. These include stimulating the channels with action potential-like commands (trains of depolarizing pulses) to assess cumulative inactivation, as well as probing the voltage-dependence of their inactivation. As Kv1.1 is rarely found *in vivo* in homotetrameric complexes, the alterations in heterotetrameric properties need to be investigated. Previous studies have indicated that the V404I and V408A mutations alter the kinetics of heterotetramers composed of tandem-linked Kv1.1-Kv1.2 or Kv1.1-Kv1.4 α-subunits (D'Adamo et al., 1999; Imbrici et al., 2006; Manganas and Trimmer, 2000). These experiments could be performed with the edited EA1 isoforms, tandem-linked with Kv1.2 or Kv1.4 (or a combination of both), with or without co-expression with β-subunits. These heterotetrameric studies will also be important

for determining whether the co-expression with Kv1.2 and Kv1.4 improves the expression of I407M and V408A non-edited and edited isoforms. Wild-type and edited EA1 characterization in tandemly-linked channels containing Kv1.2 subunits should also be specifically studied for editing-dependent changes in the use-dependent activation property (also called prepulse potentiation), which has recently been attributed to Kv1.2-containing heterotetramers (Baronas et al., 2015).

Now that we have established that the V408A/+ mice are an *in vivo* model of reduced Kv1.1 editing, it can be used as a unique model for testing editing effects and therapeutic strategies targeted towards editing. The plasma membrane versus ER expression of the different wild-type and V408A non-edited and edited isoforms could be determined by isolating different membrane fractions by differential centrifugation of brain regions and then subjecting them to mass spectrometry for protein isoform identification. Also, as described previously, there are several known drugs that can prevent the fast-inactivation mediated by β-subunits and could potentially abolish the slow recovery from inactivation of non-edited [Kv1.1(I)] (Lu et al., 2008). These drugs could be administered prior to rotarod analyses or electrophysiological recordings to determine if the decreased Kv1.1 editing of V408A/+ mice is a contributing factor to stress-induced motor dyscoordination and altered Purkinje neuron firing. These experiments could be performed on the V408A/+ mice as well as V408A mutant mice that have been bred with the non-edited [Kv1.1(I)] or edited [Kv1.1(V)] mice, for additional alterations in the wild-type allele editing level.

These further breeding experiments may reveal whether restricting the wild-type isoform to non-edited or edited could lead to dominant-negative effects on motor dyscoordination or electrophysiology.

Finally, we have also detailed how several EA1 mutations had consequences on the RNA editing process, presumably by altering the enzymatic recognition of the RNA structure. Expanding the implications of our studies for the wider scientific community, we hope that this will encourage others to see whether mutations alter the RNA editing of other substrates or, more broadly, if other mutations affect RNA interactions with other RNA-binding proteins. This could include other heritable mutations, somatic mutations arising in cancer, or synonymous variants, which could alter RNA structures while leaving the coding unchanged. Interestingly, there are many known single nucleotide polymorphisms in the region of the Kv1.1 RNA duplex (which encodes amino acids 373 through 410) as well as many documented mutations arising in a variety of cancers (Ensembl release 87 (Aken et al., 2017)) and recent studies have linked Kv1.1 expression with apoptosis and sensitivity to drug-induced cell death (Leanza et al., 2014; Szabò et al., 2010). Our studies suggest that the Kv1.1 duplex is sensitive to small perturbations, and the presence of variants in the duplex could account for RNA editing variation among the population, which could be risk factors for patients that have additional germline or somatic mutations. Of particular interest would be to test whether several known synonymous human variants around the editing site could alter Kv1.1 RNA editing similarly to the EA1 mutations we have described. To date, there are 13

synonymous variants that have been documented within the minimal duplex required for ADAR2-mediated RNA editing, on either side of the duplex, and several coincide with locations of EA1 mutations as well (Figure 4.1 and Table C.1). These silent variants may be additional factors regulating RNA editing *in vivo*. The EA1 mutations' impacts on Kv1.1 RNA editing may not be an isolated phenomenon, but could rather be an initial case-study revealing the consequences of mutations and variants on RNA-RNA interactions (such as with miRNAs) and RNA-protein interactions.

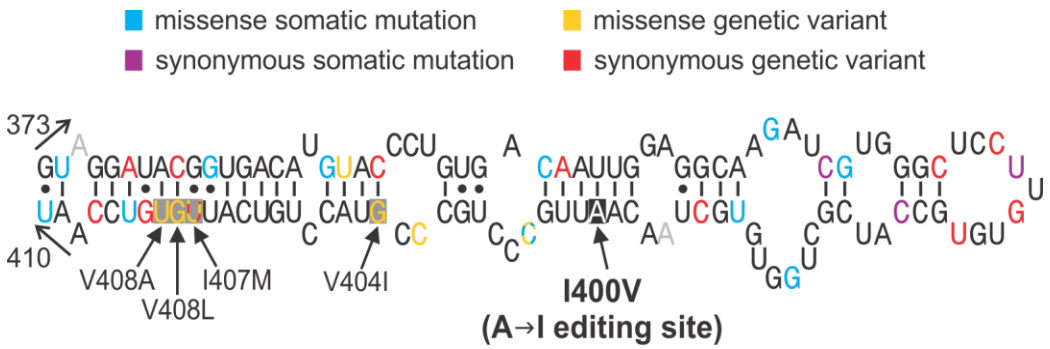

Figure 4.1. Human variants found in the Kv1.1 mRNA duplex. The predicted secondary structure for the minimal duplex required for ADAR2 editing of the wild-type human Kv1.1 pre-mRNA. Human variants are located in various positions of the duplex and color-coded for variant type, checkered letters indicate multiple types of variants at a given location (blue: missense somatic mutation, purple: synonymous somatic mutation, yellow: missense genetic variant, red: synonymous genetic variant). The position of the A-to-I editing site (I400V) is indicated with a black box and the four non-synonymous mutations associated with EA1 indicated with dark grey boxes. The numbered arrows indicate the codon positions of the associated amino acids. The locations of two human versus mouse sequence differences are indicated in light grey letters (which are both G in the mouse sequence).

We hope our studies will encourage others to continue studying the editing-dependent effects of Kv1.1 function in normal physiology and in the EA1 disorder, as well as inspire the broader scientific community to study the impacts of mutations, not only for their amino acid alterations, but also in terms of their possible altered RNA interactions.

Appendix A: Comparative analysis of editing rates determined by Sanger sequencing versus High-throughput sequence analysis

The wild-type ratio of the peak heights described in Figure 2.4 appears to diverge from the wild-type cerebellar RNA editing rate reported in (Figure 2.3). This discrepancy highlights the importance of using our high-throughput sequencing approach to quantify RNA editing rather than relying on the ratio of electropherogram peak heights, which are known to vary based on the polymerase incorporation preference for dideoxynucleotide type, sequencing direction, and sequence context (Carr et al., 2009; Li et al., 1999; Rinkevich et al., 2012). In order to highlight the differences in quantification by these two methods, I have compared three data sets where I quantified the same samples using both methods and displayed the differences in the percent editing or the rate of percent editing (Figure A.1). In Figure A.1a and b, I have detailed how the quantification methods compared for Kv1.1 editing from mouse tissues (described previously in Figures 2.3 and 2.4) and from my *in vitro* editing assay (Figure 3.3). In these data, the Sanger sequencing peak height quantification mainly overestimates the editing level or editing rate quantified by high-throughput sequencing, though it gives close to accurate measurements for the hippocampal editing level. However, Figure A.1c demonstrates that Sanger sequencing can underestimate editing levels in different contexts (these data are derived from a collaborative study I contributed to for Dr. Martin Gallagher, quantifying Gabra3 RNA editing in the thalamic reticular nucleus (nRT) dissected from mouse brain) (Zhou et al., 2015). This variation in underestimating versus

overestimating the percent editing has been documented previously (Rinkevich et al., 2012).

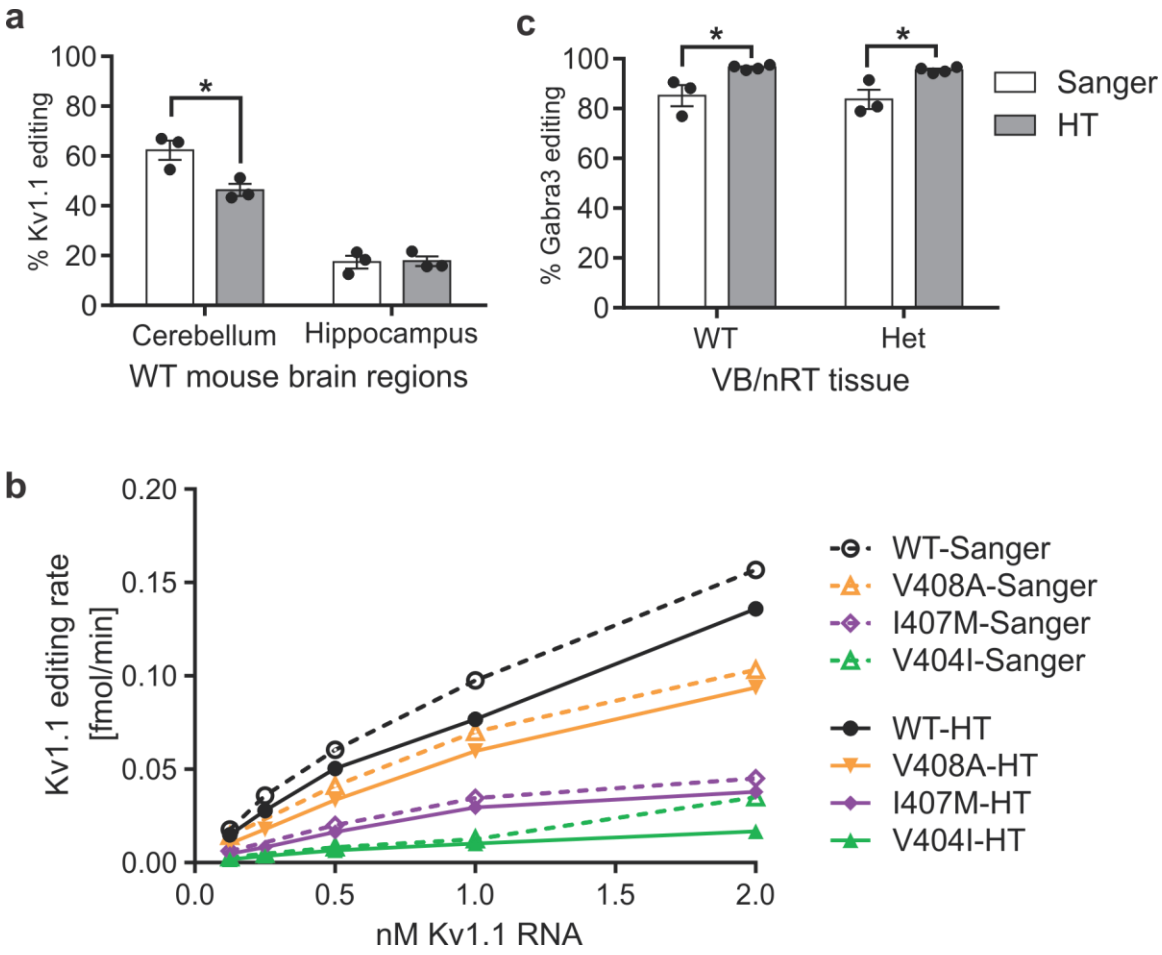

Figure A.1. Comparative analysis of editing quantification by Sanger and High-Throughput Sequencing. Editing was quantified from samples by both measuring peak heights of Sanger sequencing electropherogram traces and by high-throughput sequence analysis (HT) as described previously (Hood et al., 2014). **(a)** The extent of editing was quantified for Kv1.1 transcripts isolated from mouse brain regions (n=3, mean ± SEM) and **(b)** for the Kv1.1 in vitro editing assay (where the extent of editing was converted into the editing rate). **(c)** Gabra3 RNA editing was quantified from dissected VB/nRT brain regions in WT and heterozygous (Het) Gabra1 knock-out mice (Zhou et al., 2015). (n=3-4, mean ± SEM). Statistics could be performed for **(a)** and **(c),** determining significance by 2-way ANOVA with Sidak's multiple comparisons test ($p<0.05$).

Appendix B: Additional p-value tables

For the sake of brevity, ranges of p-values were reported in the legends for Figures 3.6, 3.8, and 3.10. P-values associated with these figures are presented below.

Table B.1: P-values corresponding to Figure 3.6 (time to half-activation)

	voltage	-10	0	10	20	30	40	50	60	70	80	significant range
Non-edited vs Edited (4 comparisons)	WT N vs WT E	0.0266	0.0443	0.0631	0.0766	0.0791	0.0695	0.052	0.0334	0.0185	0.009	0.0443>p>0.009
	significant	*	*	ns	ns	ns	ns	ns	*	*	*	
	V404I N vs V404I E	0.099	0.0574	0.0397	0.0325	0.0316	0.0364	0.0497	0.0813	0.1576	0.3391	0.0497>p>0.0316
	significant	ns	ns	*	*	*	*	*	ns	ns	ns	
	I407M N vs I407M E	0.0055	0.0018	0.001	0.0008	0.0009	0.0013	0.0029	0.0089	0.0397	0.2249	0.0397>p>0.0008
	significant	*	*	*	*	*	*	*	*	*	ns	
	V408A N vs V408A E	0.0004	0.0048	0.0432	0.2189	0.5883	0.9986	0.7067	0.5621	0.555	0.681	0.0432>p>0.0004
	significant	*	*	*	ns	ns	ns	ns	ns	ns	ns	
WT N vs mutant N (3 comparisons)	WT N vs V404I N	0.0006	0.0017	0.0043	0.0093	0.0165	0.0246	0.0309	0.0336	0.0322	0.028	0.0336>p>0.0006
	significant	*	*	*	*	*	*	*	*	*	*	
	WT N vs I407M N	<0.0001	<0.0001	<0.0001	<0.0001	<0.0001	<0.0001	<0.0001	<0.0001	<0.0001	<0.0001	all p<0.0001
	significant	*	*	*	*	*	*	*	*	*	*	
	WT N vs V408A N	0.0778	0.0804	0.0906	0.1096	0.1407	0.1905	0.2701	0.3962	0.587	0.847	none
	significant	ns	ns	ns	ns	ns	ns	ns	ns	ns	ns	
WT E vs mutant E (3 comparisons)	WT E vs V404I E	0.2704	0.1292	0.0664	0.0377	0.0236	0.0165	0.0131	0.0128	0.0165	0.0292	0.0377>p>0.0165
	significant	ns	ns	ns	*	*	*	*	*	*	*	
	WT E vs I407M E	<0.0001	<0.0001	<0.0001	<0.0001	<0.0001	<0.0001	<0.0001	<0.0001	0.0001	0.0027	0.027>p>0.0001
	significant	*	*	*	*	*	*	*	*	*	*	
	WT E vs V408A E	0.1427	0.0592	0.026	0.0122	0.006	0.0031	0.0017	0.0011	0.001	0.0013	0.026>p>0.001
	significant	ns	ns	*	*	*	*	*	*	*	*	

Individual group comparisons for p-values were based on the Wald tests of model-based predicted (least square) means. Significance was defined as p<0.05.

Table B.2: P-values corresponding to Figure 3.8 (closing kinetics)

	voltage	**-120**	**-110**	**-100**	**-90**	**-80**	**-70**	**-60**	**significant range**
Nonedited vs Edited (4 comparisons)	WT N vs WT E	0.0002	0.0004	0.001	0.0042	0.034	0.4182	0.2903	0.034>p>0.0002
	significant	*	*	*	*	*	ns	ns	
	V404I N vs V404I E	0.0066	0.0122	0.0254	0.0586	0.1447	0.3556	0.7789	0.0586>p>0.0066
	significant	*	*	*	ns	ns	ns	ns	
	I407M N vs I407M E	0.0086	0.0041	0.0036	0.0054	0.015	0.0807	0.6194	0.015>p>0.0036
	significant	*	*	*	*	*	ns	ns	
	V408A N vs V408A E	N/A	N/A	N/A	N/A	N/A	N/A	N/A	
	significant	ns	ns	ns	ns	ns	ns	ns	N/A
WT N v other N (3 comparisons)	WT N vs V404I N	<0.0001	<0.0001	<0.0001	<0.0001	<0.0001	<0.0001	<0.0001	all p<0.0001
	significant	*	*	*	*	*	*	*	
	WT N vs I407M N	<0.0001	<0.0001	<0.0001	<0.0001	<0.0001	<0.0001	<0.0001	all p<0.0001
	significant	*	*	*	*	*	*	*	
	WT N vs V408A N	<0.0001	<0.0001	<0.0001	<0.0001	<0.0001	<0.0001	<0.0001	all p<0.0001
	significant	*	*	*	*	*	*	*	
WT E v other E (3 comparisons)	WT E vs V404I E	0.0005	0.0005	0.0009	0.0024	0.01	0.0637	0.45	0.01>p>0.0005
	significant	*	*	*	*	*	ns	ns	
	WT E vs I407M E	0.0019	0.001	0.0005	0.0003	0.0001	<0.0001	<0.0001	0.0019>p>0.0001
	significant	*	*	*	*	*	*	*	
	WT E vs V408A E	N/A	N/A	N/A	N/A	N/A	N/A	N/A	
	significant	ns	ns	ns	ns	ns	ns	ns	N/A

Individual group comparisons for p-values were based on the Wald tests of model-based predicted (least square) means. Significance was defined as p<0.05.

Table B.3: P-values corresponding to Figure 3.10 (kinetics of Kvβ1.1 inactivation)

	voltage	10	20	30	40	50	60	70	80	significant range
Nonedited vs Edited (4 comparisons)	WT N vs WT E	<0.0001	<0.0001	<0.0001	<0.0001	<0.0001	<0.0001	<0.0001	<0.0001	all p<0.0001
	significant	*	*	*	*	*	*	*	*	
	V404I N vs V404I E	N/A	N/A	N/A	N/A	0.6925	0.947	0.6908	0.5607	none
	significant	ns	ns	ns	ns	ns	ns	ns	ns	
	I407M N vs I407M E	N/A	N/A	<0.0001	<0.0001	<0.0001	<0.0001	<0.0001	<0.0001	all p<0.0001
	significant	ns	ns	*	*	*	*	*	*	
	V408A N vs V408A E	0.0005	0.001	0.002	0.0051	0.017	0.0683	0.3027	0.9997	0.017>p>0.0005
	significant	*	*	*	*	*	ns	ns	ns	
WT N v other N (3 comparisons)	WT N vs V404I N	N/A	N/A	N/A	N/A	0.0052	0.0138	0.0263	0.0386	0.0386>p>0.0052
	significant	ns	ns	ns	ns	*	*	*	*	
	WT N vs I407M N	N/A	<0.0001	<0.0001	<0.0001	<0.0001	<0.0001	<0.0001	<0.0001	all p<0.0001
	significant	ns	*	*	*	*	*	*	*	
	WT N vs V408A N	<0.0001	<0.0001	<0.0001	<0.0001	<0.0001	<0.0001	<0.0001	<0.0001	all p<0.0001
	significant	*	*	*	*	*	*	*	*	
WT E v other E (3 comparisons)	WT E vs V404I E	0.0002	0.0003	0.0006	0.0012	0.0018	0.0023	0.0024	0.0025	0.0025>p>0.0002
	significant	*	*	*	*	*	*	*	*	
	WT E vs I407M E	N/A	N/A	<0.0001	<0.0001	<0.0001	<0.0001	<0.0001	<0.0001	all p<0.0001
	significant	ns	ns	*	*	*	*	*	*	
	WT E vs V408A E	<0.0001	<0.0001	<0.0001	<0.0001	0.001	0.0194	0.2455	0.8719	0.0194>p>0.0001
	significant	*	*	*	*	*	*	ns	ns	

Individual group comparisons for p-values were based on the Wald tests of model-based predicted (least square) means. Significance was defined as p<0.05.

Appendix C: Human variants found in the Kv1.1 mRNA duplex

Table C.1 was compiled from data accessed from Ensembl release 87(Aken et al., 2017) and the Human Gene Mutation Database (Stenson et al., 2014). These data further describe the information found in Figure 4.1.

http://uswest.ensembl.org/Homo_sapiens/Gene/Variation_Gene/Table?db=core;g=ENSG00000111262;r=12:4909905-4931361;t=ENST00000382545

http://www.hgmd.cf.ac.uk/ac/index.php

Table C.1: Human variants found in the Kv1.1 mRNA duplex

residue number	genomic location	variation ID	variant type	description	amino acid change	nucleotide change
373	12:4912496	COSM4042554	missense somatic mutation	stomach carcinoma	V373A	T1118C
374	12:4912500	rs778171002	synonymous variant			A1122T
374	12:4912500	rs778171002	synonymous variant			A1122C
375	12:4912503	rs144351014	synonymous variant			C1125T
376	12:4912505	COSM3461760	missense somatic mutation	skin, malignant melanoma	G376D	G1127A
378	12:4912512	COSM940253	missense somatic mutation	endometrium carcinoma	M378I	G1134A
379	12:4912513	rs774543663	missense variant		Y379D	T1135G
379	12:4912515	rs759584837	synonymous variant			C1137T
382	12:4912523	COSM4694135	missense somatic mutation	large intestine carcinoma	T382K	C1145A
382	12:4912524	rs768750670	synonymous variant			A1146C
386	12:4912536	COSM468479	missense somatic mutation	kidney carcinoma	K386N	G1158T
387	12:4912539	COSM4042555	synonymous somatic mutation	stomach carcinoma	I387I	C1161T
388	12:4912540	COSM346166	missense somatic mutation	large intestine and lung carcinoma	V388M	G1162A
389	12:4912545	rs775643582	synonymous variant			C1167A

residue number	genomic location	variation ID	variant type	description	amino acid change	nucleotide change
390	12:4912548	rs760496447	synonymous variant			C1170G
391	12:4912549	COSM219473	synonymous somatic mutation	breast carcinoma	L391L	T1171C
391	12:4912551	rs763811664	synonymous variant			G1173A
392	12:4912554	rs753733816	synonymous variant			T1176C
393	12:4912557	COSM940254	synonymous somatic mutation	endometrium carcinoma	A393A	C1179T
396	12:4912564	COSM5739544	missense somatic mutation	small intestine, adenoma	G396C	G1186T
397	12:4912568	COSM3727191	missense somatic mutation	skin malignant melanoma	V397A	T1190C
398	12:4912570	rs761868527	synonymous variant			C1192T
401	12:4912580	rs797044929	missense variant	inborn genetic disorder (Farwell et al., 2015)	A401V	C1202T
401	12:4912580	COSM5375323	missense somatic mutation	skin, malignant melanoma	A401V	C1202T
403	12:4912586	rs867232553	missense variant	Unclear, but from melanoma paper (Arafeh et al., 2015)	P403L	C1208T
404	12:4912588	rs104894355 and CM981109	missense EA1 variant	Characterized in EA1 (Scheffer et al., 1998)	V404I	G1210A
407	12:4912599	rs138936640	synonymous variant		I407I	T1221C

residue number	genomic location	variation ID	variant type	description	amino acid change	nucleotide change
407	12:4912599	CM130980	Missense EA1 variant	Characterized in EA1 (Tomlinson et al., 2013)		
408	12:4912600	rs113994117 and CM092472	missense EA1 variant	Characterized in EA1 (Demos et al., 2009)	V408L	G1222T
408	12:4912601	rs104894352 and CM940995	missense EA1 variant	Characterized in EA1 (Browne et al., 1994)	V408A	T1223C
408	12:4912602	rs142055425	synonymous variant			G1224A
409	12:4912603	COSM4042556	missense somatic mutation	stomach carcinoma	S409T	T1225A
409	12:4912605	rs757958737	synonymous variant			C1227A
410	12:4912608	COSM1747035	missense somatic mutation	urinary tract carcinoma	N410K	T1230A

REFERENCES

Adelman, J.P., Bond, C.T., Pessia, M., and Mayliet, J. (1995). Episodic ataxia results from voltage-dependent potassium channels with altered functions. Neuron *15*, 1449-1454.

Aken, B.L., Achuthan, P., Akanni, W., Amode, M.R., Bernsdorff, F., Bhai, J., Billis, K., Carvalho-Silva, D., Cummins, C., Clapham, P.*, et al.* (2017). Ensembl 2017. Nucleic Acids Res *45*, D635-D642.

Akhtar, S., McIntosh, P., Bryan-Sisneros, A., Barratt, L., Robertson, B., and Dolly, J.O. (1999). A Functional Spliced-Variant of β2 Subunit of Kv1 Channels in C6 Glioma Cells and Reactive Astrocytes from Rat Lesioned Cerebellum. Biochemistry *38*, 16984-16992.

Alekov, A.K., Rahman, M.M., Mitrovic, N., LehmannHorn, F., and Lerche, H. (2000). A sodium channel mutation causing epilepsy in man exhibits subtle defects in fast inactivation and activation in vitro. The Journal of Physiology *529*, 533-540.

Alfarez, D.N., Wiegert, O., Joels, M., and Krugers, H.J. (2002). Corticosterone and stress reduce synaptic potentiation in mouse hippocampal slices with mild stimulation. Neuroscience *115*, 1119-1126.

Arafeh, R., Qutob, N., Emmanuel, R., Keren-Paz, A., Madore, J., Elkahloun, A., Wilmott, J.S., Gartner, J.J., Di Pizio, A., Winograd-Katz, S.*, et al.* (2015). Recurrent inactivating RASA2 mutations in melanoma. Nat Genet *47*, 1408-1410.

Archer, S.L., London, B., Hampl, V., Wu, X., Nsair, A., Puttagunta, L., Hashimoto, K., Waite, R.E., and Michelakis, E.D. (2001). Impairment of hypoxic pulmonary vasoconstriction in mice lacking the voltage-gated potassium channel Kv1.5. FASEB J *15*, 1801-1803.

Avery, O.T., MacLeod, C.M., and McCarty, M. (1944). STUDIES ON THE CHEMICAL NATURE OF THE SUBSTANCE INDUCING TRANSFORMATION OF PNEUMOCOCCAL TYPES. The Journal of Experimental Medicine *79*, 137-158.

Bagchi, B., Al-Sabi, A., Kaza, S., Scholz, D., O'Leary, V.B., Dolly, J.O., and Ovsepian, S.V. (2014). Disruption of myelin leads to ectopic expression of K(V)1.1 channels with abnormal conductivity of optic nerve axons in a cuprizone-induced model of demyelination. PLoS ONE *9*, e87736.

Bardien-Kruger, S., Wulff, H., Arieff, Z., Brink, P., Chandy, K.G., and Corfield, V. (2002). Characterisation of the human voltage-gated potassium channel gene, KCNA7, a candidate gene for inherited cardiac disorders, and its exclusion as cause of progressive familial heart block I (PFHBI). European Journal of Human Genetics *10*, 36-43.

Baronas, V.A., McGuinness, B.R., Brigidi, G.S., Gomm Kolisko, R.N., Vilin, Y.Y., Kim, R.Y., Lynn, F.C., Bamji, S.X., Yang, R., and Kurata, H.T. (2015). Use-dependent activation of neuronal Kv1.2 channel complexes. J Neurosci *35*, 3515-3524.

Basilio, C., Wahba, A.J., Lengyel, P., Speyer, J.F., and Ochoa, S. (1962). Synthetic Polynucleotides and the Amino Acid Code, V. Proceedings of the National Academy of Sciences of the United States of America *48*.

Bass, B.L., and Weintraub, H. (1988). An unwinding activity that covalently modifies its double-stranded RNA substrate. Cell *55*, 1089-1098.

Baumann, A., Grupe, A., Ackermann, A., and Pongs, O. (1988). Structure of the voltage-dependent potassium channel is highly conserved from Drosophila to vertebrate central nervous systems. The EMBO Journal *7*, 2457-2463.

Begum, R., Bakiri, Y., Volynski, K.E., and Kullmann, D.M. (2016). Action potential broadening in a presynaptic channelopathy. Nat Commun *7*, 12102.

Bezanilla, F. (2004). RNA editing of a human potassium channel modifies its inactivation. Nat Struct Mol Biol *11*, 915-916.

Bhalla, T., Rosenthal, J.J.C., Holmgren, M., and Reenan, R. (2004). Control of human potassium channel inactivation by editing of a small mRNA hairpin. Nat Struct Mol Biol *11*, 950-956.

Bretschneider, F., Wrisch, A., Lehmann-Horn, F., and Grissmer, S. (1999). Expression in mammalian cells and electrophysiological characterization of two mutant Kv1.1 channels causing episodic ataxia type 1 (EA-1). European Journal of Neuroscience *11*, 2403-2412.

Brew, H.M., Gittelman, J.X., Silverstein, R.S., Hanks, T.D., Demas, V.P., Robinson, L.C., Robbins, C.A., McKee-Johnson, J., Chiu, S.Y., Messing, A.*, et al.* (2007). Seizures and reduced life span in mice lacking the potassium channel subunit Kv1.2, but hypoexcitability and enlarged Kv1 currents in auditory neurons. J Neurophysiol *98*, 1501-1525.

Brew, H.M., Hallows, J.L., and Tempel, B.L. (2003). Hyperexcitability and reduced low threshold potassium currents in auditory neurons of mice lacking the channel subunit Kv1.1. The Journal of Physiology *548*, 1-20.

Brooks, S.P., and Dunnett, S.B. (2009). Tests to assess motor phenotype in mice: a user's guide. Nat Rev Neurosci *10*, 519-529.

Browne, D.L., Gancher, S.T., Nutt, J.G., Brunt, E.R.P., Smith, E.A., Kramer, P., and Litt, M. (1994). Episodic ataxia/myokymia syndrome is associated with point mutations in the human potassium channel gene, KCNA1. Nature Genetics *8*, 136-140.

Brunetti, O., Imbrici, P., Botti, F.M., Pettorossi, V.E., D'Adamo, M.C., Valentino, M., Zammit, C., Mora, M., Gibertini, S., Di Giovanni, G.*, et al.* (2012). Kv1.1 knock-in ataxic mice exhibit spontaneous myokymic activity exacerbated by fatigue, ischemia and low temperature. Neurobiol Dis *47*, 310-321.

Buynitsky, T., and Mostofsky, D.I. (2009). Restraint stress in biobehavioral research: Recent developments. Neuroscience & Biobehavioral Reviews *33*, 1089-1098.

Campomanes, C.R., Carroll, K.I., Manganas, L.N., Hershberger, M.E., Gong, B., Antonucci, D.E., Rhodes, K.J., and Trimmer, J.S. (2002). Kvβ Subunit Oxidoreductase Activity and Kv1 Potassium Channel Trafficking. Journal of Biological Chemistry *277*, 8298-8305.

Carr, I.M., Robinson, J.I., Dimitriou, R., Markham, A.F., Morgan, A.W., and Bonthron, D.T. (2009). Inferring relative proportions of DNA variants from sequencing electropherograms. Bioinformatics *25*, 3244-3250.

Carter, R.J., Lione, L.A., Humby, T., Mangiarini, L., Mahal, A., Bates, G.P., Dunnett, S.B., and Morton, A.J. (1999). Characterization of Progressive Motor Deficits in Mice Transgenic for the Human Huntington's Disease Mutation. Journal of Neuroscience *19*, 3248-3257.

Carter, R.J., Morton, J., and Dunnett, S.B. (2001). Motor Coordination and Balance in Rodents. In Current Protocols in Neuroscience (John Wiley & Sons, Inc.).

Chen, C.X., Cho, D.S., Wang, Q., Lai, F., Carter, K.C., and Nishikura, K. (2000). A third member of the RNA-specific adenosine deaminase gene family, ADAR3, contains both single- and double-stranded RNA binding domains. RNA *6*, 755-767.

Chen, S.H., Fu, S.J., Huang, J.J., and Tang, C.Y. (2016). The episodic ataxia type 1 mutation I262T alters voltage-dependent gating and disrupts protein biosynthesis of human Kv1.1 potassium channels. Sci Rep *6*, 19378.

Chen, X., Wang, Q., Ni, F., and Ma, J. (2010). Structure of the full-length Shaker potassium channel Kv1.2 by normal-mode-based X-ray crystallographic refinement. Proceedings of the National Academy of Sciences of the United States of America *107*, 11352-11357.

Cho, D.S.C., Yang, W., Lee, J.T., Shiekhattar, R., Murray, J.M., and Nishikura, K. (2003). Requirement of dimerization for RNA editing activity of adenosine deaminases acting on RNA. Journal of Biological Chemistry *278*.

Choi, K.L., Aldrich, R.W., and Yellen, G. (1991). Tetraethylammonium blockade distinguishes two inactivation mechanisms in voltage-activated K+ channels. Proceedings of the National Academy of Sciences of the United States of America *88*, 5092.

Chung, W.K., Shin, M., Jaramillo, T.C., Leibel, R.L., LeDuc, C.A., Fischer, S.G., Tzilianos, E., Gheith, A.A., Lewis, A.S., and Chetkovich, D.M. (2009). Absence epilepsy in apathetic, a spontaneous mutant mouse lacking the h channel subunit, HCN2. Neurobiol Dis *33*, 499-508.

Clark, J.D., and Tempel, B.L. (1998). Hyperalgesia in mice lacking the Kv1.1 potassium channel gene. Neurosci Lett *251*, 121-124.

Coleman, S.K., Newcombe, J., Pryke, J., and Dolly, J.O. (1999). Subunit Composition of Kv1 Channels in Human CNS. Journal of Neurochemistry *73*, 849-858.

Connor, J.X., McCormack, K., Pletsch, A., Gaeta, S., Ganetzky, B., Chiu, S.Y., and Messing, A. (2005). Genetic modifiers of the Kvβ2-null phenotype in mice. Genes, Brain and Behavior *4*, 77-88.

Consortium, I.H.G.S. (2004). Finishing the euchromatic sequence of the human genome. Nature *431*, 931-945.

Cravatt, B.F., Demarest, K., Patricelli, M.P., Bracey, M.H., Giang, D.K., Martin, B.R., and Lichtman, A.H. (2001). Supersensitivity to anandamide and enhanced endogenous cannabinoid signaling in mice lacking fatty acid amide hydrolase. Proc Natl Acad Sci U S A *98*, 9371-9376.

D'Adamo, M.C., Hasan, S., Guglielmi, L., Servettini, I., Cenciarini, M., Catacuzzeno, L., and Franciolini, F. (2015). New insights into the pathogenesis and therapeutics of episodic ataxia type 1. Front Cell Neurosci *9*, 317.

D'Adamo, M.C., Imbrici, P., Sponcichetti, F., and Pessia, M. (1999). Mutations in the KCNA1 gene associated with episodic ataxia type-1 syndrome impair heteromeric voltage-gated K(+) channel function. FASEB journal : official publication of the Federation of American Societies for Experimental Biology *13*, 1335-1345.

D'Adamo, M.C., Liu, Z., Adelman, J.P., Maylie, J., and Pessia, M. (1998). Episodic ataxia type-1 mutations in the hKv1.1 cytoplasmic pore region alter the gating properties of the channel. EMBO J *17*, 1200-1207.

Dawson, T.R., Sansam, C.L., and Emeson, R.B. (2004). Structure and Sequence Determinants Required for the RNA Editing of ADAR2 Substrates. Journal of Biological Chemistry *279*, 4941-4951.

De Sarro, G., Ibbadu, G.F., Marra, R., Rotiroti, D., Loiacono, A., Donato Di Paola, E., and Russo, E. (2004). Seizure susceptibility to various convulsant stimuli in dystrophin-deficient mdx mice. Neuroscience Research *50*, 37-44.

Decher, N., Streit, A.K., Rapedius, M., Netter, M.F., Marzian, S., Ehling, P., Schlichthörl, G., Craan, T., Renigunta, V., Köhler, A.*, et al.* (2010). RNA editing modulates the binding of drugs and highly unsaturated fatty acids to the open pore of Kv potassium channels. EMBO J *29*, 2101-2113.

Demos, M.K., Macri, V., Farrell, K., Nelson, T.N., Chapman, K., Accili, E., and Armstrong, L. (2009). A novel KCNA1 mutation associated with global delay and persistent cerebellar dysfunction. Movement Disorders *24*, 778-782.

Dhir, A., Zolkowska, D., Murphy, R.B., and Rogawski, M.A. (2011). Seizure Protection by Intrapulmonary Delivery of Propofol Hemisuccinate. J Pharmacol Exp Ther *336*, 215-222.

Dolly, J.O., and Parcej, D.N. (1996). Molecular properties of voltage-gated K+ channels. Journal of bioenergetics and biomembranes *28*, 231-253.

Donahue, L.R., Cook, S.A., Johnson, K.R., Bronson, R.T., and Davisson, M.T. (1996). Megencephaly: a new mouse mutation on chromosome 6 that causes hypertrophy of the brain. Mamm Genome *7*, 871-876.

Dreissen, Y.E., and Tijssen, M.A. (2012). The startle syndromes: physiology and treatment. Epilepsia *53 Suppl 7*, 3-11.

England, S.K., Uebele, V.N., Kodali, J., Bennett, P.B., and Tamkun, M.M. (1995). A novel K+ channel beta-subunit (hKv beta 1.3) is produced via alternative mRNA splicing. J Biol Chem *270*, 28531-28534.

Eunson, L.H., Rea, R., Zuberi, S.M., Youroukos, S., Panayiotopoulos, C.P., Liguori, R., Avoni, P., McWilliam, R.C., Stephenson, J.B., Hanna, M.G.*, et al.* (2000). Clinical, genetic, and expression studies of mutations in the potassium channel gene KCNA1 reveal new phenotypic variability. Ann Neurol *48*, 647-656.

Farwell, K.D., Shahmirzadi, L., El-Khechen, D., Powis, Z., Chao, E.C., Tippin Davis, B., Baxter, R.M., Zeng, W., Mroske, C., Parra, M.C.*, et al.* (2015). Enhanced utility of family-centered diagnostic exome sequencing with inheritance model-based analysis: results from 500 unselected families with undiagnosed genetic conditions. Genetics in medicine : official journal of the American College of Medical Genetics *17*, 578-586.

Feil, R., and Fraga, M.F. (2012). Epigenetics and the environment: emerging patterns and implications. Nature Reviews Genetics *13*, 97-109.

Felsenfeld, G. (2014). A Brief History of Epigenetics. Cold Spring Harbor Perspectives in Biology *6*, a018200.

Feng, Y., Sansam, C.L., Singh, M., and Emeson, R.B. (2006). Altered RNA Editing in Mice Lacking ADAR2 Autoregulation. Mol Cell Biol *26*, 480-488.

Ferraro, T.N., Golden, G.T., Smith, G.G., Jean, P.S., Schork, N.J., Mulholland, N., Ballas, C., Schill, J., Buono, R.J., and Berrettini, W.H. (1999). Mapping Loci for Pentylenetetrazol-Induced Seizure Susceptibility in Mice. J Neurosci *19*, 6733-6739.

Ferrick-Kiddie, E.A., Rosenthal, J.J., Ayers, G.D., and Emeson, R.B. (2017). Mutations underlying Episodic Ataxia type-1 antagonize Kv1.1 RNA editing. Sci Rep *7*, 41095.

Franklin, R.E., and Gosling, R.G. (1953). Molecular Configuration in Sodium Thymonucleate. Nature *171*, 740-741.

Galeotti, N., Ghelardini, C., Papucci, L., Capaccioli, S., Quattrone, A., and Bartolini, A. (1997). An Antisense Oligonucleotide on the MouseShaker-like Potassium Channel Kv1.1 Gene Prevents Antinociception Induced by Morphine and Baclofen. J Pharmacol Exp Ther *281*, 941-949.

Gallo, A., Keegan, L.P., Ring, G.M., and O'Connell, M.A. (2003). An ADAR that edits transcripts encoding ion channel subunits functions as a dimer. The EMBO Journal *22*, 3421-3430.

Gan, Z., Zhao, L., Yang, L., Huang, P., Zhao, F., Li, W., and Liu, Y. (2006). RNA Editing by ADAR2 Is Metabolically Regulated in Pancreatic Islets and β-Cells. Journal of Biological Chemistry *281*, 33386-33394.

George, C.X., Gan, Z., Liu, Y., and Samuel, C.E. (2011). Adenosine Deaminases Acting on RNA, RNA Editing, and Interferon Action. J Interferon Cytokine Res *31*, 99-117.

Gerber, A., O'Connell, M.A., and Keller, W. (1997). Two forms of human double-stranded RNA-specific editase 1 (hRED1) generated by the insertion of an Alu cassette. RNA *3*, 453.

Giese, K.P., Storm, J.F., Reuter, D., Fedorov, N.B., Shao, L.-R., Leicher, T., Pongs, O., and Silva, A.J. (1998). Reduced K+ Channel Inactivation, Spike Broadening, and After-Hyperpolarization in Kvβ1.1-Deficient Mice with Impaired Learning. Learn Mem *5*, 257-273.

Glasscock, E., Yoo, J.W., Chen, T.T., Klassen, T.L., and Noebels, J.L. (2010). Kv1.1 potassium channel deficiency reveals brain-driven cardiac dysfunction as a candidate mechanism for sudden unexplained death in epilepsy. J Neurosci *30*, 5167-5175.

Glauner, K.S., Mannuzzu, L.M., Gandhi, C.S., and Isacoff, E.Y. (1999). Spectroscopic mapping of voltage sensor movement in the Shaker potassium channel. Nature *402*, 813-817.

Gonzalez-Sulser, A., Wang, J., Queenan, B.N., Avoli, M., Vicini, S., and Dzakpasu, R. (2012). Hippocampal neuron firing and local field potentials in the in vitro 4-aminopyridine epilepsy model. J Neurophysiol *108*, 2568-2580.

Gonzalez, C., Lopez-Rodriguez, A., Srikumar, D., Rosenthal, J.J.C., and Holmgren, M. (2011). Editing of human KV1.1 channel mRNAs disrupts binding of the N-terminus tip at the intracellular cavity. Nat Commun *2*.

Graves, T.D., Cha, Y.-H., Hahn, A.F., Barohn, R., Salajegheh, M.K., Griggs, R.C., Bundy, B.N., Jen, J.C., Baloh, R.W., and Hanna, M.G. (2014). Episodic ataxia type 1: clinical characterization, quality of life and genotype–phenotype correlation. Brain *137*, 1009-1018.

Graves, T.D., Rajakulendran, S., Zuberi, S.M., Morris, H.R., Schorge, S., Hanna, M.G., and Kullmann, D.M. (2010). Nongenetic factors influence severity of episodic ataxia type 1 in monozygotic twins(Video). Neurology *75*, 367-372.

Grice, L.F., and Degnan, B.M. (2015). The origin of the ADAR gene family and animal RNA editing. BMC Evolutionary Biology *15*, 4.

Griffith, F. (1928). The Significance of Pneumococcal Types. J Hyg (Lond) *27*, 113-159.

Grissmer, S., Nguyen, A.N., Aiyar, J., Hanson, D.C., Mather, R.J., Gutman, G.A., Karmilowicz, M.J., Auperin, D.D., and Chandy, K.G. (1994). Pharmacological characterization of five cloned voltage-gated K+ channels, types Kv1.1, 1.2, 1.3, 1.5, and 3.1, stably expressed in mammalian cell lines. Mol Pharmacol *45*, 1227-1234.

Grupe, A., Schröter, K.H., Ruppersberg, J.P., Stocker, M., Drewes, T., Beckh, S., and Pongs, O. (1990). Cloning and expression of a human voltage-gated potassium channel. A novel member of the RCK potassium channel family. The EMBO Journal *9*, 1749.

Gu, C., Jan, Y.N., and Jan, L.Y. (2003). A Conserved Domain in Axonal Targeting of Kv1 (Shaker) Voltage-Gated Potassium Channels. Science *301*, 646-649.

Gutman, G.A., Chandy, K.G., Grissmer, S., Lazdunski, M., McKinnon, D., Pardo, L.A., Robertson, G.A., Rudy, B., Sanguinetti, M.C., Stühmer, W.*, et al.* (2005). International Union of Pharmacology. LIII. Nomenclature and Molecular Relationships of Voltage-Gated Potassium Channels. Pharmacol Rev *57*, 473-508.

Hao, J., Padilla, F., Dandonneau, M., Lavebratt, C., Lesage, F., Noel, J., and Delmas, P. (2013). Kv1.1 channels act as mechanical brake in the senses of touch and pain. Neuron *77*, 899-914.

Hartner, J.C., Schmittwolf, C., Kispert, A., Müller, A.M., Higuchi, M., and Seeburg, P.H. (2004). Liver Disintegration in the Mouse Embryo Caused by Deficiency in the RNA-editing Enzyme ADAR1. Journal of Biological Chemistry *279*, 4894-4902.

Heilstedt, H.A., Burgess, D.L., Anderson, A.E., Chedrawi, A., Tharp, B., Lee, O., Kashork, C.D., Starkey, D.E., Wu, Y.-Q., Noebels, J.L.*, et al.* (2001). Loss of the Potassium Channel β-Subunit Gene, KCNAB2, Is Associated with Epilepsy in Patients with 1p36 Deletion Syndrome. Epilepsia *42*, 1103-1111.
Heinemann, S.H., Rettig, J., Graack, H.R., and Pongs, O. (1996). Functional characterization of Kv channel beta-subunits from rat brain. The Journal of Physiology *493*, 625.

Heinemann, S.H., Rettig, J., Wunder, F., and Pongs, O. (1995). Molecular and functional characterization of a rat brain Kv beta 3 potassium channel subunit. FEBS Lett *377*, 383-389.

Hershey, A.D., and Chase, M. (1952). INDEPENDENT FUNCTIONS OF VIRAL PROTEIN AND NUCLEIC ACID IN GROWTH OF BACTERIOPHAGE. J Gen Physiol *36*, 39-56.

Herson, P.S., Virk, M., Rustay, N.R., Bond, C.T., Crabbe, J.C., Adelman, J.P., and Maylie, J. (2003). A mouse model of episodic ataxia type-1. Nat Neurosci *6*, 378-383.

Higuchi, M., Maas, S., Single, F.N., Hartner, J., Rozov, A., Burnashev, N., Feldmeyer, D., Sprengel, R., and Seeburg, P.H. (2000). Point mutation in an AMPA receptor gene rescues lethality in mice deficient in the RNA-editing enzyme ADAR2. Nature *406*, 78-81.

Holmgren, M., Shin, K.S., and Yellen, G. (1998). The Activation Gate of a Voltage-Gated K+ Channel Can Be Trapped in the Open State by an Intersubunit Metal Bridge. Neuron *21*, 617-621.

Honoré, E., Barhanin, J., Attali, B., Lesage, F., and Lazdunski, M. (1994). External blockade of the major cardiac delayed-rectifier K+ channel (Kv1.5) by polyunsaturated fatty acids. Proceedings of the National Academy of Sciences *91*, 1937-1941.

Hood, J.L., and Emeson, R.B. (2012). Editing of Neurotransmitter Receptor and Ion Channel RNAs in the Nervous System. In Adenosine Deaminases Acting on RNA (ADARs) and A-to-I Editing, C.E. Samuel, ed. (Springer Berlin Heidelberg), pp. 61-90.

Hood, J.L., Morabito, M.V., Martinez, C.R., Gilbert, J.A., Ferrick, E.A., Ayers, G.D., Chappell, J.D., Dermody, T.S., and Emeson, R.B. (2014). Reovirus-mediated induction of ADAR1 (p150) minimally alters RNA editing patterns in discrete brain regions. Mol Cell Neurosci.

Hoopengardner, B., Bhalla, T., Staber, C., and Reenan, R. (2003). Nervous System Targets of RNA Editing Identified by Comparative Genomics. Science *301*, 832-836.

Horsch, M., Seeburg, P.H., Adler, T., Aguilar-Pimentel, J.A., Becker, L., Calzada-Wack, J., Garrett, L., Gotz, A., Hans, W., Higuchi, M.*, et al.* (2011). Requirement of the RNA-editing enzyme ADAR2 for normal physiology in mice. J Biol Chem *286*, 18614-18622.

Hoshi, T., and Armstrong, C.M. (2013). C-type inactivation of voltage-gated K+ channels: Pore constriction or dilation? J Gen Physiol *141*, 151-160.

Hoshi, T., Zagotta, W.N., and Aldrich, R.W. (1990). Biophysical and Molecular Mechanisms of Shaker Potassium Channel Inactivation. Science *250*, 533.

Huang, H., Tan, B.Z., Shen, Y., Tao, J., Jiang, F., Sung, Y.Y., Ng, C.K., Raida, M., Köhr, G., Higuchi, M.*, et al.* (2012). RNA Editing of the IQ Domain in Cav1.3 Channels Modulates Their Ca2+-Dependent Inactivation. Neuron *73*, 304-316.

Hufeldt, M.R., Nielsen, D.S., Vogensen, F.K., Midtvedt, T., and Hansen, A.K. (2010). Variation in the Gut Microbiota of Laboratory Mice Is Related to Both Genetic and Environmental Factors. Comp Med *60*, 336-342.

Hwang, T., Park, C.K., Leung, A.K., Gao, Y., Hyde, T.M., Kleinman, J.E., Rajpurohit, A., Tao, R., Shin, J.H., and Weinberger, D.R. (2016). Dynamic regulation of RNA editing in human brain development and disease. Nat Neurosci *19*, 1093-1099.

Imbrici, P., D'Adamo, M.C., Grottesi, A., Biscarini, A., and Pessia, M. (2011). Episodic ataxia type 1 mutations affect fast inactivation of K+ channels by a reduction in either subunit surface expression or affinity for inactivation domain. Am J Physiol Cell Physiol *300*, C1314-C1322.

Imbrici, P., D'Adamo, M.C., Kullmann, D.M., and Pessia, M. (2006). Episodic ataxia type 1 mutations in the KCNA1 gene impair the fast inactivation properties of the human potassium channels Kv1.4-1.1/Kvβ1.1 and Kv1.4-1.1/Kvβ1.2. Eur J Neurosci *24*, 3073-3083.

Ishida, S., Sakamoto, Y., Nishio, T., Baulac, S., Kuwamura, M., Ohno, Y., Takizawa, A., Kaneko, S., Serikawa, T., and Mashimo, T. (2012). Kcna1-mutant rats dominantly display myokymia, neuromyotonia and spontaneous epileptic seizures. Brain Research *1435*, 154-166.

Ishikawa, T., Nakamura, Y., Saitoh, N., Li, W.-B., Iwasaki, S., and Takahashi, T. (2003). Distinct Roles of Kv1 and Kv3 Potassium Channels at the Calyx of Held Presynaptic Terminal. J Neurosci *23*, 10445-10453.

Itoh, K., and Watanabe, M. (2009). Paradoxical facilitation of pentylenetetrazole-induced convulsion susceptibility in mice lacking neuronal nitric oxide synthase. Neuroscience *159*, 735-743.

Jacobs, M.M., Fogg, R.L., Emeson, R.B., and Stanwood, G.D. (2009). ADAR1 and ADAR2 Expression and Editing Activity during Forebrain Development. Dev Neurosci-Basel *31*, 223-237.

Jayabal, S., Ljungberg, L., Erwes, T., Cormier, A., Quilez, S., Jaouhari, S.E., and Watt, A.J. (2015). Rapid Onset of Motor Deficits in a Mouse Model of Spinocerebellar Ataxia Type 6 Precedes Late Cerebellar Degeneration. eNeuro *2*, ENEURO.0094-0015.2015.

Jenkins, P.M., McIntyre, J.C., Zhang, L., Anantharam, A., Vesely, E.D., Arendt, K.L., Carruthers, C.J.L., Kerppola, T.K., Iñiguez-LluhÍ, J.A., Holz, R.W.*, et al.* (2011). Subunit-Dependent Axonal Trafficking of Distinct α Heteromeric Potassium Channel Complexes. Journal of Neuroscience *31*, 13224-13235.

Kalman, K., Nguyen, A., Tseng-Crank, J., Dukes, I.D., Chandy, G., Hustad, C.M., Copeland, N.G., Jenkins, N.A., Mohrenweiser, H., Brandriff, B.*, et al.* (1998). Genomic Organization, Chromosomal Localization, Tissue Distribution, and Biophysical Characterization of a Novel MammalianShaker-related Voltage-gated Potassium Channel, Kv1.7. Journal of Biological Chemistry *273*, 5851-5857.

Kamb, A., Iverson, L.E., and Tanouye, M.A. (1987). Molecular characterization of Shaker, a Drosophila gene that encodes a potassium channel. Cell *50*, 405-413.

Kaplan, W.D., and Trout, W.E. (1969). The Behavior of Four Neurological Mutants of Drosophila. Genetics *61*, 399-409.

Karst, H., Wadman, W.J., and Joels, M. (1993). Long-term control by corticosteroids of the inward rectifier in rat CA1 pyramidal neurons, in vitro. Brain Res *612*, 172-179.

Kastner, P., Mark, M., Leid, M., Gansmuller, A., Chin, W., Grondona, J.M., Décimo, D., Krezel, W., Dierich, A., and Chambon, P. (1996). Abnormal spermatogenesis in RXR beta mutant mice. Genes & Dev *10*, 80-92.

Kayakabe, M., Kakizaki, T., Kaneko, R., Sasaki, A., Nakazato, Y., Shibasaki, K., Ishizaki, Y., Saito, H., Suzuki, N., and Yanagawa, Y. (2014). Motor dysfunction in cerebellar Purkinje cell-specific vesicular GABA transporter knockout mice. Front Cell Neurosci *7*, 286.

Kim, D., Song, I., Keum, S., Lee, T., Jeong, M.-J., Kim, S.-S., McEnery, M.W., and Shin, H.-S. (2001). Lack of the Burst Firing of Thalamocortical Relay Neurons and Resistance to Absence Seizures in Mice Lacking α1G T-Type Ca2+ Channels. Neuron *31*, 35-45.

Kim, U., Wang, Y., Sanford, T., Zeng, Y., and Nishikura, K. (1994a). Molecular cloning of cDNA for double-stranded RNA adenosine deaminase, a candidate enzyme for nuclear RNA editing. Proceedings of the National Academy of Sciences *91*, 11457-11461.

Kim, Y.S., Hong, K.S., Seong, Y.S., Park, J.B., Kuroda, S., Kishi, K., Kaibuchi, K., and Takai, Y. (1994b). Phosphorylation and activation of mitogen-activated protein kinase by kainic acid-induced seizure in rat hippocampus. Biochem Biophys Res Commun *202*, 1163-1168.

Kirchheim, F., Tinnes, S., Haas, C.A., Stegen, M., and Wolfart, J. (2013). Regulation of action potential delays via voltage-gated potassium Kv1.1 channels in dentate granule cells during hippocampal epilepsy. Front Cell Neurosci *7*.

Kirsch, G.E., Drewe, J.A., Verma, S., Brown, A.M., and Joho, R.H. (1991). Electrophysiological characterization of a new member of the RCK family of rat brain K+ channels. FEBS Letters *278*, 55-60.

Koch, R.O., Wanner, S.G., Koschak, A., Hanner, M., Schwarzer, C., Kaczorowski, G.J., Slaughter, R.S., Garcia, M.L., and Knaus, H.-G. (1997). Complex Subunit Assembly of Neuronal Voltage-gated K+Channels Basis for High-Affinity Toxin Interactions and Pharmacology. J Biol Chem *272*, 27577-27581.

Koschak, A., Bugianesi, R.M., Mitterdorfer, J., Kaczorowski, G.J., Garcia, M.L., and Knaus, H.-G. (1998). Subunit Composition of Brain Voltage-gated Potassium Channels Determined by Hongotoxin-1, a Novel Peptide Derived fromCentruroides limbatus Venom. Journal of Biological Chemistry *273*, 2639-2644.

Krestel, H., Raffel, S., von Lehe, M., Jagella, C., Moskau-Hartmann, S., Becker, A., Elger, C.E., Seeburg, P.H., and Nirkko, A. (2013). Differences between RNA and DNA due to RNA editing in temporal lobe epilepsy. Neurobiol Dis *56*, 66-73.

Krestel, H.E., Shimshek, D.R., Jensen, V., Nevian, T., Kim, J., Geng, Y., Bast, T., Depaulis, A., Schonig, K., Schwenk, F.*, et al.* (2004). A genetic switch for epilepsy in adult mice. J Neurosci *24*, 10568-10578.

Kurata, H.T., and Fedida, D. (2006). A structural interpretation of voltage-gated potassium channel inactivation. Progress in Biophysics and Molecular Biology *92*, 185-208.

Kuroda, K.O., and Tsuneoka, Y. (2013). Assessing Postpartum Maternal Care, Alloparental Behavior, and Infanticide in Mice: With Notes on Chemosensory Influences. In Pheromone Signaling: Methods and Protocols, K. Touhara, ed. (Totowa, NJ: Humana Press), pp. 331-347.

Lander, E.S., Linton, L.M., Birren, B., Nusbaum, C., Zody, M.C., Baldwin, J., Devon, K., Dewar, K., Doyle, M., FitzHugh, W.*, et al.* (2001). Initial sequencing and analysis of the human genome. Nature *409*, 860-921.

Lang, R., Lee, G., Liu, W., Tian, S., Rafi, H., Orias, M., Segal, A.S., and Desir, G.V. (2000). KCNA10: a novel ion channel functionally related to both voltage-gated potassium and CNG cation channels. American Journal of Physiology - Renal Physiology *278*, F1013-F1021.

Leanza, L., O'Reilly, P., Doyle, A., Venturini, E., Zoratti, M., Szegezdi, E., and Szabo, I. (2014). Correlation between potassium channel expression and sensitivity to drug-induced cell death in tumor cell lines. Curr Pharm Des *20*, 189-200.

Lee, T.E., Philipson, L.H., and Nelson, D.J. (1996). N-type Inactivation in the Mammalian Shaker K+ Channel Kv1.4. J Membrane Biol *151*, 225-235.

Lehmann, K.A., and Bass, B.L. (2000). Double-Stranded RNA Adenosine Deaminases ADAR1 and ADAR2 Have Overlapping Specificities. Biochemistry *39*, 12875-12884.

Li, J.B., Levanon, E.Y., Yoon, J.-K., Aach, J., Xie, B., LeProust, E., Zhang, K., Gao, Y., and Church, G.M. (2009). Genome-Wide Identification of Human RNA Editing Sites by Parallel DNA Capturing and Sequencing. Science *324*, 1210-1213.

Li, Y., Mitaxov, V., and Waksman, G. (1999). Structure-based design of Taq DNA polymerases with improved properties of dideoxynucleotide incorporation. Proceedings of the National Academy of Sciences *96*, 9491-9496.

Licatalosi, D.D., and Darnell, R.B. (2010). RNA processing and its regulation: global insights into biological networks. Nature Reviews Genetics *11*, 75-87.

Liman, E.R., Tytgat, J., and Hess, P. (1992). Subunit stoichiometry of a mammalian K+ channel determined by construction of multimeric cDNAs. Neuron *9*, 861-871.

Lipski, J., Park, T.I., Li, D., Lee, S.C., Trevarton, A.J., Chung, K.K., Freestone, P.S., and Bai, J.Z. (2006). Involvement of TRP-like channels in the acute ischemic response of hippocampal CA1 neurons in brain slices. Brain Res *1077*, 187-199.

Lohnes, D., Kastner, P., Dierich, A., Mark, M., LeMeur, M., and Chambon, P. (1993). Function of retinoic acid receptor γ in the mouse. Cell *73*, 643-658.

London, B., Wang, D.W., Hill, J.A., and Bennett, P.B. (1998). The transient outward current in mice lacking the potassium channel gene Kv1.4. The Journal of Physiology *509 (Pt 1)*, 171-182.

Long, S.B., Campbell, E.B., and MacKinnon, R. (2005). Crystal Structure of a Mammalian Voltage-Dependent Shaker Family K+ Channel. Science *309*, 897-903.

Lu, Q., Peevey, J., Jow, F., Monaghan, M.M., Mendoza, G., Zhang, H., Wu, J., Kim, C.Y., Bicksler, J., Greenblatt, L.*, et al.* (2008). Disruption of Kv1.1 N-type inactivation by novel small molecule inhibitors (disinactivators). Bioorganic & Medicinal Chemistry *16*, 3067-3075.

Lugt, N.M.v.d., Domen, J., Linders, K., Roon, M.v., Robanus-Maandag, E., Riele, H.t., Valk, M.v.d., Deschamps, J., Sofroniew, M., and Lohuizen, M.v. (1994).

Posterior transformation, neurological abnormalities, and severe hematopoietic defects in mice with a targeted deletion of the bmi-1 proto-oncogene. Genes & Dev *8*, 757-769.

Ma, Z., Lavebratt, C., Almgren, M., Portwood, N., Forsberg, L.E., Bränström, R., Berglund, E., Falkmer, S., Sundler, F., Wierup, N.*, et al.* (2011). Evidence for Presence and Functional Effects of Kv1.1 Channels in β-Cells: General Survey and Results from mceph/mceph Mice. PLoS ONE *6*.

MacDonald, P.E., and Wheeler, M.B. (2003). Voltage-dependent K(+) channels in pancreatic beta cells: role, regulation and potential as therapeutic targets. Diabetologia *46*, 1046-1062.

Madeja, M., Mußhoff, U., Lorra, C., Pongs, O., and Speckmann, E.-J. (1996). Mechanism of action of the epileptogenic drug pentylenetetrazol on a cloned neuronal potassium channel. Brain Research *722*, 59-70.

Madeja, M., Stocker, M., Muβhoff, U., Pongs, O., and Speckmann, E.-J. (1994). Potassium currents in epilepsy: effects of the epileptogenic agent pentylenetetrazol on a cloned potassium channel. Brain Research *656*, 287-294.

Manganas, L.N., and Trimmer, J.S. (2000). Subunit Composition Determines Kv1 Potassium Channel Surface Expression. J Biol Chem *275*, 29685-29693.

Manganas, L.N., Wang, Q., Scannevin, R.H., Antonucci, D.E., Rhodes, K.J., and Trimmer, J.S. (2001). Identification of a trafficking determinant localized to the Kv1 potassium channel pore. Proceedings of the National Academy of Sciences of the United States of America *98*, 14055-14059.

Mannion, Niamh M., Greenwood, S.M., Young, R., Cox, S., Brindle, J., Read, D., Nellåker, C., Vesely, C., Ponting, Chris P., McLaughlin, Paul J.*, et al.* (2014). The RNA-Editing Enzyme ADAR1 Controls Innate Immune Responses to RNA. Cell reports *9*, 1482-1494.

Marcucci, R., Brindle, J., Paro, S., Casadio, A., Hempel, S., Morrice, N., Bisso, A., Keegan, L.P., Sal, G.D., and O'Connell, M.A. (2011). Pin1 and WWP2 regulate GluR2 Q/R site RNA editing by ADAR2 with opposing effects. The EMBO Journal *30*, 4211-4222.

Marsh, D.J., Baraban, S.C., Hollopeter, G., and Palmiter, R.D. (1999). Role of the Y5 neuropeptide Y receptor in limbic seizures. Proc Natl Acad Sci U S A *96*, 13518-13523.

Matsuo, N., Takao, K., Nakanishi, K., Yamasaki, N., Tanda, K., and Miyakawa, T. (2010). Behavioral profiles of three C57BL/6 substrains. Front Behav Neurosci *4*, 29.

Maylie, B., Bissonnette, E., Virk, M., Adelman, J.P., and Maylie, J.G. (2002). Episodic Ataxia Type 1 Mutations in the Human Kv1.1 Potassium Channel Alter hKvβ1-Induced N-Type Inactivation. J Neurosci *22*, 4786-4793.

McCormack, K., Connor, J.X., Zhou, L., Ho, L.L., Ganetzky, B., Chiu, S.-Y., and Messing, A. (2002). Genetic Analysis of the Mammalian K+ Channel β Subunit Kvβ2 (Kcnab2). Journal of Biological Chemistry *277*, 13219-13228.

McCormack, K., McCormack, T., Tanouye, M., Rudy, B., and Stühmer, W. (1995). Alternative splicing of the human Shaker K+ channel β1 gene and functional expression of the β2 gene product. FEBS Letters *370*, 32-36.

McKinnon, D. (1989). Isolation of a cDNA clone coding for a putative second potassium channel indicates the existence of a gene family. Journal of Biological Chemistry *264*, 8230-8236.

Meiri, N., Ghelardini, C., Tesco, G., Galeotti, N., Dahl, D., Tomsic, D., Cavallaro, S., Quattrone, A., Capaccioli, S., Bartolini, A.*, et al.* (1997). Reversible antisense inhibition of Shaker-like Kv1.1 potassium channel expression impairs associative memory in mouse and rat. Proceedings of the National Academy of Sciences *94*, 4430-4434.

Mestre, T.A., Manole, A., MacDonald, H., Riazi, S., Kraeva, N., Hanna, M.G., Lang, A.E., Mannikko, R., and Yoon, G. (2016). A novel KCNA1 mutation in a family with episodic ataxia and malignant hyperthermia. Neurogenetics.

Monteiro, S., Roque, S., de Sa-Calcada, D., Sousa, N., Correia-Neves, M., and Cerqueira, J.J. (2015). An efficient chronic unpredictable stress protocol to induce stress-related responses in C57BL/6 mice. Frontiers in psychiatry *6*, 6.

Moore, A.N., Waxham, M.N., and Dash, P.K. (1996). Neuronal activity increases the phosphorylation of the transcription factor cAMP response element-binding protein (CREB) in rat hippocampus and cortex. J Biol Chem *271*, 14214-14220.

Morabito, M.V., Ulbricht, R.J., O'Neil, R.T., Airey, D.C., Lu, P., Zhang, B., Wang, L., and Emeson, R.B. (2010). High-Throughput Multiplexed Transcript Analysis Yields Enhanced Resolution of 5-Hydroxytryptamine2C Receptor mRNA Editing Profiles. Mol Pharmacol *77*, 895-902.

Nakamura, K., Oshima, T., Morimoto, T., Ikeda, S., Yoshikawa, H., Shiwa, Y., Ishikawa, S., Linak, M.C., Hirai, A., Takahashi, H.*, et al.* (2011). Sequence-specific error profile of Illumina sequencers. Nucleic Acids Research *39*, e90-e90.

Need, A.C., Irvine, E.E., and Giese, K.P. (2003). Learning and memory impairments in Kvβ1.1-null mutants are rescued by environmental enrichment or ageing. European Journal of Neuroscience *18*, 1640-1644.

Nishikura, K. (2010). Functions and Regulation of RNA Editing by ADAR Deaminases. Annual review of biochemistry *79*, 321-349.

Niswender, C.M., Copeland, S.C., Herrick-Davis, K., Emeson, R.B., and Sanders-Bush, E. (1999). RNA Editing of the Human Serotonin 5-Hydroxytryptamine 2C Receptor Silences Constitutive Activity. Journal of Biological Chemistry *274*, 9472-9478.

O'Leary, H., Bernard, P.B., Castano, A.M., and Benke, T.A. (2016). Enhanced long term potentiation and decreased AMPA receptor desensitization in the acute period following a single kainate induced early life seizure. Neurobiol Dis *87*, 134-144.

O'Neil, R.T., and Emeson, R.B. (2012). Quantitative analysis of 5HT(2C) receptor RNA editing patterns in psychiatric disorders. Neurobiol Dis *45*, 8-13.

Oliver, D., Lien, C.-C., Soom, M., Baukrowitz, T., Jonas, P., and Fakler, B. (2004). Functional Conversion Between A-Type and Delayed Rectifier K+ Channels by Membrane Lipids. Science *304*, 265-270.

Ovsepian, S.V., LeBerre, M., Steuber, V., O'Leary, V.B., Leibold, C., and Oliver Dolly, J. (2016). Distinctive role of KV1.1 subunit in the biology and functions of low threshold K(+) channels with implications for neurological disease. Pharmacol Ther *159*, 93-101.

Parcej, D.N., Scott, V.E., and Dolly, J.O. (1992). Oligomeric properties of alpha-dendrotoxin-sensitive potassium ion channels purified from bovine brain. Biochemistry *31*, 11084-11088.

Peng, P.L., Zhong, X., Tu, W., Soundarapandian, M.M., Molner, P., Zhu, D., Lau, L., Liu, S., Liu, F., and Lu, Y. (2006). ADAR2-dependent RNA editing of AMPA receptor subunit GluR2 determines vulnerability of neurons in forebrain ischemia. Neuron *49*, 719-733.

Pennacchio, P., Noe, F., Gnatkovsky, V., Moroni, R.F., Zucca, I., Regondi, M.C., Inverardi, F., de Curtis, M., and Frassoni, C. (2015). Increased pCREB expression and the spontaneous epileptiform activity in a BCNU-treated rat model of cortical dysplasia. Epilepsia *56*, 1343-1354.

Persson, A.-S., Klement, G., Almgren, M., Sahlholm, K., Nilsson, J., Petersson, S., Århem, P., Schalling, M., and Lavebratt, C. (2005). A truncated Kv1.1 protein in the brain of the megencephaly mouse: expression and interaction. BMC Neurosci *6*, 65.

Persson, A.-S., Westman, E., Wang, F.-H., Khan, F.H., Spenger, C., and Lavebratt, C. (2007). Kv1.1 null mice have enlarged hippocampus and ventral cortex. BMC Neurosci *8*, 10.

Pertea, M., and Salzberg, S.L. (2010). Between a chicken and a grape: estimating the number of human genes. Genome Biology *11*, 206.

Petersson, S., Persson, A.-S., Johansen, J.E., Ingvar, M., Nilsson, J., Klement, G., Århem, P., Schalling, M., and Lavebratt, C. (2003). Truncation of the Shaker-like voltage-gated potassium channel, Kv1.1, causes megencephaly. European Journal of Neuroscience *18*, 3231-3240.

Petitjean, D., Kalstrup, T., Zhao, J., and Blunck, R. (2015). A Disease Mutation Causing Episodic Ataxia Type I in the S1 Links Directly to the Voltage Sensor and the Selectivity Filter in Kv Channels. J Neurosci *35*, 12198-12206.

Piredda, S., Yonekawa, W., Whittingham, T.S., and Kupferberg, H.J. (1985). Potassium, Pentylenetetrazol, and Anticonvulsants in Mouse Hippocampal Slices. Epilepsia *26*, 167-174.

Po, S., Roberds, S., Snyders, D.J., Tamkun, M.M., and Bennett, P.B. (1993). Heteromultimeric assembly of human potassium channels. Molecular basis of a transient outward current? Circulation Research *72*, 1326-1336.

Po, S., Snyders, D.J., Baker, R., Tamkun, M.M., and Bennett, P.B. (1992). Functional expression of an inactivating potassium channel cloned from human heart. Circulation Research *71*, 732-736.

Pongs, O., and Schwarz, J.R. (2010). Ancillary subunits associated with voltage-dependent K+ channels. Physiol Rev *90*, 755-796.

Pozo, E.D., Barrios, M., and Baeyens, J.M. (1990). Effects of Potassium Channel Openers on Pentylenetetrazole-Induced Seizures in Mice. Pharmacology & Toxicology *67*, 182-184.

Ramanjaneyulu, R., and Ticku, M.K. (1984). Interactions of pentamethylenetetrazole and tetrazole analogues with the picrotoxinin site of the benzodiazepine-GABA receptor-ionophore complex. Eur J Pharmacol *98*, 337-345.

Rasband, M.N., Park, E.W., Vanderah, T.W., Lai, J., Porreca, F., and Trimmer, J.S. (2001). Distinct potassium channels on pain-sensing neurons. Proc Natl Acad Sci USA *98*, 13373-13378.

Rettig, J., Heinemann, S.H., Wunder, F., Lorra, C., Parcej, D.N., Oliver Dolly, J., and Pongs, O. (1994). Inactivation properties of voltage-gated K+ channels altered by presence of β-subunit. Nature *369*, 289-294.

Rho, J.M., Szot, P., Tempel, B.L., and Schwartzkroin, P.A. (1999). Developmental Seizure Susceptibility of Kv1.1 Potassium Channel Knockout Mice. Dev Neurosci-Basel *21*, 320-327.

Rhodes, K.J., Monaghan, M.M., Barrezueta, N.X., Nawoschik, S., Bekele-Arcuri, Z., Matos, M.F., Nakahira, K., Schechter, L.E., and Trimmer, J.S. (1996). Voltage-gated K+ channel beta subunits: expression and distribution of Kv beta 1 and Kv beta 2 in adult rat brain. J Neurosci *16*, 4846-4860.

Rhodes, K.J., Strassle, B.W., Monaghan, M.M., Bekele-Arcuri, Z., Matos, M.F., and Trimmer, J.S. (1997). Association and Colocalization of the Kvβ1 and Kvβ2 β-Subunits with Kv1 α-Subunits in Mammalian Brain K+Channel Complexes. J Neurosci *17*, 8246-8258.

Rinkevich, F.D., Schweitzer, P.A., and Scott, J.G. (2012). Antisense sequencing improves the accuracy and precision of A-to-I editing measurements using the peak height ratio method. BMC Research Notes *5*, 63.

Risher, W.C., Andrew, R.D., and Kirov, S.A. (2009). Real-time passive volume responses of astrocytes to acute osmotic and ischemic stress in cortical slices and in vivo revealed by two-photon microscopy. Glia *57*, 207-221.

Robbins, C.A., and Tempel, B.L. (2012). Kv1.1 and Kv1.2: Similar channels, different seizure models. Epilepsia *53*, 134-141.

Roeper, J., Sewing, S., Zhang, Y., Sommer, T., Wanner, S.G., and Pongs, O. (1998). NIP domain prevents N-type inactivation in voltage-gated potassium channels. Nature *391*, 390-393.

Rula, E.Y., Lagrange, A.H., Jacobs, M.M., Hu, N., Macdonald, R.L., and Emeson, R.B. (2008). Developmental modulation of GABA(A) receptor function by RNA editing. J Neurosci *28*, 6196-6201.

Sandberg, R., Yasuda, R., Pankratz, D.G., Carter, T.A., Rio, J.A.D., Wodicka, L., Mayford, M., Lockhart, D.J., and Barlow, C. (2000). Regional and strain-specific gene expression mapping in the adult mouse brain. Proceedings of the National Academy of Sciences *97*, 11038-11043.

Sands, Z., Grottesi, A., and Sansom, M.S. (2005). Voltage-gated ion channels. Current biology : CB *15*, R44-47.

Sanguinetti, M.C., Jiang, C., Curran, M.E., and Keating, M.T. (1995). A mechanistic link between an inherited and an acquired cardiac arrhythmia: HERG encodes the IKr potassium channel. Cell *81*, 299-307.

SantaLucia, J., Jr. (1998). A unified view of polymer, dumbbell, and oligonucleotide DNA nearest-neighbor thermodynamics. Proc Natl Acad Sci USA *95*, 1460-1465.

Scheffer, H., Brunt, E.R.P., Mol, G.J.J., van der Vlies, P., Stulp, Verlind, E., Mantel, G., Averyanov, Y.N., Hofstra, R.M.W., and Buys, C.H.C.M. (1998). Three novel KCNA1 mutations in episodic ataxia type I families. Human Genetics *102*, 464-466.

Schirmer, M., Ijaz, U.Z., D'Amore, R., Hall, N., Sloan, W.T., and Quince, C. (2015). Insight into biases and sequencing errors for amplicon sequencing with the Illumina MiSeq platform. Nucleic Acids Research, gku1341.

Schreiber, E., Matthias, P., Müller, M.M., and Schaffner, W. (1989). Rapid detection of octamer binding proteins with 'mini extracts', prepared from a small number of cells. Nucleic Acids Res *17*, 6419-6419.

Schulte, U., Thumfart, J.-O., Klöcker, N., Sailer, C.A., Bildl, W., Biniossek, M., Dehn, D., Deller, T., Eble, S., Abbass, K.*, et al.* (2006). The Epilepsy-Linked Lgi1 Protein Assembles into Presynaptic Kv1 Channels and Inhibits Inactivation by Kvβ1. Neuron *49*, 697-706.

Scott, V.E.S., Muniz, Z.M., Sewing, S., Lichtinghagen, R., Parcej, D.N., Pongs, O., and Dolly, J.O. (1994). Antibodies specific for distinct Kv subunits unveil a heterooligomeric basis for subtypes of .alpha.-dendrotoxin-sensitive potassium channels in bovine brain. Biochemistry *33*, 1617-1623.

Shi, G., Nakahira, K., Hammond, S., Rhodes, K.J., Schechter, L.E., and Trimmer, J.S. (1996). βSubunits Promote K+ Channel Surface Expression through Effects Early in Biosynthesis. Neuron *16*, 843-852.

Smart, S.L., Lopantsev, V., Zhang, C.L., Robbins, C.A., Wang, H., Chiu, S.Y., Schwartzkroin, P.A., Messing, A., and Tempel, B.L. (1998). Deletion of the KV1.1 Potassium Channel Causes Epilepsy in Mice. Neuron *20*, 809-819.

Sokolov, M.V., Shamotienko, O., Dhochartaigh, S.N., Sack, J.T., and Dolly, J.O. (2007). Concatemers of brain Kv1 channel alpha subunits that give similar K+ currents yield pharmacologically distinguishable heteromers. Neuropharmacol *53*, 272-282.

Sommer, B., Köhler, M., Sprengel, R., and Seeburg, P.H. (1991). RNA editing in brain controls a determinant of ion flow in glutamate-gated channels. Cell *67*, 11-19.

Speake, T., Kibble, J.D., and Brown, P.D. (2004). Kv1.1 and Kv1.3 channels contribute to the delayed-rectifying K+ conductance in rat choroid plexus epithelial cells. Am J Physiol Cell Physiol *286*, C611-C620.

Stefani, E., and Bezanilla, F. (1998). [17] Cut-open oocyte voltage-clamp technique. In Meth Enzymol, P.M. Conn, ed. (Academic Press), pp. 300-318.

Stefl, R., Oberstrass, F.C., Hood, J.L., Jourdan, M., Zimmermann, M., Skrisovska, L., Maris, C., Peng, L., Hofr, C., Emeson, R.B.*, et al.* (2010). The Solution Structure of the ADAR2 dsRBM-RNA Complex Reveals a Sequence-Specific Readout of the Minor Groove. Cell *143*, 225-237.

Stein, E.A., Fuller, S.A., Edgemond, W.S., and Campbell, W.B. (1996). Physiological and behavioural effects of the endogenous cannabinoid, arachidonylethanolamide (anandamide), in the rat. Br J Pharmacol *119*, 107-114.

Stenson, P.D., Mort, M., Ball, E.V., Shaw, K., Phillips, A., and Cooper, D.N. (2014). The Human Gene Mutation Database: building a comprehensive mutation repository for clinical and molecular genetics, diagnostic testing and personalized genomic medicine. Hum Genet *133*, 1-9.

Streit, A.K., Derst, C., Wegner, S., Heinemann, U., Zahn, R.K., and Decher, N. (2011). RNA editing of Kv1.1 channels may account for reduced ictogenic potential of 4- aminopyridine in chronic epileptic rats. Epilepsia *52*, 645-648.

Streit, A.K., Matschke, L.A., Dolga, A.M., Rinné, S., and Decher, N. (2014). RNA Editing in the Central Cavity as a Mechanism to Regulate Surface Expression of the Voltage-gated Potassium Channel Kv1.1. J Biol Chem *289*, 26762-26771.

Stühmer, W., Ruppersberg, J.P., Schröter, K.H., Sakmann, B., Stocker, M., Giese, K.P., Perschke, A., Baumann, A., and Pongs, O. (1989). Molecular basis of functional diversity of voltage-gated potassium channels in mammalian brain. The EMBO Journal *8*, 3235.

Swanson, R., Marshall, J., Smith, J.S., Williams, J.B., Boyle, M.B., Folander, K., Luneau, C.J., Antanavage, J., Oliva, C., Buhrow, S.A.*, et al.* (1990). Cloning and expression of cDNA and genomic clones encoding three delayed rectifier potassium channels in rat brain. Neuron *4*, 929-939.

Szabò, I., Zoratti, M., and Gulbins, E. (2010). Contribution of voltage-gated potassium channels to the regulation of apoptosis. FEBS Lett *584*, 2049-2056.

Tempel, B.L., Jan, Y.N., and Jan, L.Y. (1988). Cloning of a probable potassium channel gene from mouse brain. Nature *332*, 837-839.

Tempel, B.L., Papazian, D.M., Schwarz, T.L., Jan, Y.N., and Jan, L.Y. (1987). Sequence of a probable potassium channel component encoded at Shaker locus of Drosophila. Science *237*, 770-775.

Thorneloe, K.S., Chen, T.T., Kerr, P.M., Grier, E.F., Horowitz, B., Cole, W.C., and Walsh, M.P. (2001). Molecular Composition of 4-Aminopyridine-Sensitive Voltage-Gated K+ Channels of Vascular Smooth Muscle. Circulation Research *89*, 1030-1037.

Tomlinson, S.E., Rajakulendran, S., Tan, S.V., Graves, T.D., Bamiou, D.-E., Labrum, R.W., Burke, D., Sue, C.M., Giunti, P., Schorge, S.*, et al.* (2013). Clinical, genetic, neurophysiological and functional study of new mutations in episodic ataxia type 1. J Neurol Neurosurg Psychiatry *84*, 1107-1112.

Trimmer, J.S., and Rhodes, K.J. (2004). Localization of Voltage-Gated Ion Channels IN Mammalian Brain. Annual Review of Physiology *66*, 477-519.

Tsaur, M.L., Sheng, M., Lowenstein, D.H., Jan, Y.N., and Jan, L.Y. (1992). Differential expression of K+ channel mRNAs in the rat brain and down-regulation in the hippocampus following seizures. Neuron *8*, 1055-1067.

Vennekamp, J., Wulff, H., Beeton, C., Calabresi, P.A., Grissmer, S., Hänsel, W., and Chandy, K.G. (2004). Kv1.3-Blocking 5-Phenylalkoxypsoralens: A New Class of Immunomodulators. Mol Pharmacol *65*, 1364-1374.

Venter, J.C., Adams, M.D., Myers, E.W., Li, P.W., Mural, R.J., Sutton, G.G., Smith, H.O., Yandell, M., Evans, C.A., Holt, R.A.*, et al.* (2001). The Sequence of the Human Genome. Science *291*, 1304-1351.

Wagner, R.W., Smith, J.E., Cooperman, B.S., and Nishikura, K. (1989). A double-stranded RNA unwinding activity introduces structural alterations by means of adenosine to inosine conversions in mammalian cells and Xenopus eggs. Proceedings of the National Academy of Sciences *86*, 2647-2651.

Wahlstedt, H., Daniel, C., Ensterö, M., and Öhman, M. (2009). Large-scale mRNA sequencing determines global regulation of RNA editing during brain development. Genome Research *19*, 978-986.

Wang, F.C., Parcej, D.N., and Dolly, J.O. (1999). α Subunit compositions of Kv1.1-containing K+ channel subtypes fractionated from rat brain using dendrotoxins. Eur J Biochem *263*, 230-237.

Wang, H., Kunkel, D.D., Martin, T.M., Schwartzkroin, P.A., and Tempel, B.L. (1993). Heteromultimeric K+ channels in terminal and juxtaparanodal regions of neurons. Nature *365*, 75-79.

Wang, H., Kunkel, D.D., Schwartzkroin, P.A., and Tempel, B.L. (1994). Localization of Kv1.1 and Kv1.2, two K channel proteins, to synaptic terminals, somata, and dendrites in the mouse brain. J Neurosci *14*, 4588-4599.

Wang, Q., Miyakoda, M., Yang, W., Khillan, J., Stachura, D.L., Weiss, M.J., and Nishikura, K. (2004). Stress-induced Apoptosis Associated with Null Mutation of ADAR1 RNA Editing Deaminase Gene. Journal of Biological Chemistry *279*, 4952-4961.

Wang, Z., Kiehn, J., Yang, Q., Brown, A.M., and Wible, B.A. (1996). Comparison of Binding and Block Produced by Alternatively Spliced Kvβ1 Subunits. Journal of Biological Chemistry *271*, 28311-28317.

Watson, J.D., and Crick, F.H.C. (1953). Molecular Structure of Nucleic Acids: A Structure for Deoxyribose Nucleic Acid. Nature *171*, 737-738.
Weber, E.M., Algers, B., Hultgren, J., and Olsson, I.A.S. (2013). Pup mortality in laboratory mice – infanticide or not? Acta Vet Scand *55*, 83.

Xu, J., Koni, P.A., Wang, P., Li, G., Kaczmarek, L., Wu, Y., Li, Y., Flavell, R.A., and Desir, G.V. (2003). The voltage-gated potassium channel Kv1.3 regulates energy homeostasis and body weight. Hum Mol Genet *12*, 551-559.

Xu, J., and Li, M. (1997). Kvβ2 Inhibits the Kvβ1-mediated Inactivation of K+ Channels in Transfected Mammalian Cells. Journal of Biological Chemistry *272*, 11728-11735.

Yao, X., Segal, A.S., Welling, P., Zhang, X., McNicholas, C.M., Engel, D., Boulpaep, E.L., and Desir, G.V. (1995). Primary structure and functional expression of a cGMP-gated potassium channel. Proceedings of the National Academy of Sciences *92*, 11711-11715.

Yellen, G. (2002). The voltage-gated potassium channels and their relatives. Nature *419*, 35-42.

Yu, W., Xu, J., and Li, M. (1996). NAB Domain Is Essential for the Subunit Assembly of both α–α and α–β Complexes of Shaker-like Potassium Channels. Neuron *16*, 441-453.

Zagotta, W.N., Hoshi, T., and Aldrich, R.W. (1990). Restoration of inactivation in mutants of Shaker potassium channels by a peptide derived from ShB. Science *250*, 568-571.

Zerr, P., Adelman, J.P., and Maylie, J. (1998). Episodic Ataxia Mutations in Kv1.1 Alter Potassium Channel Function by Dominant Negative Effects or Haploinsufficiency. J Neurosci *18*, 2842-2848.

Zhang, C.-L., Messing, A., and Chiu, S.Y. (1999). Specific Alteration of Spontaneous GABAergic Inhibition in Cerebellar Purkinje Cells in Mice Lacking the Potassium Channel Kv1.1. J Neurosci *19*, 2852-2864.

Zhao, S., and Fernald, R.D. (2005). Comprehensive Algorithm for Quantitative Real-Time Polymerase Chain Reaction. J Comput Biol *12*, 1047-1064.

Zhou, C., Ding, L., Deel, M.E., Ferrick, E.A., Emeson, R.B., and Gallagher, M.J. (2015). Altered intrathalamic GABAA neurotransmission in a mouse model of a human genetic absence epilepsy syndrome. Neurobiol Dis *73*, 407-417.

Zhou, L., Zhang, C.-L., Messing, A., and Chiu, S.Y. (1998). Temperature-Sensitive Neuromuscular Transmission in Kv1.1 Null Mice: Role of Potassium Channels under the Myelin Sheath in Young Nerves. J Neurosci *18*, 7200-7215.

Zhou, M., Morais-Cabral, J.H., Mann, S., and MacKinnon, R. (2001). Potassium channel receptor site for the inactivation gate and quaternary amine inhibitors. Nature *411*, 657-661.

Zuker, M. (2003). Mfold web server for nucleic acid folding and hybridization prediction. Nucleic Acids Res *31*, 3406-3415.